August 1970
Report No. EVE 24-70-4

WATER TREATMENT SLUDGE DRYING AND DRAINAGE ON SAND BEDS

Edward E. Clark

Partially Supported by Water Quality Office, Environmental Protection Agency, Research Grant 17070-DZS, and Research Fellowship 1-F1-WP-26, 453-01

ENVIRONMENTAL ENGINEERING
DEPARTMENT OF CIVIL ENGINEERING
UNIVERSITY OF MASSACHUSETTS
AMHERST, MASSACHUSETTS

WATER TREATMENT SLUDGE DRYING AND DRAINAGE ON SAND BEDS

BY

Edward E. Clark

Ph.D.

VITA

Edward E. Clark was born February 18, 1940 in Cincinnati, Ohio. He attended Cumberland County High School at Crossville, Tennessee. In 1962 he received a Bachelor of Science in Civil Engineering from Tennessee Technological University, Cookeville, Tennessee. From 1962 to 1965 he worked in Nashville, Tennessee as a field engineer and designer for Burkhalter, Hickerson and Associates, and Turner Engineering Company, respectively. In 1966 he received a Master of Science in Sanitary Engineering from Vanderbilt University, Nashville, Tennessee.

From 1966 to 1968 he worked as a consulting engineer for Turner Engineering Company, Nashville, and Ryckman, Edgerley, Tomlinson, and Associates, St. Louis, Missouri.

In 1968 he entered the Environmental Engineering Program in the Civil Engineering Department at the University of Massachusetts for the degree of Doctor of Philosophy.

After September, 1970 he will be associated with the consulting frim Connell Associates, Inc., Miami, Florida.

He is a registered professional engineer in Tennessee and member of Sigma Xi, American Society of Civil Engineers, the Water Pollution Control Federation, American Institute of Chemical Engineers, and American Water Works Association.

Water Treatment Sludge Drying and Drainage

on Sand Beds. (August 1970)

Edward E. Clark
B.S., Tennessee Technological University
M.S., Vanderbilt University
Directed by: Dr. Donald D. Adrian

The collection, handling, and disposal of water treatment sludges is one of the most exigent problems in environmental engineering. Reduction of the water content by drying and drainage on sand dewatering beds reduces the volume of material for ultimate disposal.

Sludges from four types of treatment processes were studied. Evaporation, drying, and dewatering (drying and drainage) studies were conducted under controlled drying conditions. Moisture profiles of the sludge cakes and supporting sand layers were determined by a gamma-ray attenuation method. Various chemical analyses were performed on sludge, filtrate, and decant samples.

The sludges varied widely in chemical characteristics depending upon the raw water source, the type and degree of treatment, and the method of sludge removal from the sedimentation basins. A large percentage of the chemical constituents were adsorbed to the sludge solids leaving a relatively clean filtrate and decant to be disposed.

For the drying period of interest in sludge drying, the major resistance to drying is at the surface and the drying rate approximates that of a free water surface. The moisture gradient of the sludge cake, as determined by the gamma-ray attenuation method, was negligible. Thus, the internal resistance to moisture move by diffusion, or capillary,

flow was small.

Water treatment sludges have lower media factors than sewage sludges due to the smaller particle size and flocculant nature of the material.

Equations and methodology were presented which will enable the design engineer to predict the drying bed area required for water treatment sludges.

ACKNOWLEDGMENTS

The author wishes to express his appreciation to the dissertation committee for their assistance and guidance. Until June, 1969, the committee consisted of Dr. John H. Nebiker, chairman; Dr. Rolf T. Skrinde, and Dr. Donald D. Adrian. After June, 1969, the committee consisted of Dr. Donald D. Adrian, chairman; Dr. Tsuan H. Feng, and Dr. Chin S. Chen.

Special thanks are also expressed to Mr. Philip Lutin, Mr. John Ramsay, and Mrs. Dorothy Jabarin for their assistance in conducting the experiments. Prof. Armand Costa and the Engineering Research Shop are acknowledged for their assistance in the fabrication of the equipment.

The work was supported in part by the Federal Water Quality Administration in the form of Research Grant 17070-DZS (formerly WP-01239) and by Research Fellowship 1-F1-WP-26, 453-01.

TABLE OF CONTENTS

LIST OF TABLES

List of Tables Continued . . .

LIST OF FIGURES

List of Figures Continued. . . .

List of Figures Continued . . .

NOMENCLATURE

Symbol	Definition and Dimensions in Mass (M), Length (L), Time (t), and Temperature (T).
A	Area (L^2)
A_s	Radiation strength (t^{-1})
$B(\mu,z')$	Radiation build-up factor (dimensionless)
C_h	Henry's-law constant ($ML^{-1}t^{-2}$)
c	Weight of dry cake solids per unit volume ($ML^{-2}t^{-2}$)
D	Constant diffusion coefficient (L^2t^{-1})
$D(U)$	Moisture dependent diffusion coefficient (L^2t^{-1})
$D.R.$	Radiation dose rate (L^2t^{-3})
d	Diameter (L)
E	Evaporation ratio (dimensionless)
E_o	Energy (ML^2t^{-2})
E_r	Evaporation rate (Lt^{-1})
E_w	Evaporation flux rate ($ML^{-1}t^{-3}$)
g	Acceleration due to gravity (Lt^{-2})
H	Hydraulic head at time t (L)
H_o	Initial hydraulic head (L)
I	Drying rate ($ML^{-2}t^{-1}$)
I_c	Drying rate in constant-rate period ($ML^{-2}t^{-1}$)
I_f	Drying rate in falling-rate period ($ML^{-2}t^{-1}$)
I_n	Net intensity of solar radiation (Mt^{-3})
K	Transfer coefficient ($M^{-1}L^3t$)

K_e	Evaporation transfer coefficient (t^{-1})
L	Thickness (L)
L_f	Thickness of filter (L)
L_i	Thickness of material i (L)
ℓ	Slab half-thickness (L)
m	Media factor (dimensionless)
N	Intensity of transmitted beam (dimensionless)
N_o	Intensity of incident beam (dimensionless)
N_p	Intensity of beam transmitted through empty sludge column (dimensionless)
n	Recorded counting rate (t^{-1})
n_o	True counting rate (t^{-1})
P	Pressure at time t ($ML^{-1}t^{-2}$)
P_c	Reference pressure at R_c ($ML^{-1}t^{-2}$)
ΔP	Pressure drop ($ML^{-1}t^{-2}$)
p_a	Partial pressure of component a ($ML^{-1}t^{-2}$)
p_g	Partial pressure, or vapor pressure of water in main gas stream ($ML^{-1}t^{-2}$)
p_i	Partial pressure, or vapor pressure, of water at interface ($ML^{-1}t^{-2}$)
R	Specific resistance ($M^{-1}t^{2}$)
$\overline{R}$	Average specific resistance ($M^{-1}t^{2}$)
R'	Hydraulic resistance of sludge (L^{-2})
R_c	Reference specific resistance at H_c or P_c ($M^{-1}t^{2}$)
R'_f	Hydraulic resistance of filter (L^{-2})

$R(P)$	Specific resistance as a function of pressure ($M^{-1}t^2$)
R_t	Hydraulic resistance of flow (L^{-1})
R_v	Gas constant for water ($L^2t^{-2}T^{-1}$)
S	Percent solids content (dimensionless)
S_f	Percent final solids (dimensionless)
S_o	Percent initial solids (dimensionless)
T	Temperature (T)
T_a	Dry bulb temperature of air (T)
T_{am}	Mean daily air temperature (T)
T_{dp}	Mean daily dew-point temperature (T)
t	time (t)
t_c	Drying time in constant-rate period (t)
t_f	Drying time in falling-rate period (t)
t_r	Resolving time (t)
U	Average moisture content (dimensionless)
U_{CR}	Critical moisture content (dimensionless)
U_o	Initial moisture content (dimensionless)
U_s	Moisture content at surface (dimensionless)
U_t	Final moisture content (dimensionless)
U_x	Moisture content at a specific location (dimensionless)
V_f	Volume of filtrate (L^3)
V_i	Volume of material i (L^3)
V_t	Total volume of filtrate collected (L^3)
v_c	Volume of cake deposited per unit volume of filtrate (dimensionless)

W_{TS}	Mass of dry solids (M)
W_w	Mass of water (M)
x	Distance (L)
Y	Ratio of N_p to N (dimensionless)
Z	Elevation (L)
z	Distance (L)
z^T	Shield thickness (L)
β	Regression coefficient
Δ	Finite difference
ϵ	Percent error (dimensionless)
μ	Attenuation coefficient ($M^{-1}L^2$)
μ_i	Attenuation coefficient of material i ($M^{-1}L^2$)
ν	Dynamic viscosity ($ML^{-1}t^{-1}$)
ρ	Mass density (ML^{-3})
ρ_b	Bulk density of dry material (ML^{-3})
ρ_v	Mass density of water vapor (ML^{-3})
σ	Standard deviation (statistics)
σ	Coefficient of compressibility (dimensionless)
χ	Mole fraction of component a in liquid phase (dimensionless)
ω	Velocity (Lt^{-1})

CHAPTER I

INTRODUCTION

Problem Background

The collection, treatment, and disposal of water treatment solid residues, or sludge, is one of the most exigent problems in environmental engineering. Population growth combined with increased per capita water demand, stringent drinking water standards, and a concern that water treatment plants set an exemplary example of waste disposal makes the problem even more pressing.

Hudson (1) states that the United States alone uses 150 tons of water per capita annually via public water supplies and 360 tons per capita annually in industry. This is followed by use of coal and oil (4.4 and 3.1 tons per person per year, respectively). Removal of solids constitutes the major treatment of water and sludge from water treatment amounts to more than one million tons per year of dry solids or 15 pounds per year per capita. Most water treatment sludges contain only 1/2 to 6 per cent solids by weight when they are removed from the sedimentation basins; thus the amount of water treatment sludge to be disposed of is some 50,000,000 tons per year.

The majority of water treatment plants in the United States are of three broad classifications: sedimentation, coagulation-sedimentation and water softening. Two waste streams, filter backwash and sludge, may originate at conventional water treatment plants. Filter backwash results from washing sand filters through which relatively

clean water has passed. Eventually the filter becomes clogged (head loss becomes excessive) and the filtering process is terminated. Treated water is generally used to backwash the filter thereby removing debris, chemical precipitates, and small amounts of the filter media. The backwash stream generally comprises 2 to 5% of plant flow, and according to Russelmann (2), is relatively clean, containing 120 to 1500 mg/l of solids. Some plants recycle the washwater, practically eliminating the filter backwash problem. Other plants perform a minimal amount of treatment, or none whatever, before discharge of the backwash to a watercourse. Of the two waste streams emanating from a water treatment plant filter backwash disposal seems to be a lesser problem than sedimentation sludge disposal.

Sludge is produced by sedimentation of particles present in the raw water, by compounds added in the treatment processes to aid sedimentation, and by chemical precipitates formed in water softening processes. Various other types of treatment processes such as ion exchange and microscreening produce waste streams but these problems are less vexing than sludge disposal in that the solids from an ion exchange unit are dissolved while microscreening solids are of low concentration.

The quantity and characteristics of sludge produced by water treatment plants depend on the quality of the raw water, the degree of treatment obtained, the amounts and kinds of chemicals added, and the rate and method of removal of the collected sludge. The quantity of sludge removed may represent from 1/2 to 5% of plant flow. Some of the constituents removed from raw water--and hence found in water treatment sludges--

include sand, silt, organic materials, and plankton. Some of the compounds added in the treatment process include chlorine, alum, iron salts, polyelectrolytes, clay, lime, soda ash, and activated carbon.

The impact of water treatment sludges on receiving watercourse was outlined by Russelmann (2) as follows: (1) Suspended solids may collect and deposit on stream beds clogging gills of fish as well as causing aesthetic problems. (2) Oxygen-demanding substances utilize oxygen needed for fish life and aerobic conditions in the stream. (3) Turbidity and color are aesthetically objectionable and interfere with light transmission for photosynthetic processes. (4) Acids, alkaline materials, and certain ions present in sludge may be directly destructive to plant and animal life.

The ultimate disposal of sludge solids requires their discharge to the atmosphere, ocean, or land. According to Dean (3) organic compounds, which are oxidizable to carbon dioxide, are most amenable to atmospheric disposal. Some water treatment sludges are low in organic material so that their oxidation would leave a substantial fraction of ash for further disposal. For communities near the ocean, direct discharge of the sludge into the ocean may be practicable although serious questions are currently being raised about the prudence of using the oceans as a waste disposal site. For the overwhelming majority of the United States communities water treatment sludge must be disposed of on land. In order to reduce the volume and weight of material handled, removal of water is necessary. Reduction of the volume of water may be carried out by a variety of mechanical and non-mechanical methods. Mechanical methods include

centrifugation, vacuum filtration, pressing, vibration, and artificial freezing and thawing. Non-mechanical methods include compaction and decantation in lagoons, natural freezing and thawing, and sand beds.

Historical Development

The study of the water treatment sludge disposal problem dates back many years. In 1946 the American Water Works Association appointed a committee to study and report on disposal methods from water purification and softening plants. From 1946 to 1953 the sludge disposal problem was studied and reports were made by Aultman (4), Black (5), Haney (6,7), Hall (8), and Dean (9). The report by Dean (9) included the results of a survey which showed that 96% of the 1530 reporting plants discharged sludge to streams or lakes without treatment. Sludge beds or disposal on low ground accounted for 75% of the treatment methods employed.

Water quality standards imposed by the Federal Water Quality Act of 1965, led to more emphasis on the problem of sludge disposal. Recent research studies and reports, however, have concentrated on the problem definition and characterization. A status report was recently published by the American Water Works Association Research Foundation (10) which covered research, engineering, plant operation, and regulatory aspects of the problem. Current technology and cost of disposal methods based on fifteen operating plants were presented. Other recent studies on plant operation and sludge properties have been presented by O'Brien and Gere (11) and Gates and McDermott (12). These reports, prepared for the New

York State Department of Health, give insight to problems occurring at specific plants. Surveys of disposal methods and research trends have been recently presented by Doe (13), Russelmann (2), Gauntlett (14,15, 16), Wertz (17), Mace (18), and Burd (19).

In total, little work has been published on the various sludge disposal methods. Proprietary devices such as centrifuges, vacuum filters, filter presses, freezing apparatus, and vibration devices are being evaluated by the various manufacturers for design criteria but comparison between alternatives still seems to be more of an art than a science. Usually a pilot plant operation can be made before final selection but scale-up methods are not well developed. Field adjustment and modification are often required. The problem is further compounded for the design engineer since no rational design methods exist which would allow comparisons of alternative methods.

Engineers designing facilities for drainage and drying of sludge on sand beds or lagoons for the most cases utilize empirical data derived for specific problems, rule of thumb, or practices from other installations. Even though land increases in value whereas mechanical equipment depreciates, the scarcity of available land in some locations necessitates optimum dewatering bed design. No rational methods exist to delineate the role of each parameter prior to design. Most importantly, engineering and economic comparison of land methods with the various mechanical dewatering methods are virtually impossible due to a lack of rational design criteria. The basic theoretical topics involved--evaporation, drainage, and drying--have been studied separately in fields such as hydrology, civil

engineering, and chemical engineering. To assimilate and supplement the pertinent knowledge that is available into an integrated treatment could provide the desired basis for rational design of land disposal methods.

One factor urgently needed to evaluate the applicability of different models to the sand bed dewatering process is the distribution of moisture within the sludge as dewatering takes place. Traditional sampling methods have either been destructive or unsatisfactory. Drying studies in chemical engineering have utilized samples cut into thin slices with moisture determined by oven drying. The destructive method terminates the experiment. In situ methods determine and correlate with the moisture content, the electrical resistance or temperature within the sample. These methods have usually been unsuccessful. Fortunately, gamma-ray attenuation methods have been used successfully in soil studies, and have most recently been applied to sewage sludge studies by Tang (20). This method offers the advantage of being both accurate and non-destructive.

The basic processes involved in the dewatering of water treatment sludge are filtration, evaporation or drying, and consolidation. The filtration process is one of fluid flow through porous media and has been studied extensively for certain materials such as soil. Recent work on sewage sludge filtration by Sanders (21), O'Brien and Gere (11), and Adrian and Nebiker (22) provides some insight toward the filtration of water treatment sludge. Similarly, evaporation and drying have been studied by various disciplines but applicability toward sludge drying has been limited to sewage sludge studies such as those by Nebiker (23), Quon

and Tamblyn (24), Quon and Ward (25), and Coackley and Allos (26). The fundamental principles of water treatment sludge drainage and drying clearly remains largely undeveloped. Research in this area must be conducted if this deficiency is to be replaced with sound and proven knowledge of both scientific and practical concepts.

Objectives

The objectives of this investigation were varied due to the rudimentary nature of the water treatment sludge problem. The overriding objective was the development of sound sampling and laboratory investigation procedures for determining the dewatering rates of water treatment sludge. Other objectives were to assemble technology from various disciplines that would be of direct benefit to the design engineer. The specific scientific objectives were:

1. To determine the chemical and physical properties of various types of water treatment sludges.
2. To assimilate technology from other disciplines that is applicable to sludge dewatering with particular emphasis on evaporation, drying, and drainage.
3. To develop a non-destructive method for measuring moisture or solids contents in situ.
4. To develop experimental apparatus and methodology for studying sludge dewatering on sand beds.
5. To determine the applicability of some of the more rational sewage sludge dewatering formulas to water treatment sludge.

CHAPTER II

THEORETICAL CONSIDERATIONS

Dewatering of water treatment sludge comprises several basic operations for which the specific role of some is not fully understood. The dewatering process consists of drainage and drying over a wide range of moisture and solids concentrations. Sludge initially at 0.5% solids (99.5% water) undergoing drying and drainage simultaneously may behave as a dilute suspension. Any water lost by evaporation will approximate that of a free water surface, especially if some sedimentation has occurred exposing clear supernatant to the drying atmosphere. Drainage alone may concentrate the sludge to a gelatin-like mass of 5 to 15% solids content in a relatively short time. Drying will further concentrate the sludge causing it to behave like a solid. This stage is accompanied by compression and shrinkage with cracks appearing throughout the sludge cake. Continued drying to equilibrium produces a hard, dry solid with characteristics ranging from those of a dry sand to ceramic. The transition between the various stages is not pronounced and more than one basic mechanism may be present at any one time.

Moisture

Different classifications of moisture and water are used in different disciplines depending upon the particular area of interest. In environmental engineering water content is usually associated with large amounts of water and is defined as the mass of water divided by the total mass (solids plus liquid). Moisture content refers to much smaller

amounts of water and is defined as the mass of water per mass of dry solids. The term water content is convenient during the drainage and early stages of water treatment sludge drying, whereas the term moisture content is more convenient during the later stages of drying. The term solids content is also frequently used in sludge dewatering studies. Solids content is defined as the mass of solids divided by the total mass. Thus solids content plus water content is unity.

There is no agreement on the nomenclature of the various kinds of water involved in the various disciplines. According to Spangler (27) one method of classification is the Briggs classification of soil water. Each class of water is referred to according to the kind of force primarily controlling its movement. The three types are:

1. Hygroscopic water - water tightly adhering to solid particles in thin films and can be removed only as a vapor.
2. Capillary water - water which is held by cohesion as a continuous film around the soil particles and in the capillary spaces.
3. Gravitational water - water which exists in large pores of soil and which the force of gravity will remove from the soil when conditions for free drainage exist.

Chemical engineering literature usually refers to four types of moisture. The four types as listed by Treybal (28) are:

1. Bound moisture - moisture contained by a substance which exerts an equilibrium vapor pressure less than that of the pure liquid at the same temperature.

2. Unbound moisture - moisture contained by a substance which exerts an equilibrium vapor pressure equal to that of the pure liquid at the same temperature.

3. Equilibrium moisture - the moisture content of a substance when at equilibrium with a given partial pressure of the vapor.

4. Free moisture - that moisture contained by a substance in excess of the equilibrium moisture.

These relationships are shown in Figure 1 for a material exposed to an atmosphere of relative humidity A. Bound water may exist in several conditions. Liquid water in fine capillaries exerts an abnormally low vapor pressure because of the highly concave curvature at the surface. Bound moisture in cell or fiber walls may have a lower vapor pressure due to dissolved solids. Bound water in many substances is both in physical and chemical combination, the nature and strength of which vary with the nature and moisture content of the solid. Unbound water, however, exerts its full vapor pressure and is largely held in the voids of the solid. McCabe and Smith (29) state that the distinction between bound and unbound water depends on the material itself, while the distinction between free and equilibrium moisture depends on the drying conditions.

Evaporation of Water

Differentiation of evaporation from drying is difficult. The term drying usually refers to the removal of relatively small amounts of water from solid or nearly solid material. According to Badger and Banchero (30), the term evaporation is usually limited to the removal of relatively large amounts of water from solutions. Exhaustive studies

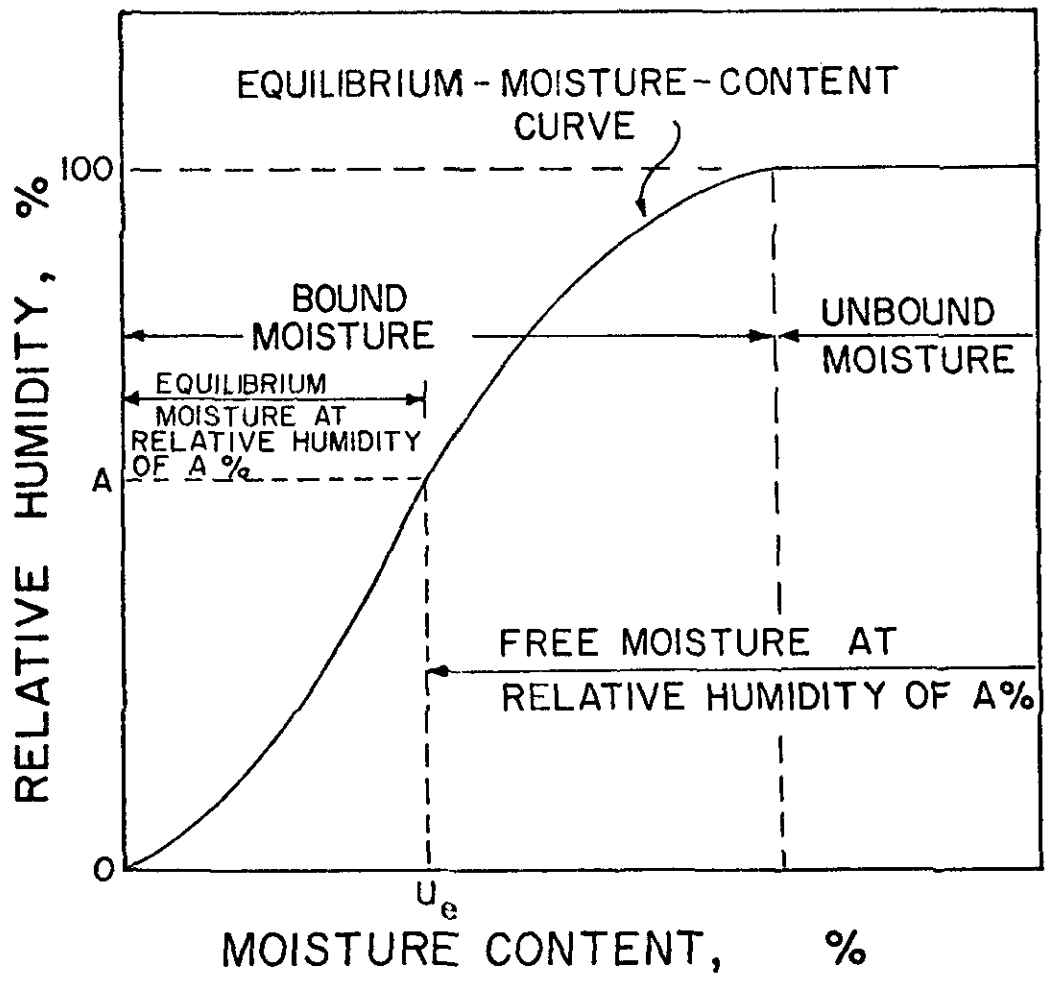

FIGURE 1 -- Types of Moisture (Reference 28)

on evaporation have been conducted by engineers and hydrologists but a complete review is beyond the scope of this investigation. Only some pertinent terminology and principles that may have application to sludge dewatering will be presented here.

A net input of thermal energy to a flat free-water surface increases the free (kinetic) energy of the water molecules to the point where some are able to escape across the liquid-gas interface. The amount of heat absorbed by a unit mass of water, while passing from the liquid to the vapor state at constant temperature, is called the latent heat of evaporation or latent heat of vaporation (31). Molecules of water that leave the liquid surface cannot re-enter readily due to the decrease in kinetic energy. Under equilibrium conditions water vapor may be treated as an ideal gas yielding the following equation:

$$p_i = \rho_v R_v T \qquad (1)$$

where p_i = partial pressure of water vapor $(ML^{-1}t^{-2})$

ρ_v = mass density of water vapor (ML^{-3})

R_v = gas constant for water $(L^2t^{-2}T^{-1})$

T = absolute temperature (T)

Further vaporization causes a continued increase in p in the air above the liquid until condensation begins. When the rate of condensation and the rate of vaporization become equal, the air is saturated with vapor, and molecules are crossing the interface in both directions at the same rate. The partial pressure of the vapor in the air at which this equilibrium takes place is known as the saturation vapor pressure, or simply the vapor pressure of the liquid. This vapor pressure is an increasing

function of the liquid temperature. Equilibrium never exists under natural conditions since the volume of air into which vaporization takes place is essentially infinite. Also, various convective transport processes will operate to transport the vapor both parallel and perpendicular to the liquid surface, thus preventing equilibrium from occurring.

Laboratory studies on evaporation from free water surfaces have been reported by many investigators in various disciplines. Buelter et al. (32) presented the following empirical equation for evaporation rate into a quiescent atmosphere which was produced under laboratory conditions:

$$E_w = K_e(p_i - p_g) \qquad (2)$$

where E_w = evaporation flux rate ($ML^{-1}t^{-3}$)

K_e = evaporation transfer coefficient (t^{-1})

P_i = partial pressure of water at interface ($ML^{-1}t^{-2}$)

P_g = partial pressure of water in main gas stream ($ML^{-1}t^{-2}$)

The value of K is 0.054 when pressures are reported in inches of mercury. Equation 2 is inadequate to explain the evaporation mechanism under normal conditions since quiescent conditions seldom occur.

When evaporation is taking place from a free-water surface, it is helpful to assume that a thin film of vapor saturated air forms adjacent to the water surface. The film temperature is assumed to be the temperature of water. Whenever the saturation vapor pressure at film temperature is greater than the partial pressure of the water vapor in the air immediately above the film, a gradient in vapor pressure

will exist and the evaporation function may be written as

$$E_r = - K \frac{dp_g}{dZ} \tag{3}$$

where E_r = evaporation rate (Lt^{-1})

Z = elevation (L)

K = transfer coefficient ($M^{-1}L^3t$)

The dependence of E_r upon total atmospheric pressure and salinity as well as upon temperature is implied through variation of p_g with these variables. The presence of wind will have a major effect on E_r, since by convection it will remove the vapor-laden air, thereby keeping the film thin and maintaining a high transfer rate. Other factors influencing the evaporation rate, either directly or indirectly, are solar radiation, air temperature, and vapor pressure.

The depression of the evaporation rate due to salinity or dissolved solids can be formulated by Henry's law which may be written as

$$p_a = C_h \chi \tag{4}$$

where p_a = partial pressure of component a ($ML^{-1}t^{-2}$)

C_h = Henry's law constant ($ML^{-1}t^{-2}$)

χ = mole fraction of component a in liquid phase (dimensionless).

Since χ is defined as the ratio of moles of component a (in this case water) to the total moles, a dilute solution will exert a higher vapor pressure and the driving force ($p_i - p_g$) in Equation 2 will approach the maximum (that of pure water). For increasing values of χ (dense

solutions), the driving force decreases, hence the evaporation rate decreases.

According to Eagleson (31) there are two fundamental approaches to the theoretical study of evaporation from a freewater surface. The diffusion method involves a mass-transfer process by which vapor is removed from the liquid surface. The energy-balance method involves determining an average rate of water loss by evaporation over a given time interval. Penman (33) first utilized the best features of both of the theoretical approaches in order to derive a water-surface evaporation relation which is dependent upon a limited number of fairly easily measured meteorological variables. Kohler et al. (34) further developed Penman's model to obtain an equation correlating the appropriate meteorological variables which allows prediction of daily water surface evaporation. The analytical form of this model is

$$E_r = \frac{\exp[(T_{am}-212)\ (0.1024-0.01066\ \ln I_n)]\ \ 10^{-4} + 0.0105\ \Delta p^{0.88}(0.37+0.0041\omega)}{0.015 + (T_{am} + 398.36)^{-2}\ (6.8554)\ 10^{10}\ \exp[-74826 / (T_{am} + 398.36)]} \qquad (5)$$

where

$$\Delta p = (6.41326)\ 10^{6}\ [\exp(- \frac{7482.6}{T_{am}+398.36}) - \exp (- \frac{7482.6}{T_{dp}+398.36})] \qquad (6)$$

where E_r = free-water evaporation, in. day^{-1} (Lt^{-1})

T_{am} = mean daily air temperature, °F (T)

T_{dp} = mean daily dew point temperature, °F (T)

I_n = net intensity of solar radiation, Langleys/day (Mt^{-3})

ω = wind movement at Z = 2 ft., miles day^{-1} (Lt^{-1})

The graphical form of Equations 5 and 6 is shown as Figure 2.

In order to apply Equations 5 and 6 or Figure 2, to natural water bodies, adjustments must be made for advected energy and for changes in heat storage. This adjustment is in the form of a pan coefficient which is the ratio of the rate of evaporation in a pan of water to the rate of evaporation in a large body of water. Pans of water are used for routine measurements due to the difficulty in making measurements on a natural body of water. Measurements are somewhat simplified by using a standard circular pan which may be installed on the ground (land pan) or in the water (floating pan). A U.S. Weather Bureau Class A pan is the most widely used and measures 4 ft. in diameter and 10 in. deep (inside dimensions). Conversion of the pan values to natural-water surface values is difficult since temperature of the small volume of water in the pan more closely follows air temperatures than does a moderate-sized natural body of water. The evaporation rate in a pan will be correspondingly higher; consequently, results of these experiments must be reduced by a factor less than unity known as the pan coefficient. The average coefficient for the land pan is about 0.7 and for the floating pan, 0.8. Complete instructions for making these measurements are given by the U.S. Weather Bureau (35).

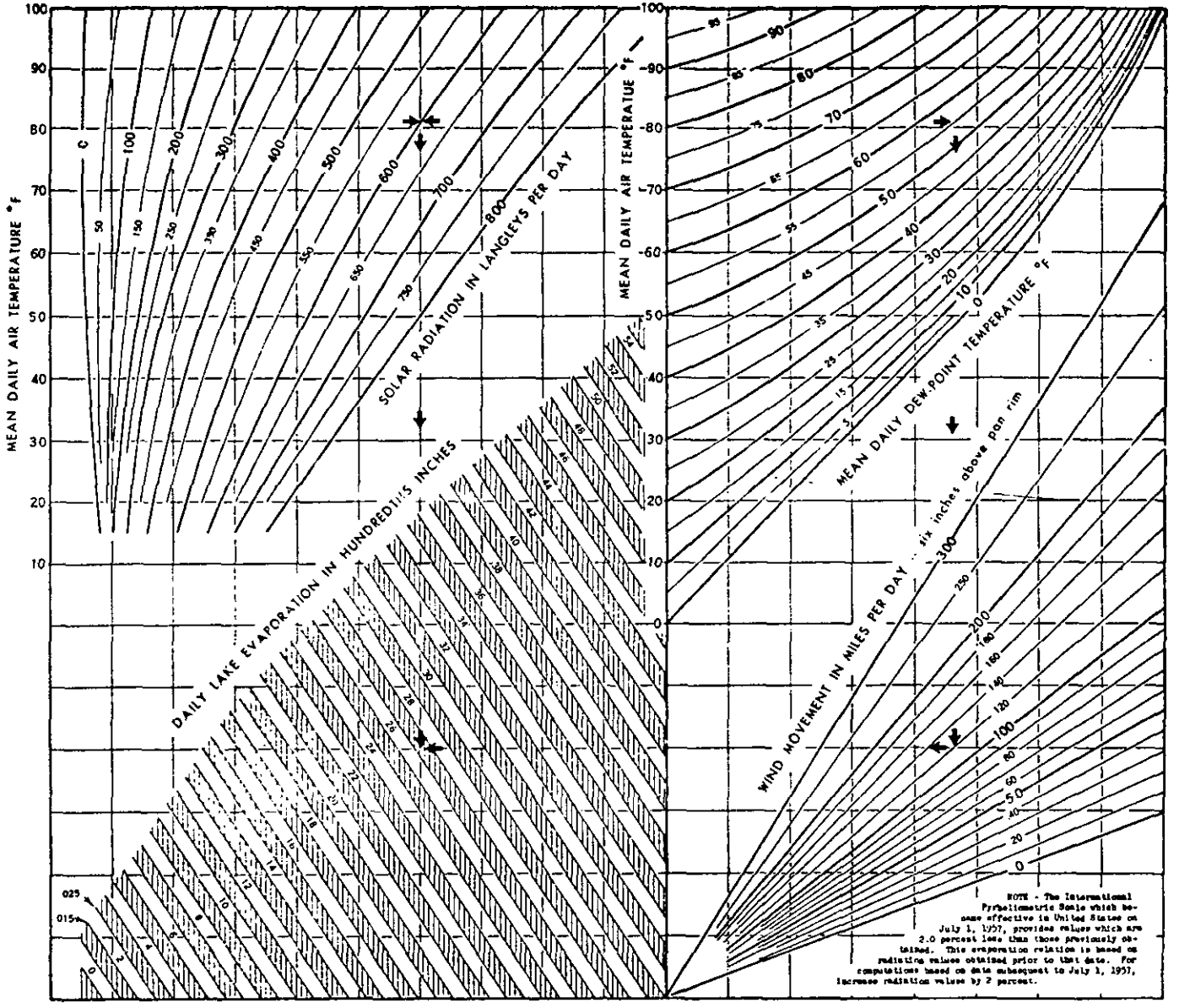

FIGURE 2 -- An Empirical Water-Surface-Evaporation Relation Assuming No Change in Heat Storage (Reference 36).

Average annual evaporation rates for lakes in the United States have been complied by the U.S. Weather Bureau. The average annual lake evaporation, in inches, for the period 1946-1955 is presented in Figure 3 as taken from Kohler et al. (36).

Drying

When a solid dries, two fundamental and simultaneous processes occur. These are transfer of heat to evaporate liquid and transfer of mass as internal moisture and evaporated liquid. Drying of solids encompasses two different types of solids, porous and nonporous. It is customary to assume that a drying solid is either porous or nonporous. Although McCabe and Smith (29) state that most solids are intermediate between the two extremes. Either type may also be hygroscopic or non-hygroscopic. The drying of a solid may be studied from the standpoint of how the drying rate varies with external conditions such as temperature and humidity or with changes in the moisture in the interior of the solid. Internal liquid flow may occur by several mechanisms, depending on the structure of the solid. Some of the possible mechanisms as listed by Marshall and Friedman (37) are as follows: (1) diffusion in continuous homogeneous solids, (2) capillary flow in granular or porous solids, (3) flow caused by shrinkage and pressure gradients, (4) flow caused by gravity, and (5) flow caused by a vaporization-condensation sequence. In general, one mechanism predominates at a given time in a solid during drying and it is not uncommon to find different mechanisms predominating at different times during the drying cycle.

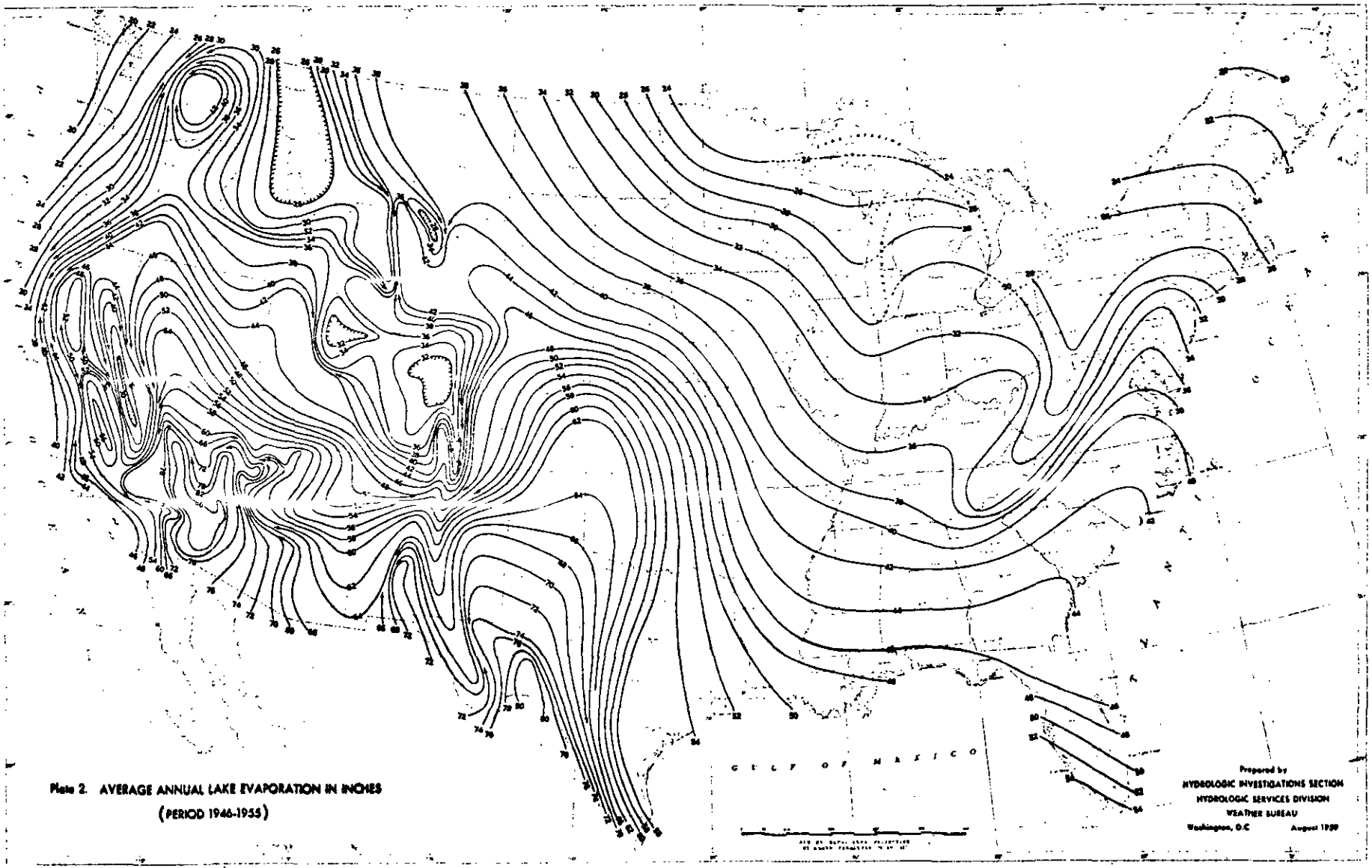

FIGURE 3 -- Mean Annual Evaporation (inches) from Shallow Lakes and Reservoirs (Reference 36).

Drying theories vary somewhat, however the theories presented by Sherwood (38, 39) are generally accepted and their applicability toward sludge drying will be briefly reviewed.

The intial stages of water treatment sludge drying would be expected to approximate that of a free water surface. Ample water is available for evaporation as some sedimentation may take place. It is not uncommon to see relatively clear supernatant on some types of water treatment sludges. As drying continues the volume changes in proportion to the amount of water lost. A thin film of water at the surface is replenished from within as fast as it can evaporate. Eventually a solid cake forms and the internal resistance to moisture movement becomes large enough that the rate of replenishing the water at the surface is less than the rate the air can absorb it. The moisture content at which this occurs is called the first critical moisture content.

Additional drying continues at the solid surface but at a decreased rate. This is known as the falling-rate period. The zone of evaporation may gradually move into the sludge mass; into the pores in any cracks that develop, with the rate of vapor transport through the empty pores becoming a major factor. A second critical moisture content is often reached at which evaporation takes place solely within the interior of the solid. At this point and beyond, internal resistance is large and resistance to evaporation from the surface of the solid is small. Some water such as hygroscopic water and hydrate water cannot be removed at atmospheric temperature even though the solid may be considered to be dry. Significant elevation of temperature is required to remove this moisture. During the falling rate drying period the rate may be

determined either by the resistance to water removal at the surface or by the resistance to moisture movement within the material. A plot of drying rate versus moisture content for the falling rate period will vary significantly with different materials.

Sherwood (40) presented drying curves for various substances as shown in Figure 4. Curve A is for porous ceramic plate and follows the drying process as described above. Curve B represents the drying-rate curve obtained in the drying of soap and wood. This case is typical where internal diffusion controls throughout the falling-rate period. Curves C and D represent drying-rate curves which may be obtained in cases where vapor removal is largely controlling throughout the falling-rate period. Curve C is for sulfite pulp slab. Curve D represents the drying of newsprint, bond, or blotting papers, where vapor removal and not internal diffusion controls the drying.

Diffusion of Moisture

Drying of nonporous solids such as soap, glue and plastic clay have been described by diffusion. These substances are essentially colloidal gels of solids and water which retain considerable amounts of bound water.

Sherwood (41), Newman (42) and Luikov (43) studied the movement of moisture during the drying process for various drying conditions and materials. The general flux equation for moisture movement can be presented as

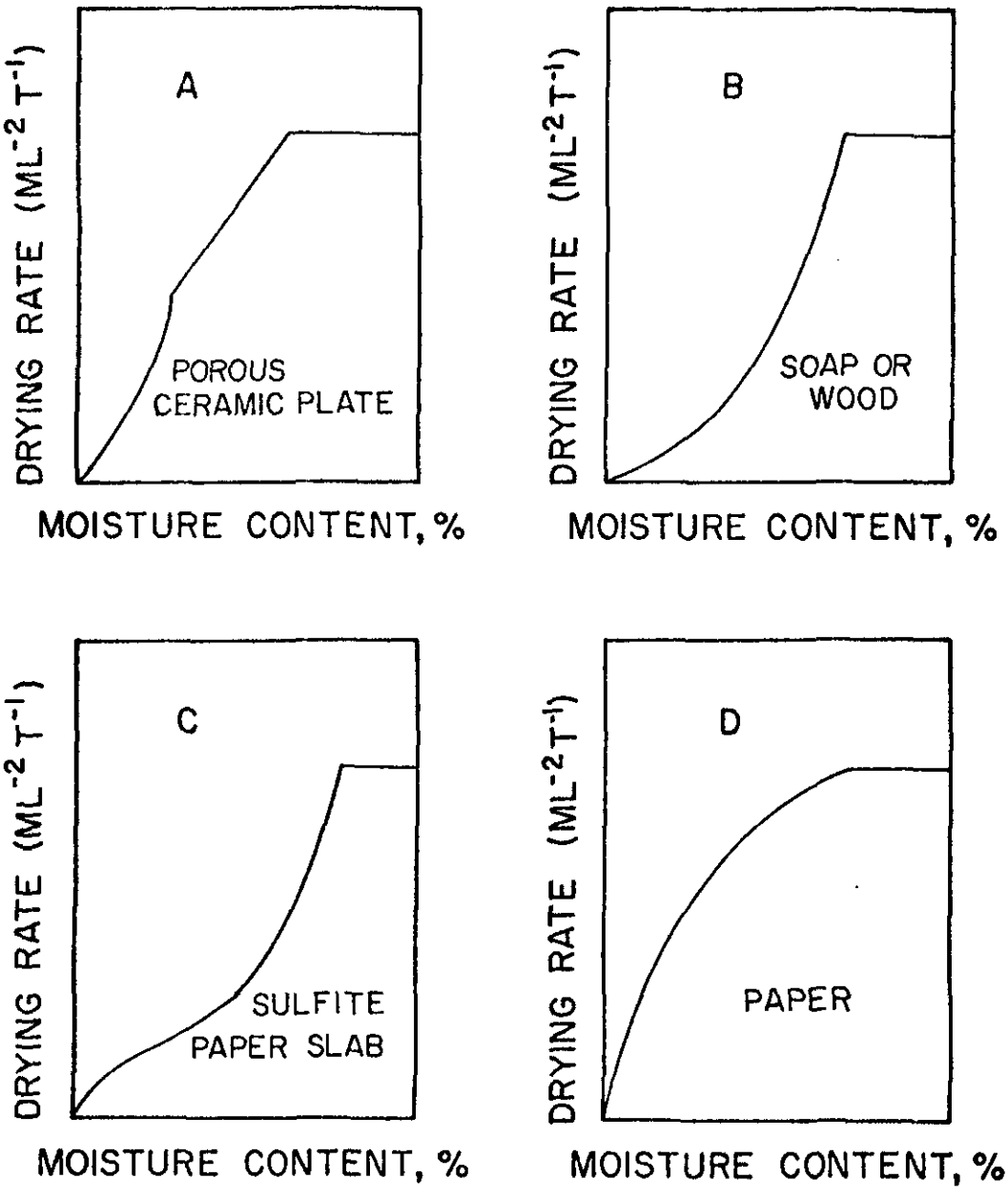

FIGURE 4 -- Drying Curves for Various Substances (Reference 40).

$$I = -\frac{1}{A}\frac{dW_w}{dt} = D\rho\frac{\partial U}{\partial x} \qquad (7)$$

where I = drying rate ($ML^{-2}t^{-1}$)

A = area (L^2)

W_w = mass of water (M)

t = time (t)

D = constant diffusion coefficient (L^2t^{-1})

ρ = density (ML^{-3})

U = average moisture content (dimensionless)

x = distance (L)

The general partial differential equation for variation in moisture content with time for unidirectional flow is given by the diffusion equation

$$\frac{\partial U}{\partial t} = D\frac{\partial^2 U}{\partial x^2} \qquad (8)$$

The solutions of Equation 8 for several boundary and initial conditions have been presented by Carslaw and Jaeger (44), Crank (45), and Ozisik (46). All solutions assume a slab of thickness 2ℓ drying from both surfaces, where shrinkage is negligible, the diffusion coefficient is a constant, and all moisture is subject to diffusion. Two common cases encountered in the drying literature are cited. When the initial moisture content U_o, is uniform and where the surface moisture content, U_s, is constant, a solution of Equation 8 is given by Equation 9. When the rate of drying at the surface is constant, I_c, and the initial moisture content, U_o, is uniform, the solution of Equation 8, given by Gilliland and Sherwood (47), is Equation 10.

$$\frac{U-U_s}{U_o-U_s} = \frac{4}{\pi}\left\{\left[\cos\frac{\pi x}{2\ell}\ \exp\left[-Dt\left(\frac{\pi}{2\ell}\right)^2\right]-\frac{1}{3}\cos\frac{3\pi x}{2\ell}\right.\right.$$
$$\exp\left[-9Dt\left(\frac{\pi}{2\ell}\right)^2\right]+\frac{1}{5}\cos\frac{5\pi x}{2\ell}$$
$$\left.\left.\exp\left[-25Dt\left(\frac{\pi}{2\ell}\right)^2\right]\ .\ .\ .\ .\right\}\right. \qquad (9)$$

$$(U_o-U)\left(\frac{D\rho}{I_c\ell}\right) = \left[\left(\frac{x-\ell}{2\ell^2}\right) - \frac{1}{6} + \frac{Dt}{\ell^2} - \frac{2}{\pi^2}\right.$$
$$\sum_1^{\infty}\frac{(-1)^n}{n}\ \exp\left(-n^2\pi^2\ \frac{Dt}{\ell^2}\right)$$
$$\left.\cos-n\pi\ \frac{(x-\ell)}{\ell}\right] \qquad (10)$$

The main limitations to describing moisture movement by diffusion during drying are the assumptions of constant diffusion coefficient and negligible shrinkage (constant thickness). Hougen et al. (48) and Ceaglske and Hougen (49) found that diffusivity varied with moisture content for various solids such as paper pulp and sand. Variable diffusivities for wood and other building materials are also reported by Luikov (43).

If diffusivity is a function of the moisture content, the moisture transport rate may be written

$$\text{Moisture Flux Rate} = -D(U)\frac{\partial U}{\partial x} \qquad (11)$$

which, when combined into a conservation of mass equation, yields

$$\frac{\partial U}{\partial t} = \frac{\partial}{\partial x}\ \left[D(U)\ \frac{\partial U}{\partial x}\ \right] \qquad (12)$$

as the concentration dependent diffusion equation. The variation of the diffusion coefficient with moisture content must be evaluated from experimental data.

Drying-Rate Studies

The drying-rate approach presents a less fundamental study of internal moisture conditions, however it is experimentally straightforward and its application is insensitive to problems of shrinkage.

The drying-rate method makes calculations of drying times straightforward. Drying studies can often be conducted under conditions identical to those the materials will be exposed to during actual processing. Moisture-time curves can be constructed requiring only an initial moisture content measurement and measurements of the loss of water at various times. The time to dry the material to any desired moisture concentration can then be read from the moisture-time directly. Such a curve is shown in Figure 5. Note that the sludge mass-time curve is the only experimental curve, the others being constructed from the data. The general case involves predicting drying times for materials under a variety of drying conditions only a few of which need be simulated in the laboratory.

The evaporation of unbound moisture from a solid exposed to constant drying conditions has been explained by Treybal (28). Since evaporation of moisture absorbs latent heat, the liquid surface will come to and remain at an equilibrium temperature such that the rate of heat flow from the surroundings to the surface equals the rate of heat absorption. If the solid and liquid surface are at a different temperature than the surroundings, the evaporation rate will vary until equilibrium conditions are reached as shown by points A and B. The vapor pressure at the surface thereafter remains constant causing

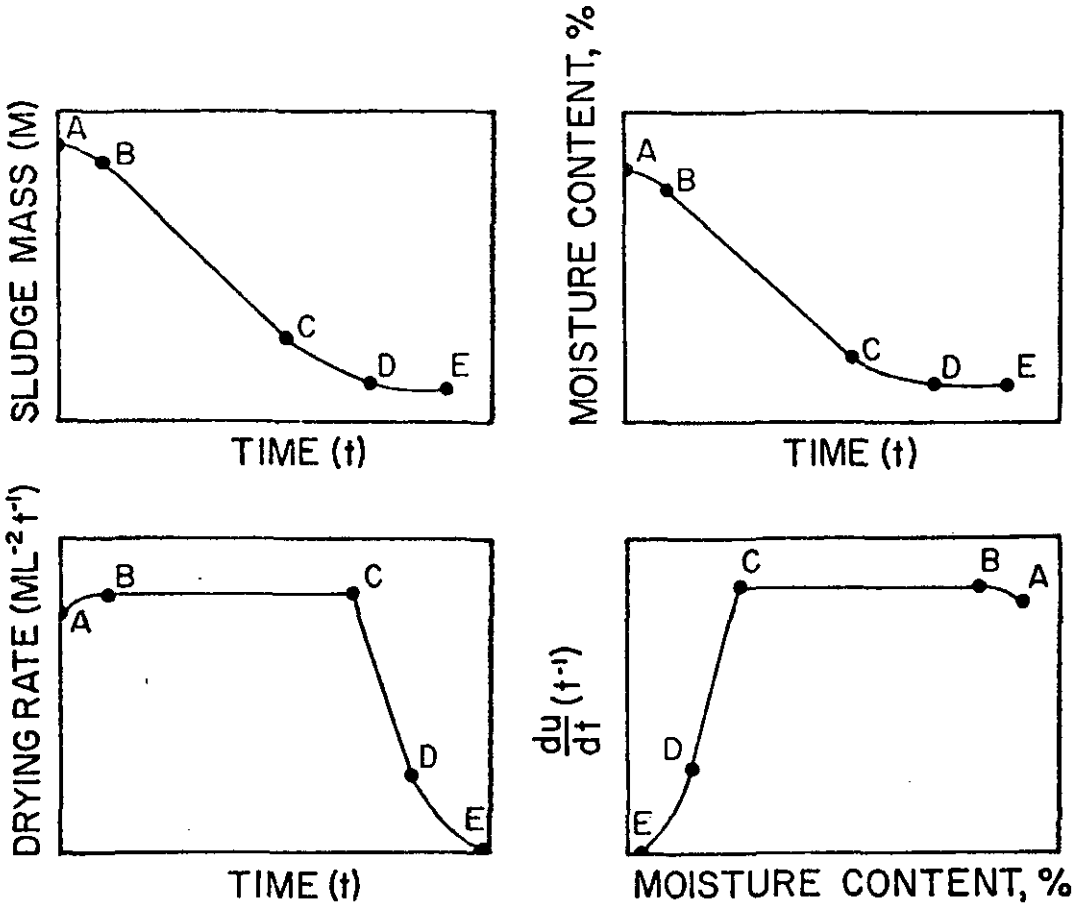

FIGURE 5 -- Typical Drying Relations for Batch Drying with Constant Drying Conditions

the rate of evaporation to remain constant. This period is the constant-rate drying period previously described and shown between points B and C.

When the average moisture content reaches the first critical moisture content (point C), the surface film of moisture is so reduced by evaporation that dry spots appear upon the surface. This gives rise to the first falling-rate period (point C to point D). The moisture content at point D is the second critical moisture content and the second falling-rate period is shown between points C and D. The moisture content at point E is the equilibrium moisture content and is the minimum moisture content obtained under this drying condition.

This method was used by Nebiker (23) to describe the drying of digested sewage sludges on open air drying beds. Since the expression for moisture content is

$$U = 100\frac{W_w}{W_{TS}} \tag{13}$$

where W_{TS} = mass of dry solids (M)

the rate of drying is

$$I = -\frac{dW_w}{Adt} = -\frac{W_{TS}}{100\ A}\ \frac{dU}{dt} \tag{14}$$

Rearranging and integrating over the time interval while the moisture content changes from its initial value U_o to its final value U_t,

$$t = \frac{W_{TS}}{100\ A}\int_{U_t}^{U_o}\frac{dU}{I} \tag{15}$$

If the drying takes place entirely in the constant rate period so that U_o and $U_t > U_{CR}$ and $I = I_c$, Equation 15 becomes

$$t = \frac{W_{TS}}{100A\ I_c} \quad (U_o - U_t) \tag{16}$$

$$(U_o > U_t \geq U_{CR})$$

If the entire falling rate period is taken as a straight line then

$$I_f = I_c \ \frac{(U_t - U_e)}{(U_{CR} - U_e)} \tag{17}$$

$$(U_{CR} > U_t > U_e)$$

where U_e = equilibrium moisture content (dimensionless).

I_f = drying rate in falling-rate period ($ML^{-2}t^{-1}$)

Upon substitution of Equation 17 into Equation 15 and using an upper integration limit of U_{CR}, the following is derived:

$$t_f = \frac{W_{TS}(U_{CR} - U_e)}{A\ I_c\ 100} \quad \ln \ \frac{(U_{CR} - U_e)}{(U_t - U_e)} \tag{18}$$

where t_f = drying time in falling-rate period (t).

If the equilibrium moisture content is negligibly small, Equation 18 may be written as

$$t_f = \frac{W_{TS}}{A\ I_c} \quad \frac{U_{CR}}{100} \ \ln \ \frac{(U_{CR})}{U_t} \tag{19}$$

$$(U_{CR} > U_t > U_e)$$

For a material drying in both the constant and falling rate periods, the total drying time would be

$$t = t_c + t_f$$

$$= \frac{W_{TS}}{A\ I_c\ 100} \left[U_o - U_{CR} + U_{CR} \ln \frac{(U_{CR})}{U_t} \right] \qquad (20)$$

$$(U_o \geq U_{CR} \geq U_t).$$

where t_c = drying time in constant-rate period (t).

Critical Moisture Content

The importance of the first critical moisture content is evident from inspection of the previous equations. Most of the relationships to predict the critical moisture content were derived using the diffusion method of moisture movement in the interior of the solid. Methods to calculate the critical moisture content have been presented by Sherwood and Gilliland (50), Luikov (43), and Broughton (51).

Broughton (51) derived a relationship for the critical moisture content on the assumption that the surface-free moisture concentration at the critical point is dependent on the nature of the material but not the drying conditions. If the constant-rate period is long enough the steady state is achieved and Equation 8 results in a parabolic moisture distribution across the slab as shown in Figure 6, the equation for which is

$$\frac{U_m - U}{U_m - U_s} = \frac{(x - \ell)^2}{\ell^2} \qquad (21)$$

where U_s = moisture content at the surface (dimensionless)

U_m = moisture content at the midplane (dimensionless).

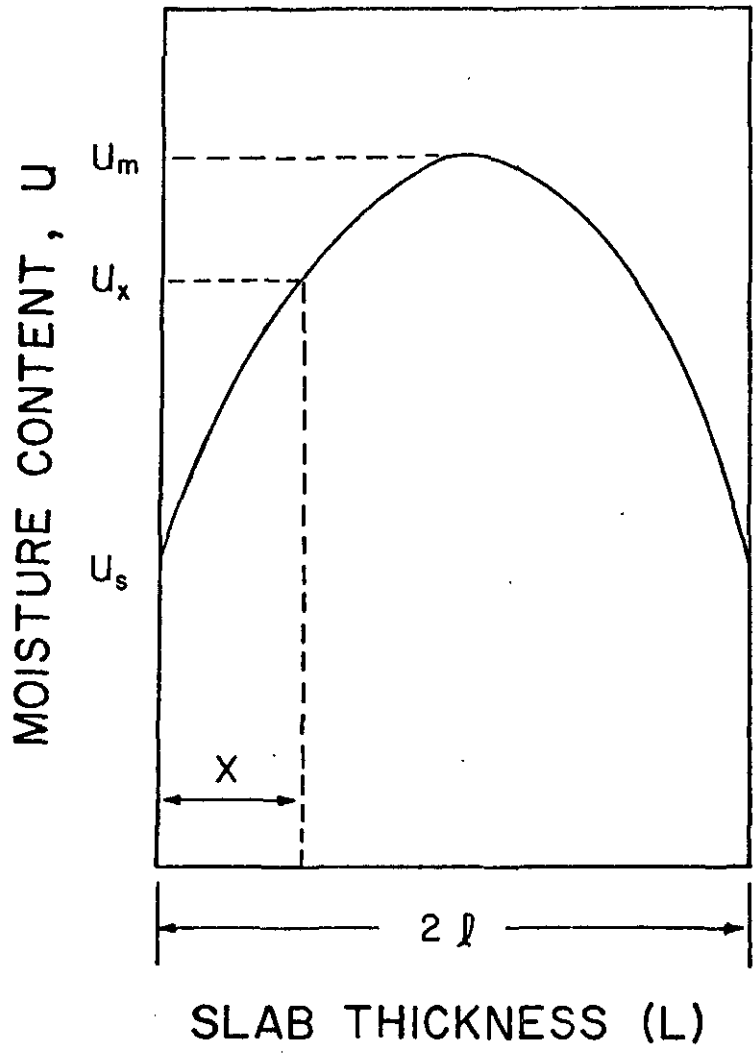

FIGURE 6 -- Moisture Distribution in a Slab Drying at Steady State Conditions (Reference 51).

Differentiating and substituting x = o and x = 2ℓ gives gradients at the surface as

$$\left(\frac{dU}{dx}\right)_s = \pm \frac{2(U_m - U_s)}{\ell} \tag{22}$$

At any time U can be determined from Equation 23,

$$U = \frac{1}{\ell} \int_0^{\ell} U_x \, dx \tag{23}$$

where U_x = moisture content at a specific location (dimensionless). Substituting U from Equation 23 and integrating,

$$U - U_s = \frac{2}{3} (U_m - U_s) \tag{24}$$

Equations 7, 22, and 24 may be combined to give

$$\ell\rho \frac{dU}{dT} = \frac{3D(U - U_s)}{\ell} \tag{25}$$

which when rearranged results in

$$U_{CR} = U_s + \frac{I_c \ell}{3\rho D} \tag{26}$$

where I_c = the constant drying rate ($ML^{-2}t^{-1}$).

The diffusion coefficient, D, would be expected to depend on the nature of the material and the viscosity of the liquid. Assuming that D varies inversely as the viscosity and using the fact that the variation of viscosity of water is practically linear with temperature

$$D = \frac{K_1}{\nu} = K_1(a+b\ T_a) \tag{27}$$

where ν = dynamic viscosity ($ML^{-1}t^{-1}$)

K_1 = constant (MLt^{-2})

a = constant ($M^{-1}Lt$)

b = constant ($M^{-1}Lt\ T^{-1}$)

T_a = dry bulb temperature (T)

Using the dry bulb temperature of the air and substituting for D in Equation 26,

$$U_{CR} = U_s + \left(\frac{\ell}{3\rho K_1}\right) \quad \left(\frac{I_c}{(a+b\ T_a)}\right) \tag{28}$$

For some materials of given thickness the term ($\ell/3\ \rho K_1$) is constant, therefore a plot of U_{CR} versus $I/(a+b\ T_a)$ can be fitted with a straight line with intercept U_{sc} and slope $\ell/3\rho K_1$. Values of a and b may be taken from viscosity data on water in their temperature range. Good fits were reported for various types of clay using this method.

The main limitations to Equation 28 are the assumptions of diffusion mechanism and no shrinkage. The applicability of Equation 28 to predicting the critical moisture content in water treatment sludge drying is questionable.

Nebiker (23) simplified the above procedure by assuming thickness to be a function of the mass of solids, allowing Equation 26 to be expressed as

$$U_{CR} = f\ (I_c, W_{TS}/A) \tag{29}$$

Nebiker also assumed a constant diffusivity and a negligible equilibrium moisture content. For open-air drying of wastewater sludges the following empirical equation was developed from Equation 29.

$$U_{CR} = 500 \ (I_c \cdot W_{TS} \ / \ A)^{1/2} \qquad (30)$$

Values of U_{CR} from Equation 30 when used with Equation 20 gave calculated drying times which compared favorably with actual drying times.

Drainage Theory

Drainage is an important factor in the dewatering of wastewater treatment sludge on sand beds. Drainage may concentrate a sludge considerably representing savings in overall dewatering bed costs.

Drainage of sludges has not been studied to the extent of drainage and fluid flow in other non-compressible materials. Despite much research on gravity dewatering dating back over fifty years, there exists few formulations equating dewatering rates to inherent sludge characteristics. Early research on the drainage characteristics of sewage sludges by Haseltine (52) was of an empirical nature where the gross bed loading ($ML^{-2}t^{-1}$) was a function of the solids content of the sludge. Other work by Jeffery (53) gave an exponential formula from pilot-plant data. More complete reviews of drainage theories have been presented by Adrian et al. (54) and Sanders (21).

The concept of specific resistance holds promise as a basis for development of a model to describe the drainage of water and wastewater sludge. Work by Carmen (55,56,57) which was later refined by

Coackley and Jones (58) has proven adequate in describing dewatering of a compressible material by means of a vacuum filtration unit.

The specific resistance concept has been utilized by Sanders (21) and Adrian and Nebiker (22) to describe the gravity drainage of sewage sludges over most of the drainage period. This seems to be a logical extension of the methods developed for vacuum filters since a major difference between the two methods is a constant pressure is applied to the sludge in vacuum filtration while in dewatering by gravity there is a continually decreasing pressure or head applied to the sludge.

The Hagen-Poiseuille equation has been the basis for drainage models for sewage sludge on sand beds. The basic equation is written as:

$$\Delta P = \frac{32 L \omega \nu}{d^2} \tag{31}$$

where ΔP = pressure drop $(ML^{-1}t^{-2})$

L = length (L)

ω = velocity (Lt^{-1})

ν = viscosity $(ML^{-1}t^{-1})$

d = diameter (L)

The velocity ω may be written as

$$\omega = \frac{1}{A} \frac{dV_f}{dt} \tag{32}$$

where V_f = volume of fi trate (L^3)

A = cross-sectional area of flow (L^2)

t = time (t)

Therefore Equation 32 may be written as

$$\frac{dV_f}{dt} = \frac{Ad^2\Delta P}{32L\nu} = \frac{A\ \Delta P}{R_t\nu} \tag{33}$$

where R_t = hydraulic resistance to flow (L^{-1})

The pressure drop ΔP may be written as

$$\Delta P = \rho g\ H \tag{34}$$

where ρ = mass density (ML^{-3})

g = acceleration due to gravity (LT^{-2})

H = hydraulic head at time t (L)

Substituting Equation 34 into Equation 33, the resulting equation is

$$\frac{dV_f}{dt} = \frac{A\ \rho g\ H}{R_t\nu} \tag{35}$$

The resistance R_t may be thought of as the sum of the resistance of the cake and supporting media, thus

$$R_t = L_s\ R' + L_f\ R'_f \tag{36}$$

where R' = hydraulic resistance of sludge (L^{-2})

R'_f = hydraulic resistance of filter (L^{-2})

L_f = thickness of filter (L)

L_s = thickness of sludge (L)

Substituting Equation 36 into Equation 35, the resulting equation is

$$\frac{dV_f}{dt} = \frac{Ag\,\rho\,H}{(R'L_s+R_f' L_f)\nu} \tag{37}$$

Equation 37 is the basis for work done by Coackley and Jones (57) as previously mentioned. Carmen (55,56,57) introduced the concept that the thickness of the compressible filter cake L_s is proportional to the volume of filtrate:

$$L_s = v_c \; V_f / A \tag{38}$$

where v_c = volume of cake deposited per unit volume of filtrate (dimensionless).

Due to the difficulty of measuring the volume of a compressible cake, weight is measured instead and the filter resistance can then be defined using the relationship

$$v_c R' = c\,R \tag{39}$$

where c = weight of dry cake solids per unit volume $(ML^{-2}t^{-2})$

R = specific resistance $(M^{-1}t^{2})$

Substitution of Equations 38 and 39 into Equation 37 results in the following

$$\frac{dV_f}{dt} = \frac{\rho\,g\,H\,A}{\nu\,(cRV + AL_fR_f')} \tag{40}$$

The term dV_f/dt may be written in terms of the head as the rate of drop of the sludge surface by drainage:

$$\frac{dV_f}{dt} = -A \frac{dH}{dt} \tag{41}$$

The terms referring to the resistance of the supporting media are usually small compared to the resistance of the sludge and may be ignored. The term R is the specific resistance of the sludge cake which forms and has been found to vary with pressure and may be simplified as:

$$R = R_c \left(\frac{H}{H_c}\right)^{\sigma} \tag{42}$$

where R_c = reference specific resistance at H_c $(M^{-1}t^2)$

H_c = reference head (L)

σ = coefficient of compressibility (dimensionless).

The term c in Equation 39 is the weight of dry cake solids deposited per unit volume of filtrate. This is expressed in terms of the initial and final solids content, S_o and S_f (both percent wet basis) as

$$c = \frac{\rho g}{\frac{100}{S_o} - \frac{100}{S_f}} \tag{43}$$

where S_o = percent initial solids (dimensionless)

S_f = percent final solids (dimensionless).

Since S_f is usually an order of magnitude larger than S_o for wastewater sludges, Equation 43 may be expressed as

$$c = \frac{\rho g S_o}{100} \tag{44}$$

The accumulated volume of filtrate is

$$V_f = A(H_o - H) \tag{45}$$

where H_o = initial hydraulic head (L).

Combining Equations 40,42, 43, and 45 and rearranging, the resultant equation is

$$\frac{dH}{dt} = \frac{100\ \rho\ g\ H}{\nu\ R_c(\frac{H}{H_c})^{\sigma}\ \ g\ S_o\ (H_o - H)} \tag{46}$$

Integrating Equation 46 from $H = H_o$ at $t = 0$ gives

$$t = \frac{S_o \nu\ R_c}{100 H_c^{\sigma}} \left[\frac{H^{\sigma+1} - H_o^{\sigma+1}}{\sigma+1} + \frac{H_o^{\sigma+1} - H_o H^{\sigma}}{\sigma} \right] \tag{47}$$

Equation 47 has been used to predict the drainage times for wastewater sludges. Laboratory determinations of σ, S_o, and R comprise the laboratory operations. Equation 47 is the basic equation used by Sanders (21) and Nebiker et al. (59) in predicting drainage times for wastewater sludges.

The specific resistance, R, in Equation 47 is determined by the Buchner funnel or fritted glass funnel method. Standard laboratory procedures for measuring specific resistance by the various methods have been reported by Lutin et al. (60). An adjustment to the specific resistance so determined is necessary to account for the pressure variation across the cake in the funnel. In the Buchner or fritted glass funnel the specific resistance is a function of pressure where

$$R(P) = R_c \left(\frac{P}{P_c}\right)^{\sigma} \tag{48}$$

where P = pressure at time t $(ML^{-1}t^{-2})$

P_c = reference pressure at R_c $(ML^{-1}t^{-2})$

The pressure varies from near zero at the surface of the cake to ΔP at the outlet of the testing funnel. An average value $\overline{R}$ is measured by the funnel and could be defined as

$$\overline{R} = \frac{1}{\Delta P} \int_0^{\Delta P} R(P)\, dP \tag{49}$$

where R(P) is the local specific resistance at each horizon in the sludge cake. Substituting the value of R(P) from Equation 48 into Equation 49 and performing the integration

$$\overline{R} = \frac{R_c}{P_c} \frac{1}{\sigma + 1} (\Delta P)^{\sigma} \tag{50}$$

or rearranging,

$$\overline{R} = \frac{1}{\sigma + 1} R_c \left(\frac{P}{P_c}\right)^{\sigma} \tag{51}$$

Then from Equation 48, Equation 51 may be written as

$$\overline{R} = \frac{1}{\sigma+1} R(P) \tag{52}$$

This indicates that the values for t determined from Equation 47 should be multiplied by the term $1/(\sigma + 1)$ so that proper account is taken of

the specific resistance of the sludge cake.

It is interesting to note that Nebiker et al. (59) in a study of the drainage time required for sludge applied to sand columns found it necessary to multiply the drainage times predicted from Equation 47 by a media factor, a function of the ratio of the size of the sludge particle to the size of the sand particle. Media factors of magnitude 0.45, 0.60 and 0.75 for three different sands were used so that the theoretical equation would agree with experimental values. They used the unadjusted specific resistance values instead of $\overline{R}$. The sludges studies had coefficients of compressibility ranging from 0.63 to 0.64, which would yield values of the correction $1/(\sigma + 1)$ of 0.62. Clearly much of the discrepancy between the theoretical formulation and their experimental values was due not to the media used, but to using the unadjusted specific resistance.

The assumption that the final solids content term can be ignored in Equation 43 may be invalid for water treatment sludges. In water treatment sludges the initial and final solids content may be on the order of 0.5 and 1.5%, respectively. Using Equation 43 for c, employing the media factor , and correcting for the variation of specific resistance with pressure, the equation for drainage of water treatment sludge may be expressed as

$$t = \frac{m\, R_c\, S_o\, S_f\, \nu}{(\sigma+1)\,(100S_f - 100S_o)\, H_c^{\sigma}} \left[\frac{H^{\sigma+1} - H_o^{\sigma+1}}{\sigma + 1} + \frac{H_o^{\sigma+1} - H_o H^{\sigma}}{\sigma} \right] \quad (53)$$

where m = media factor (dimensionless).

the specific resistance of the sludge cake.

It is interesting to note that Nebiker et al. (59) in a study of the drainage time required for sludge applied to sand columns found it necessary to multiply the drainage times predicted from Equation 47 by a media factor, a function of the ratio of the size of the sludge particle to the size of the sand particle. Media factors of magnitude 0.45, 0.60 and 0.75 for three different sands were used so that the theoretical equation would agree with experimental values. They used the unadjusted specific resistance values instead of $\overline{R}$. The sludges studies had coefficients of compressibility ranging from 0.63 to 0.64, which would yield values of the correction $1/(\sigma + 1)$ of 0.62. Clearly much of the discrepancy between the theoretical formulation and their experimental values was due not to the media used, but to using the unadjusted specific resistance.

The assumption that the final solids content term can be ignored in Equation 43 may be invalid for water treatment sludges. In water treatment sludges the initial and final solids content may be on the order of 0.5 and 1.5%, respectively. Using Equation 43 for c, employing the media factor , and correcting for the variation of specific resistance with pressure, the equation for drainage of water treatment sludge may be expressed as

CHAPTER III

MATERIALS AND APPARATUS

Sludges from four types of water treatment plants were used for the dewatering studies and moisture profile measurements. Equipment for dewatering studies consisted of sample containers and an environmental chamber capable of controlling temperature and relative humidity within close tolerances. The moisture profile determinations utilized gamma-ray attenuation equipment.

Types of Sludges

The four different types of water treatment sludges studied in this investigation represented the following treatment processes: alum coagulation, alum coagulation with iron removal, alum coagulation with activated carbon, and softening. A brief description of each plant follows.

Albany. The raw water supply for Albany, New York, consists of two impounding reservoirs, Alcove and Basic, which contain 12.5 and 1.0 billion gallons, respectively. The Alcove watershed has an area of 32.33 square miles with a flooded area of 1440 acres. The Basic watershed has a drainage area of 16.37 square miles with a flooded area of 265 acres. Water from the Basic reservoir passes into the Alcove reservoir by means of a tunnel 3200 feet long. The impounding reservoirs are treated with copper sulfate at times of sudden onset of algae blooms.

The filtration plant in Fuera Bush is of the conventional rapid sand type, with aeration, alum coagulation-flocculation and sedimentation, preceding filtration, followed by chlorination. There are provisions for pH stabilization with lime and taste and odor control with activated carbon, however, the sludge samples collected for this investigation contained only alum. Sludge is stored in the sedimentation tanks for approximately 6 months and then discharged to a nearby receiving stream.

Amesbury. The raw water supply for the Town of Amesbury, Massachusetts, is a well field consisting of some 300 shallow wells of 2 to 9 inches diameter. The raw water contains an abundant supply of iron and treatment thus consists of aeration, flocculation with alum, caustic soda and activated carbon, sedimentation in a manually cleaned basin, filtration through manually cleaned slow sand filters, and chlorination. The sludge is decanted before being discharged twice a year into a nearby lagoon where it dewaters in approximately 6 months time.

Billerica. The raw water supply for the Billerica, Massachusetts, water treatment plant is the Concord River. Various industrial wastes are discharged into the Concord River, causing the water to be very turbid and promoting algae growth. Treatment consists of flocculation with alum and activated carbon, sedimentation in a continuous mechanically cleaned basin, rapid sand filtration, and chlorination. The sludge is discharged daily to a nearby lagoon. The capacity of the lagoon is overtopped by the sludge discharges. The overflowing sludge enters

directly into the Concord River.

Murfreesboro. The raw water supply for Murfreesboro, Tennessee, is the East Fork of Stones River. The intake is on the back water from Walter Hill Dam, which marks the beginning of Percy Priest Reservoir. The raw water contains a hardness of approximately 160 mg/l and is treated to a final hardness of approximately 67 mg/l. The treatment plant is a relatively new plant consisting of softening, sedimentation, rapid sand filtration and chlorination. Chemicals added during the treatment process include ferric sulfate, lime, soda ash, and activated carbon. Sludge is continuously transferred from the softening and settling basins to two lagoons. The lagoons are used alternately, each having approximately 2 years capacity. Supernatant is withdrawn from the lagoons by means of an overflow weir and discharged to the river.

Sample Containers

Two types of containers were used in the drying and evaporation studies. Drying studies utilized heavy-duty glass pans, 0.5 cm thick. The inside dimensions of the pans were 22 x 35 x 4.5 cm and 19 x 30 x 4.5 cm. Evporation studies were conducted in heavy-duty plastic pails, 27.5 cm diameter and 35.5 cm high (inside dimensions).

Plastic columns were fabricated for the dewatering studies. The column walls were 1/2 inch thick and were connected with machine screws. The inside dimensions of the columns were 5 x 5 x 36 inches. The columns were aligned and supported by a metal stand as shown in Figure 7. This arrangement permitted measurements of the

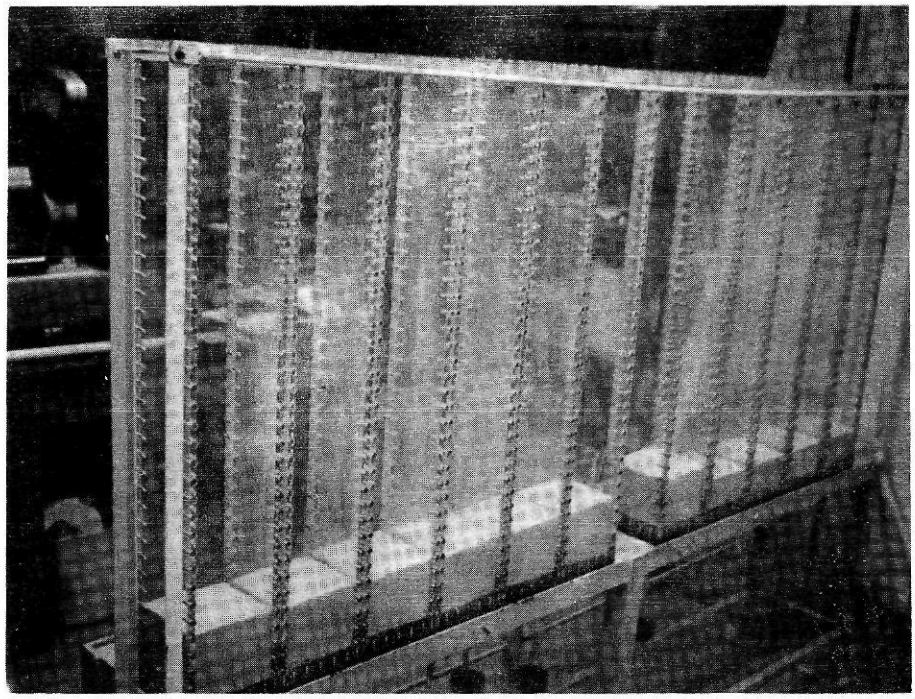

FIGURE 7 -- Photograph of Sludge Dewatering Columns

filtrate volume and facilitated other measurements and observations.

Environmental Chamber

In order to maintain constant known environmental conditions, an environmental chamber was constructed and utilized for all evaporation, drying, and dewatering studies. This chamber consisted of a room approximately 14 x 16 x 10 feet, especially modified to minimize heat and moisture losses. Constant temperature and low relative humidities were maintained by a 31,000 BTU/hr air conditioner with electric heat and reheat capabilities. High relative humidities were maintained by two humidifiers, each with a capacity of 80 lbs. per day. An electronic control system was capable of maintaining relative humidity between 30 and 80 ±2% and temperature between 65 and 85 ±2°F. A continuous record of both temperature and relative humidity was maintained by a wall-mounted recorder. A schematic diagram of the environmental chamber is shown in Figure 8.

Some of the drying experiments were conducted with slight wind velocities in order to facilitate drying and enhance air circulation in the tall dewatering columns. Air was provided by a 1.5 cfm blower and a 4-1/2 x 1-1/2 inch duct served as a manifold supply. Equally spaced 3/8 inch diameter holes provided a uniform air stream to each column.

Moisture Measurement Apparatus

The basic equipment for measuring moisture profiles by gamma-ray attenuation included scintillation, detection, and counting

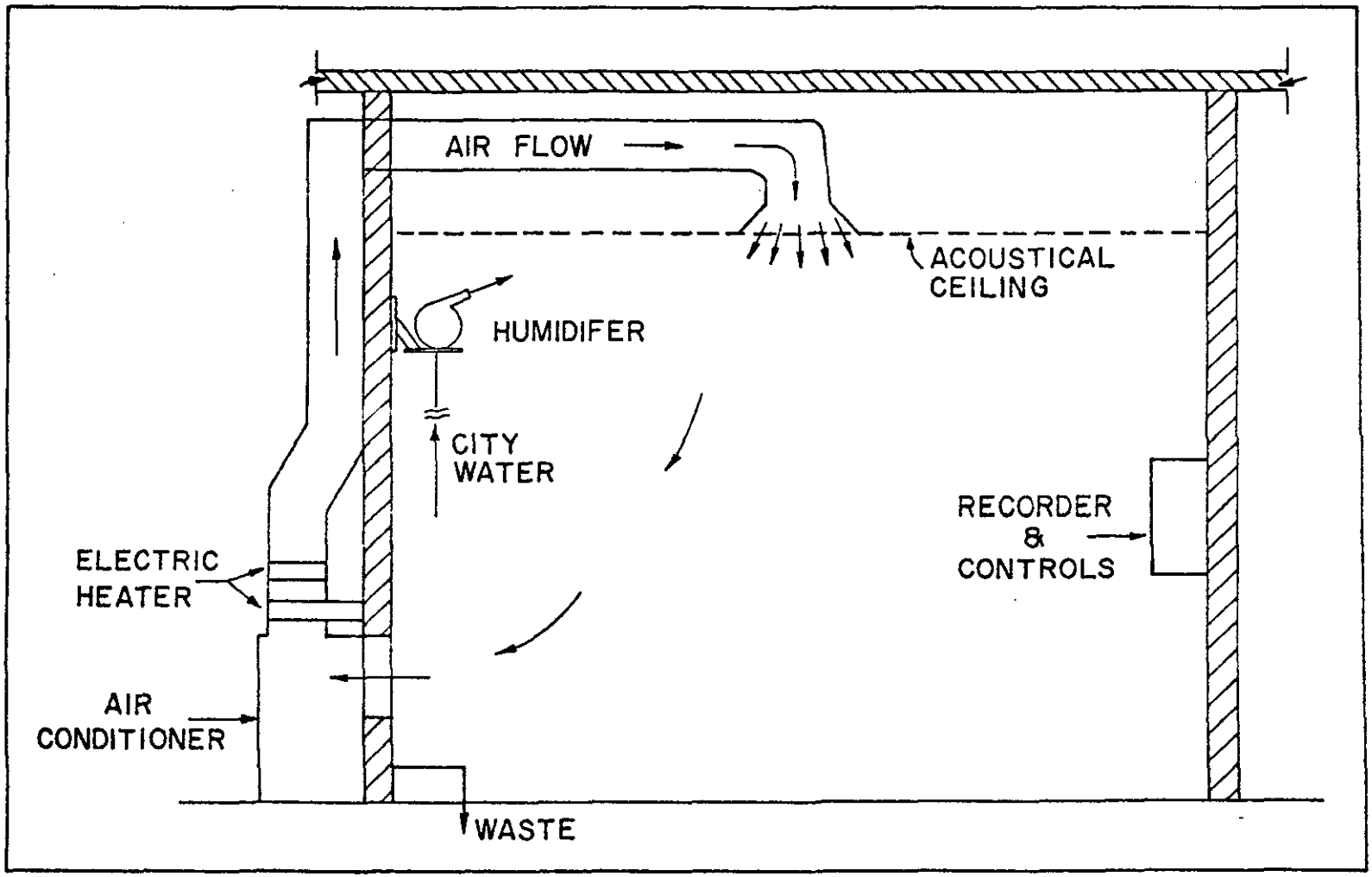

FIGURE 8 -- Diagram of Environmental Chamber.

equipment; shielding, and auxiliary equipment arranged as shown in Figure 9.

A rigid structural truss assured alignment of the detector with source beam. All were mounted on a hydraulic fork lift, permitting measurements at any elevation desired. The entire apparatus could be moved forward manually along the support for measurements at the various columns.

In order to assure repetitive measurements at a particular vertical location on a column, machined metal spacers of various thicknesses were placed on the vertical shaft of the hydraulic cylinder of the fork lift. The hydraulic pressure could then be released and the weight of the apparatus would then be supported by the spacers, thus fixing the vertical position of the source and detector. A tape measure mounted on the side of the fork lift allowed measurements of the vertical elevation to millimeter accuracy.

Five plastic boxes were fabricated to obtain attenuation coefficient measurements of sludge and water. These boxes were constructed of 0.5 inch plastic, carefully machined, with all connections made with machine screws. The plastic boxes had inside dimensions of 5 x 4 inches, with widths of 1.5, 3.0, 4.5, 6.0 and 7.5 inches.

Scintillation Counting Equipment

The scintillation counting system included a scintillator-photomultiplier assembly, high voltage supply, voltage stabilizer, linear amplifier, discriminator, and scaler-timer. The equipment is

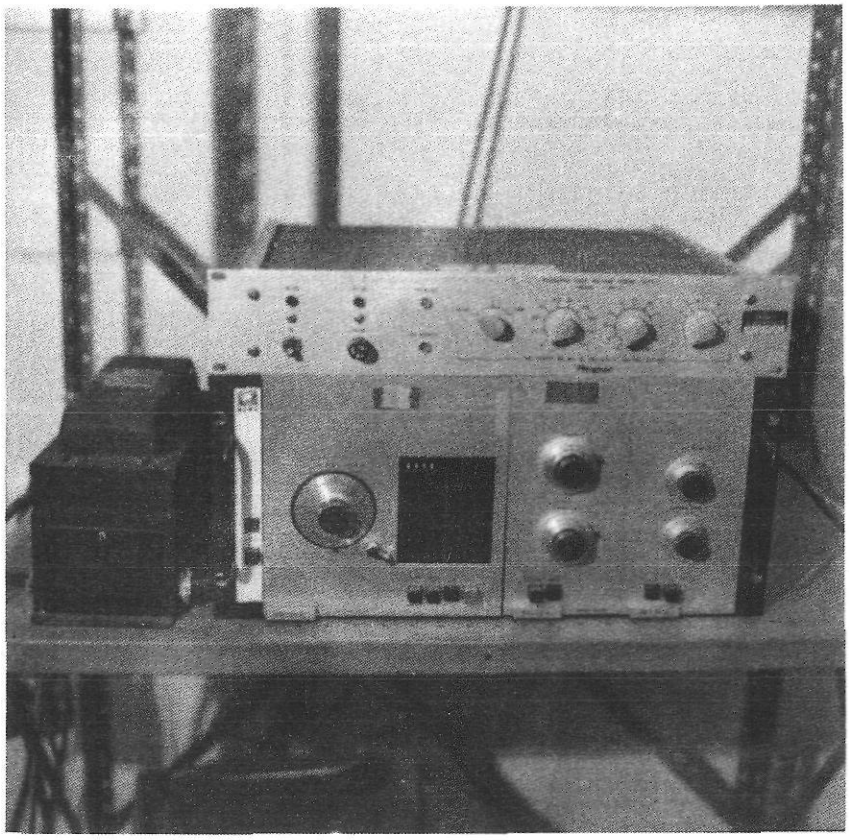

FIGURE 9 -- Photograph of Moisture Measurement Apparatus

shown in Figure 10 and Figure 11.

A gamma-ray photon, or ionizing event, struck the crystal in the detector and generated photons which caused a flash of light. These photons were reflected by the crystal housing over to the photocathode of the photomultiplier tube. The photomultiplier multiplied the initial number of electrons by a factor of about one million and delivered a charge proportional to the radiant energy spent in the scintillator. The preamplifier received the charge from the photomultiplier, gave it added gain, and served as an impedance matching device to assure the maximum transfer of the signal from the detector to the amplifier. The amplifier accepted the voltage input pulse and increased it in a linear manner, thus the relative sizes of the pulses were preserved. A differential discriminator followed the linear amplifier, and provided the analysis of the pulse height information, sorted out the pulses which satisfied the preset requirements, and rejected those that did not. The difference in energy levels between the upper limit and the baseline was the window width. The scaler-timer served as the collecting point for all the information from the detector. The timer determined the interval during which pulses from the discriminator were collected. The high voltage supply furnished the required dynode voltages to the photomultiplier tube.

The amplifier, single channel analyzer, and scaler-timer were of the RIDL series, manufactured by Nuclear-Chicago Corporation. The amplifier was a model 30-23. The scaler-timer was a model 49-25. The scaler portion was composed of three cascaded transistorized decades which drove a four-digit mechanical register with a total storage of

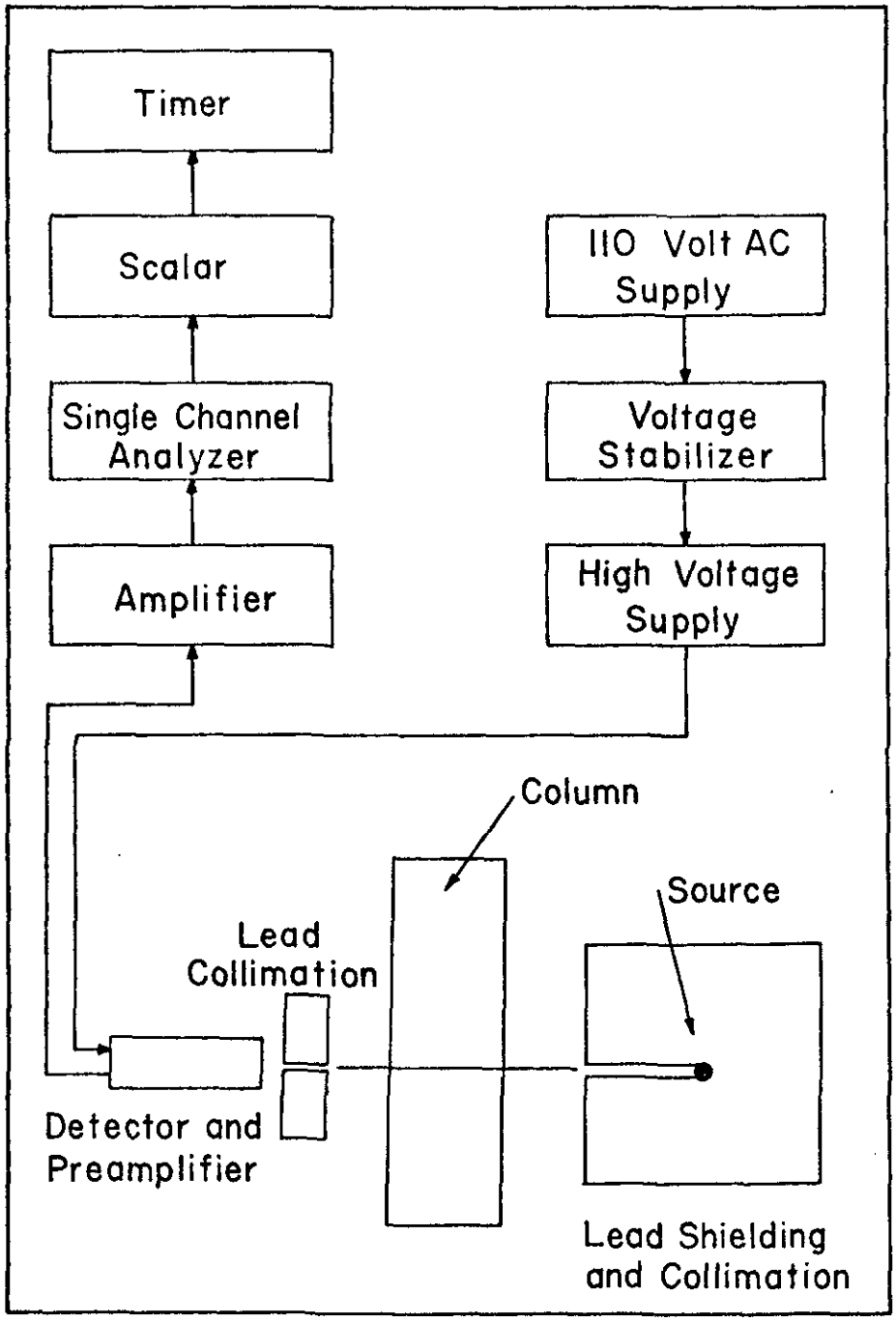

FIGURE 10 -- Schematic Diagram of Gamma-Ray Attenuation System.

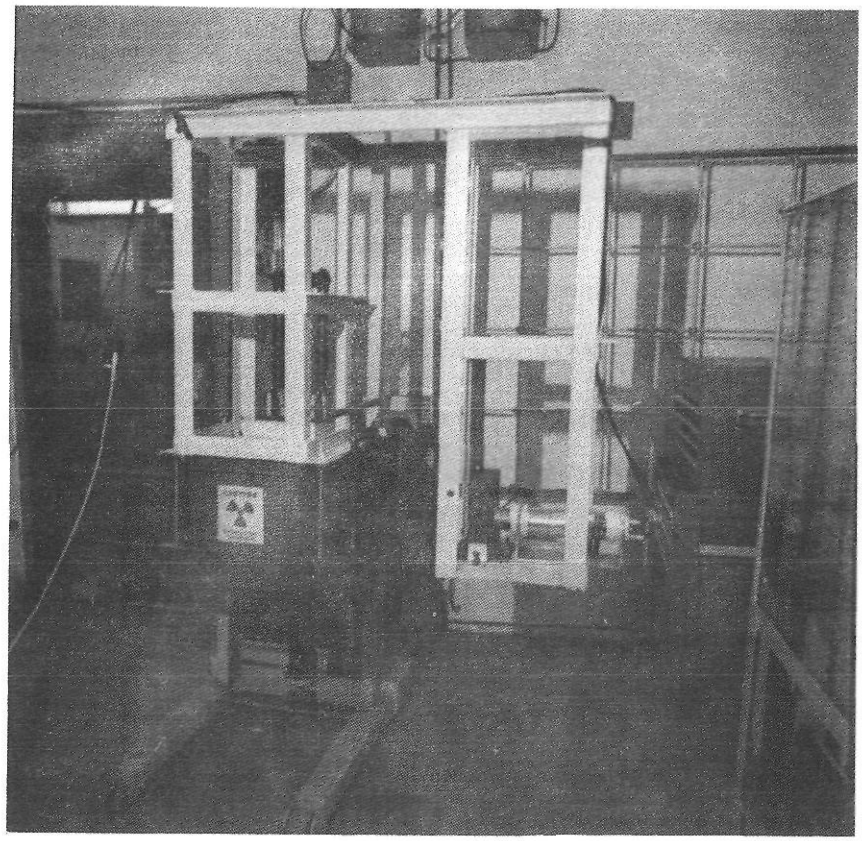

FIGURE 11 -- Photograph of Counting Equipment

up to 10^7 counts. The register responded to a maximum input rate of 20,000 pulses per second on a continuous basis. A mechanical timing dial could be set manually for any desired time, and then operated electrically to return its indicators to zero during the elapsed time for which it was set.

The voltage stabilizer, manufactured by the Raytheon Corporation, had an input voltage range of 95 - 130 volts, with an output voltage of 115 volts. The high voltage supply was of the 2 KV. type, manufactured by the Harshaw Company. The scintillator-photomultiplier system, a 2" x 2" Na(Tl) crystal, also was manufactured by the Harshaw Company. A Baird-Atomic survey meter and Nuclibadge film-badge service provided additional monitoring devices.

Shielding and Collimation

The shielding consisted of a specially constructed lead block for collimating the gamma beam and providing radiation safety to operating personnel. The shielding and scintillation detection equipment were maneuvered by means of a hydraulic fork lift previously described.

Since the weight of the lead shield was not an important factor, the shielding was designed to reduce the radiation to values only slightly greater than background levels. According to Gardner (61) normal background varies from 0.01 to 0.03 mR (milliroentgen) per hour. One milliroentgen is approximately equal to one millirad (mrad), the unit of physical radiation dose. The dose rate in mrad. per hour at a distance z in cm. from a point source of gamma radiation

at strength A_s in mc. (millicuries) was calculated from

$$D.R.\ (z,z') = 2.134 \times 10^6\ B(\mu,z')\ \frac{\mu_a}{\rho}\ E_o\ \frac{A_s}{4\pi z^2}\ \exp(-\mu z') \qquad (54)$$

where D.R. = radiation dose rate (L^2t^{-3})

$B(\mu,z')$ = buildup factor

μ_a/ρ = mass-attenuation coefficient ($M^{-1}L^2$)

μ = attenuation coefficient ($M^{-1}L^2$)

E_o = energy, Mev (ML^2t^{-2})

A_s = radiation strength (t^{-1})

z = distance, cm (L)

z' = shield thickness, cm (L).

For gamma radiation from a Cs^{137} source the energy, E_o, is primarily 0.661 Mev. The mass attenuation coefficient measured in tissue is about 0.0317 cm^2/gm, μ is 1.134 cm^{-1} and the buildup factor $B(\mu,z')$ for lead(from 3 to 20 cm thick) is approximated by the relationship by Blizzard (62) as

$$B(\mu,z') = 1.2 + 0.13z' \qquad (55)$$

Therefore, the dose rate in mrad/hr is:

$$D.R.\ (z,z') = (4.27 + 0.463z')10^3\ \frac{A_s}{z^2}\ \exp(-1.134z') \qquad (56)$$

For the 250-mc Cs^{137} source with 14 cm minimum lead thickness, the radiation at the surface was approximately 0.0017 mrad/hr, well below normal background values (0.01 to 0.03 mrad/hr). In addition to adequate thickness, care must be exercised in the design to minimize radiation leakage. A diagram of the shielding used in this method is shown in Figure 12. "Good geometry" conditions are required for successful gamma-ray attenuation measurements. Gamma rays from the source should be collimated so that only a narrow beam strikes the absorber. A collimation slit of 0.04 x 0.75 inches provided a narrow beam from the source, and a detector collimation slit of 0.08 x 0.75 inches minimized buildup due to scatter.

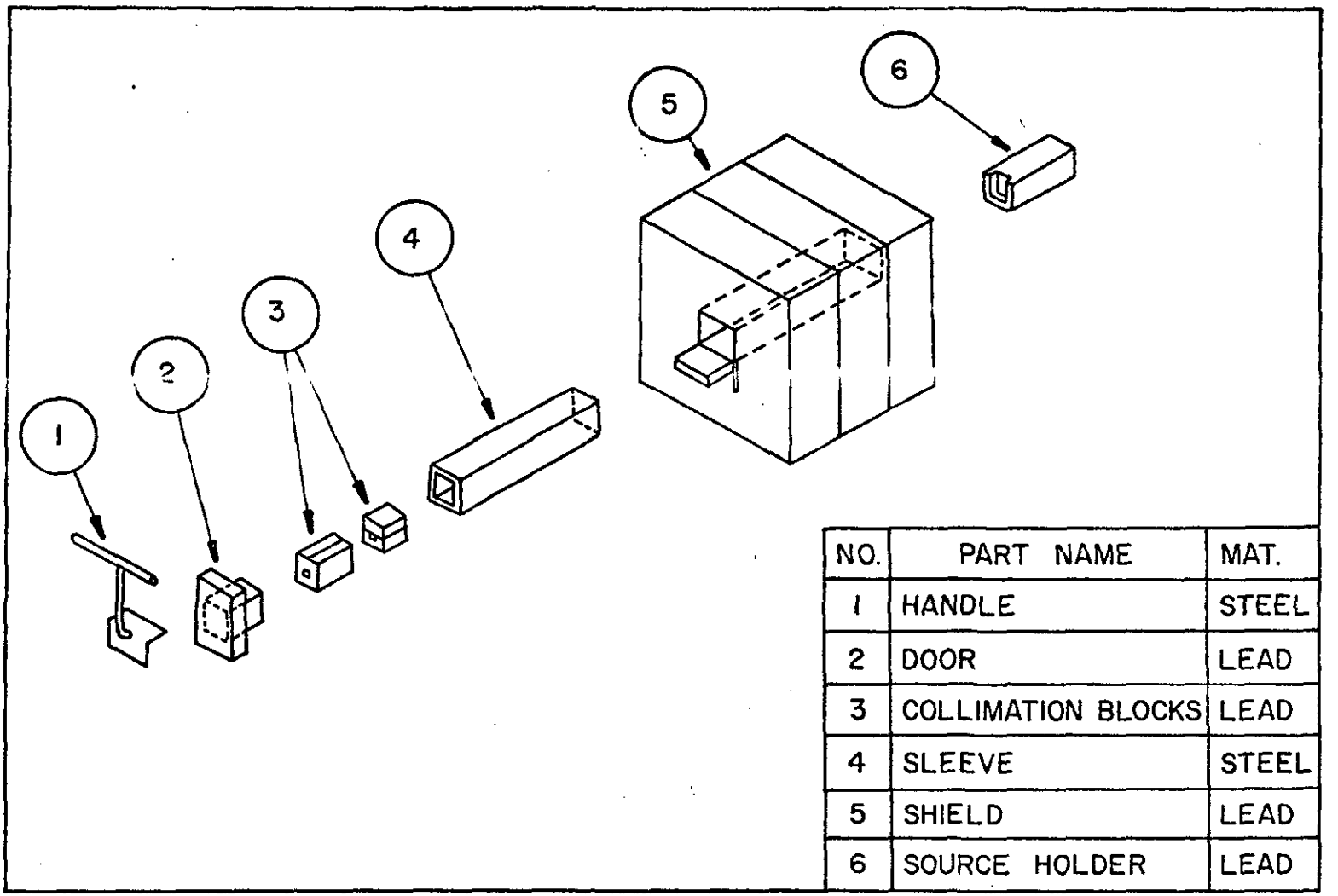

NO.	PART NAME	MAT.
1	HANDLE	STEEL
2	DOOR	LEAD
3	COLLIMATION BLOCKS	LEAD
4	SLEEVE	STEEL
5	SHIELD	LEAD
6	SOURCE HOLDER	LEAD

FIGURE 12 -- Diagram of Source Shielding and Collimation.

CHAPTER IV

METHODOLOGY

The methodology of this investigation consisted of measurements on the chemical characteristics, dewatering rates, and moisture profile analysis of four types of water treatment sludges. Chemical analyses were performed on sludge, decant, and filtrate samples. Dewatering studies required measurement of the evaporation rates of water, the drying rates of thin layers of sludge, the drying rates of thick layers of sludge on sand, and the dewatering (drying plus drainage) rates of sludge on sand. All studies were conducted in the environmental chamber under controlled temperature, relative humidity, and wind conditions.

The moisture profile studies required refinements in the gamma-ray attenuation method and determination of the physical parameters required by the method. The required parameters were attenuation coefficients of dry sand, dry sludge solids, and water as well as particle densities of the sand and sludge.

Sludge Characteristics

Chemical characteristics of the sludge, decant, and filtrate were determined for representative samples of the four water treatment sludges. Physical properties such as particle density, specific resistance, and total solids were determined for each individual study. Samples of the clear supernatant which resulted from sedimentation, were taken as representative decant samples. Filtrate samples were collected

during the dewatering studies. The filtrate had passed through 9.0 cm of Ottawa sand. Unless otherwise specified, all analyses were performed according to Standard Methods (63) and FWPCA Methods for Chemical Analysis of Water and Wastes (64). The nature of the sludge characteristics and the paucity of laboratory methods necessitated alternative procedures in some cases. The average value of triplicate analyses was reported.

Solids analyses were determined by the method reported by Adrian et al. (54). This method consists of heating the samples for 8 hours at 103°C for total solids and 20 minutes at 600°C for total volatile solids. Specific resistance analyses were performed by the Buchner funnel method as outlined by Lutin et al. (60).

Evaporation and Drying Studies

The evaporation studies required determination of the evaporation rates from free water surfaces for control purposes. Cylindrical plastic pails, 27.5 cm diameter and 35.5 cm high (inside dimensions) were filled with water at depths of 9.6, 19.3, and 29.1 cm. The pails were placed at three locations within the environmental chamber. The mass of containers plus water were determined to the nearest gram on a triple-beam balance at intervals of approximately 1.5 days.

Since a plot of mass of water versus time is linear for constant drying conditions, the slope is equal to the drying rate (Mt^{-1}). This allows comparison of drying rates using the method of comparison of regression lines. The procedure is outlined from Hald (65) as follows.

Straight lines were fitted to the data by linear regression analysis.

First the hypothesis that the theoretical variances of the two populations are equal was tested by means of the variance ratio. If the test did not reveal a significant difference between the two variances, the slopes of the two regression lines were compared by means of a t-test where

$$\tau = \frac{\beta_1 - \beta_2}{s\sqrt{\frac{1}{SSD_{x_1}} + \frac{1}{SSD_{x_2}}}} \tag{57}$$

where

$$SSD_{t_i} = \Sigma N\ (t_i - \bar{t})^2 \tag{58}$$

and had a t-distribution with $f = N_1 + N_2 - 4$ degrees of freedom. If τ exceeded the significance limit the test hypothesis was rejected and the two lines were considered to have different slopes.

If τ was not significant the two regression lines were considered parallel. A common estimate of the slope β was obtained by forming the weighted mean of the two slopes β_1 and β_2, using the reciprocal values of the variances as

$$\beta = \frac{SPD_{t_1} + SPD_{t_2 w_2}}{SSD_{t_1} + SSD_{t_2}} \tag{59}$$

$$\text{where } SPD_{t_1 w_1} = \Sigma(t_i - \bar{t})\ (w_i - \bar{w}) \tag{60}$$

$$\text{and } \bar{t} = \frac{1}{N} \sum t_i \tag{61}$$

Analysis of variance were also performed considering the average evaporation rates as variables.

Two methods were considered in the data analyses of water treatment sludge drying studies. The first method consisted of taking the derivative of the sludge mass-time data. Various relationships were then fitted to certain portions of the data. The second method considered the sludge mass-time curve only.

The first method is the traditional one for analyzing drying data in environmental and chemical engineering equations. The equation for obtaining the derivative of a function $W = f(t)$ for unequal spacing of the independent variable t, as given by Salvadori and Baron (66) may be written:

$$\frac{dW}{dt}(t_n) = \frac{1}{a(a+1)h}\left[W_{n+1} - (1-a^2)W_n - a^2 W_{n-1}\right] \qquad (62)$$

where a is the ratio between the spacings of the three points t_{n-1}, t_n, t_{n+1} written as:

$$a = (t_{n+1} - t_n) / (t_n - t_{n-1}) \qquad (63)$$

and

$$h = t_{n+1} - t_n \qquad (64)$$

Moisture contents may be obtained from the relationship

$$U = \left(\frac{W-W_{TS}}{W_{TS}}\right)100 = 100\left(\frac{W}{W_{TS}} - 1\right) \tag{65}$$

where W_{TS} = mass of sludge solids (M).

The evaporation ratio E, in %, is defined as the rate of evaporation of sludge divided by the rate of evaporation of water. The shape of the drying rate curve and the rate of change of moisture content curve are the same since

$$I = \frac{W_{TS}}{100A} \frac{dU}{dt} \tag{66}$$

when W_{TS} and A are assumed constant.

It is known from theory that a constant-rate drying period should occur under certain conditions. Thus the mass of water, W_w, is a direct function of time,

$$\frac{dW_w}{dt} = \frac{d(W-W_{TS})}{dt} = B(\text{constant}) \tag{67}$$

The mass versus time curve is therefore the integral of Equation 67 or a straight line of the form

$$W_w = A + Bt \tag{68}$$

In some cases the falling rate portion of the drying curve has been shown to be approximately linear in the form

$$\frac{dW_w}{dt} = D+Et \tag{69}$$

Equation 69 dictates that the weight-time curve for the falling-rate portion should be of the form

$$\int dW_w = \int (D+Et)dt \tag{70}$$

therefore

$$W_w = C + Dt + Et^2 \tag{71}$$

which is a second degree polynomial.

Statistical analyses of the constant-rate portions of the curves were conducted by the same procedure used for the evaporation studies.

Sludge Dewatering Studies

The primary methodology for sludge dewatering studies, was to determine the amount of water lost by drainage, the solids content at the end of drainage, and the solids content at the end of dewatering (drainage plus drying).

All dewatering studies were conducted in the plastic columns supported by the metal frame as shown in Figure 7. Temperature and relative humidity were carefully controlled during the experiments. All sludges were dewatered on a 3.5 inch layer of saturated Ottawa sand, supported by a 1 inch layer of washed stone. Each sludge was thoroughly mixed in large quantities in a 30 gallon capacity concrete mixer for a minimum of 20 minutes. The sludge was carefully placed in the columns by means of a specially constructed splash rod which prevented damage to the sand bed while charging the

columns. (Aliquot samples were taken simultaneously for laboratory analyses). Initial mass of container (tare), tare plus mass of dry sand, and tare plus mass of saturated sand were recorded. Sludge surface elevations, volume of filtrate, and mass of sludge were recorded at various intervals. The sludge mass and time were both recorded when drainage stopped. Samples of the filtrate were taken for chemical analyses after drainage had continued for some time. This insured a more representative sample since the sand and other media were previously saturated with distilled water.

The columns were permitted to drain throughout the entire dewatering study. The total filtrate collected when drainage ceased consisted of water drained from the sludge and the distilled water used to saturate the sand beds initially. The procedure for calculating the solids content at the end of drainage was as follows. The percentage of the total filtrate which came from the sludge (excluding the water to saturate the support media) was determined from

$$V_f = 100(1 - V/V_t) \tag{72}$$

where V_f = volume of filtrate (L^3)

V = volume of distilled water (L^3)

V_t = total volume collected (L^3)

The corresponding drainage time for V_f was then determined from the cumulative filtrate-time curve and the corresponding sludge mass was determined from the sludge mass-time curve. The solids content at the

end of sludge drainage was calculated as the mass of total solids (previously determined) to the total sludge mass.

Moisture Profile

Gamma-ray attenuation techniques have been used widely to follow the rapid water content change in soil columns undergoing wetting (67, 68, 69, 70). More recently, this method was used by Tang (14) to determine moisture profiles in sewage sludges. Because gamma-ray attenuation provides a convenient, rapid, non-destructive method for repeatedly measuring the solids or moisture content of sludges, it was selected for determining in situ the solids and moisture profiles in columns of water treatment sludge undergoing dewatering.

Attenuation equations. Evans (71) relates the intensity of monoenergetic gamma rays after passing through several layers of material to their incident intensity:

$$N = N_o \exp\left(-\Sigma \mu_i \rho_i L_i\right) \tag{73}$$

where N = intensity of transmitted beam (dimensionless)

N_o = intensity of incident beam (dimensionless)

μ_i = attenuation coefficient of material i $(M^{-1}L^2)$

ρ_i = density of material i (ML^{-3})

L_i = thickness of material i (L)

As an example, consider a plastic column which contains sludge and is subjected to a monoenergetic beam of gamma rays as shown in Figure 13. The gamma ray beam traverses the two column walls, each

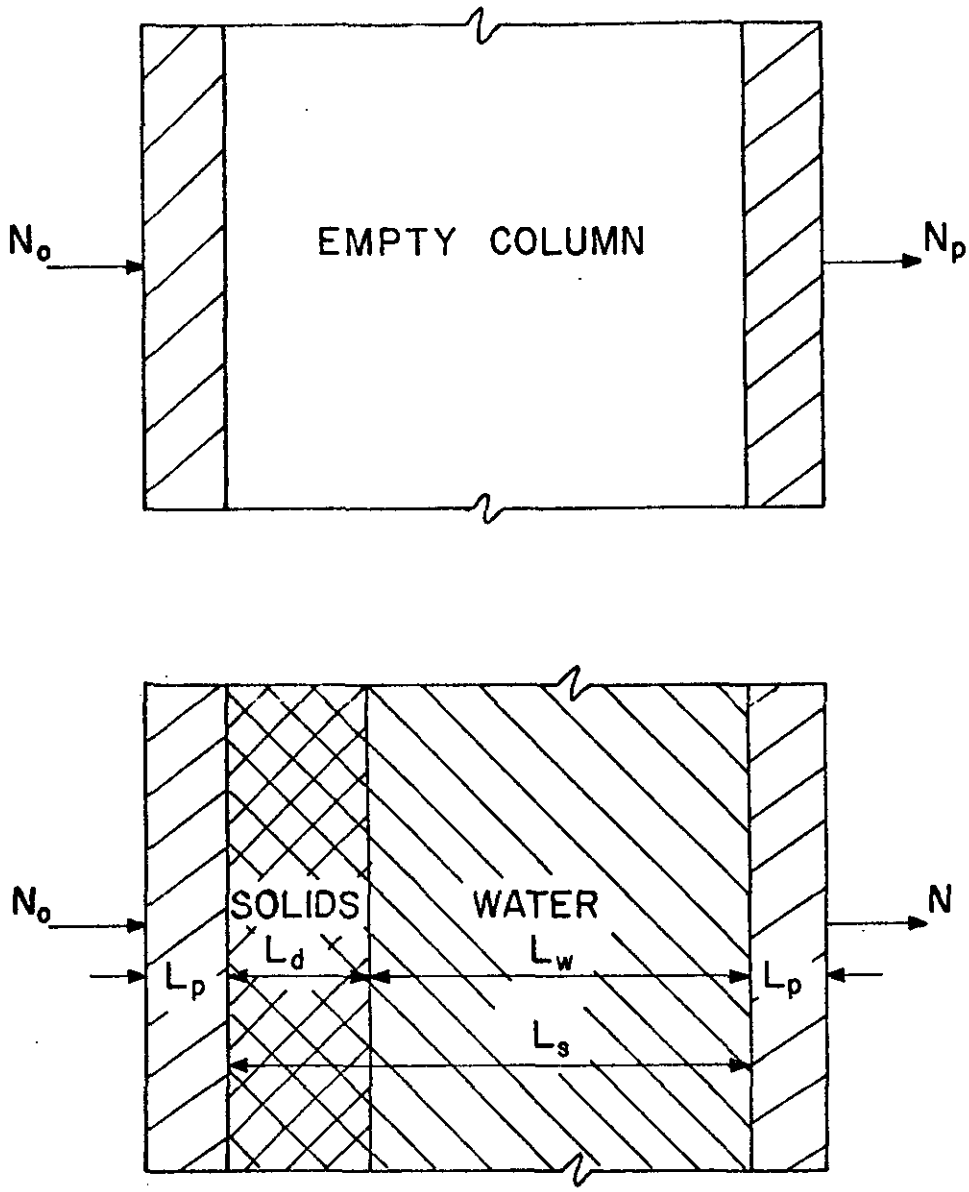

FIGURE 13 -- Attenuation Relations Used in Moisture Profile Measurements.

of thickness L_p, and the sludge of thickness L_S. The applicable attenuation relation is

$$N = N_o \exp - (2\mu_p\rho_p L_p + \mu_s\rho_s L_s) \tag{74}$$

where μ_p = attenuation coefficient of plastic $(M^{-1}L^2)$

ρ_p = density of plastic (ML^{-3})

μ_s = attenuation coefficient of sludge $(M^{-1}L^2)$

ρ_s = density of sludge (ML^{-3}).

Sludge consists of water and solids therefore Equation 74 can be expanded to

$$N = N_o \exp -(2\mu_p\rho_p L_p + \mu_w\rho_w L_w + \mu_d\rho_d L_d) \tag{75}$$

where the subscripts p, w, and d refer to plastic, water and solids, respectively. Attenuation of the plastic is described by the equation

$$N_p = N_o \exp (-2\mu_p\rho_p L_p) \tag{76}$$

where N_p = intensity of beam transmitted through plastic (dimensionless).

Division of Equation 75 by Equation 76 results in a simplified form:

$$N = N_p \exp - (\mu_w\rho_w L_w + \mu_d\rho_d L_d) \tag{77}$$

Adrian (54) showed a relationship between L_w, L_d, L_S, and the water content, w, can be derived from the basic relationship

$$L_s = L_w + L_d \tag{78}$$

and the definition of solids content

$$\frac{S}{100} = \frac{W_{TS}}{W_w + W_{TS}} = \frac{\rho_d \quad V_d}{\rho_w V_w + \rho_d V_d} \tag{79}$$

where S = % solids content (dimensionless)

W_{TS} = mass of solids (M)

W_w = mass of water (M)

V_d = volume of solids (L^3)

V_w = volume of water (L^3).

Solving Equation 79 for V_d results in

$$V_d = \frac{S\ \rho_w\ V_w}{100\ \rho_d\ (1 - S/100)} \tag{80}$$

The respective volumes are related by area A and Equation 78 by the relation

$$V_T = AL_s = A(L_w + L_d) = V_w + V_d \tag{81}$$

so the distance through the water may be expressed as

$$L_w = L_s \left[\frac{\rho_d\ (1 - S/100)}{S/100\ \ \rho_w + \rho_d\ (1 - S/100)} \right] \tag{82}$$

The distance through the solids becomes

$$L_d = L_s \left[\frac{S/100 \ \rho_w}{S/100 \ \rho_w + \rho_d \ (1 - S/100)} \right] \tag{83}$$

The distance L_s can be readily measured. Therefore, a combination of Equations 80, 82, and 83 are related to the counting measurements N and N_p through the equation

$$N = N_p \exp - \rho_d \rho_w L_s \left[\frac{\mu_w - S/100 \ (\mu_d - \mu_w)}{\rho_d + S/100 \ (\rho_w - \rho_d)} \right] \tag{84}$$

Equation 84 can be rearranged as

$$\frac{S}{100} = \frac{\rho_d [\mu_w \rho_w L_s - \ln (N_p/N)]}{(\rho_w - \rho_d) \ln (N_p/N) + \rho_w \rho_d L_s (\mu_w - \mu_d)} \tag{85}$$

and since moisture content

$$U = \left(\frac{100}{S} - 1 \right) 100 \tag{86}$$

Equation 85 may be expressed in terms of moisture content as

$$\frac{U}{100} = \left[\frac{(\rho_w - \rho_d) \ln (\frac{N_p}{N}) + \rho_w \rho_d L_s (\mu_w - \mu_d)}{\rho_d \ (\mu_w \rho_w L_s - \ln (N_p/N)} \right] - 1.0 \tag{87}$$

Equations 85 and 87 were the equations used for moisture profile measurements in this investigation. Attenuation coefficients were determined by measuring the attenuation of gamma-rays through small plastic boxes filled with water or dry solids. The particle density

of sludge solids was measured by standard soil testing procedures for specific gravity. Specific gravity, the ratio of the unit weight of solid per unit weight of water at 4°C, is numerically equal to density in the cgs system. Values for the density of water were taken from reference tables.

Radiation counting. The radioisotope source emitted a complete energy spectrum rather than monoenergetic gamma rays assumed for the attenuation theory. Therefore a differential discriminator was used to permit measurements over a narrow energy range. The advantages and disadvantages of using a Cs^{137} source for attenuation studies have been discussed by Van Bavel et al. (72). The long half life (30 yr.) of Cs^{137} eliminates any need for compensating for radioactive decay. The cesium spectrum with the well defined peak at 0.661 Mev facilitated attenuation measurements. The base-line discriminator was calibrated to read directly in kilo electron volts (kev) using the procedure outlined by Chase and Rabinowitz (73). Thus the channel number corresponded directly with energy. For this investigation the window width was set to accept gamma radiation of 0.661 ± 0.13 Mev.

The average number of radiation counts for a given time interval must be known. An estimate of the average true number of counts was obtained from single observations of the number of counts, N, in a given time period, t. Since the radioactive decay process is a Poisson distribution, Kohl et al. (74) gives the standard deviation as

$$\sigma(N) \cong (N)^{1/2} \tag{88}$$

The relative standard deviation, R.S.D. is defined as

$$\text{R.S.D.} = \frac{\sigma(N)}{N} = \frac{(N)^{1/2}}{N} = \frac{1}{(N)^{1/2}} \tag{89}$$

Since the number of observed counts depends on the counting interval, the R.S.D. can be decreased by extending the counting time. For example, if a source of about 100 counts per minute were counted for 1 minute, an average count rate of 100 would be observed and from Equation 89 the R.S.D. would be

$$\text{R.S.D.} = 1 \,/\, (100)^{1/2} = 0.1 \tag{90}$$

If the observation time were extended to 100 minutes, then approximately 10,000 counts would be observed and the R.S.D. would be

$$\text{R.S.D.} = 1 \,/\, (10{,}000)^{1/2} = 0.01 \tag{91}$$

making the advantages of increased counting time apparent.

The counting rate observed during a time t was defined as

$$n = \frac{N}{t} \tag{92}$$

where n = counting rate (t^{-1})

Excluding errors in the measurement of time t, the standard deviation of the counting rate would be

$$\sigma(n) = \frac{\sigma(N)}{t} \cong \frac{(N)^{1/2}}{t} = \frac{(nt)^{1/2}}{t} = \left(\frac{n}{t}\right)^{1/2} \tag{93}$$

A counting time of 16 minutes was chosen for this study and provided a standard deviation of $(n)^{1/2}/4$ for the counting rate. To reduce the standard deviation by half, i.e., to $(n)^{1/2}/8$, would have required a counting time of 64 minutes.

The radioactivity detection instruments have finite resolving times within which two occurring events may be distinguished and recorded separately. Thus some counts are missed; the fraction lost increasing with increasing counting rate. A coincidence correction allows the mean number of counts occurring to be calculated by the method given by Kohl et al. (74) as

$$n_o = \frac{n}{1 - nt_r} \tag{94}$$

where n_o = mean count rate occurring (t^{-1})

n = mean count rate recorded (t^{-1})

t_r = resolving time (t).

The number of lost counts is

$$n_o - n = n\, n_o\, t_r \tag{95}$$

and

$$n_{max} \rightarrow 1/t_r \tag{96}$$

All count rates in this investigation were corrected for coincidence losses using the previous equations and the published value for the counting equipment of $t_r = 1\mu$ sec.

Attenuation coefficient measurements. Values for the attenuation coefficients for water and dry solids are needed in the gamma-ray attenuation equations. The basic attenuation equation as used by Davidson et al. (68) can be written as

$$N = N_p \exp [- (\mu_d \rho_b + \mu_w \theta) L] \quad (97)$$

where ρ_b = bulk density of the dry material (ML^{-3})

θ = water content (ML^{-3})

L = thickness of sample (L).

For distilled water, Equation 97 reduces to

$$N = N_p \exp (-\mu_w \rho_w L) \quad (98)$$

where ρ_w = density of water (ML^{-3}).

Equation 98 can be written as

$$\ln N/N_p = - \mu_w \rho_w L \quad (99)$$

or in linear fashion

$$Y = BX \quad (100)$$

where $Y = \ln N/N_p$

$B = -\mu_w$

$X = \rho_w L = L$

since the density of water in the cgs system is approximately 1.0.

Plastic boxes of various thicknesses were used for making several measurements of Y. The term B was found by regression analysis for a line passing through the origin (75):

$$B = \frac{\Sigma X_i Y_i}{\Sigma X_i^2} \tag{101}$$

the variance

$$\sigma^2 = \frac{1}{N-1} \Sigma(Y_i - BX_i)^2 \tag{102}$$

and the correlation coefficient r from

$$r = \frac{\Sigma X_i Y_i}{(\Sigma X_i^2 \Sigma Y_i^2)^{1/2}} \tag{103}$$

Attenuation coefficients for dry sludge solids or dry sand required measuring the attenuation of the dry material for a constant thickness at various bulk densities. To this end the sludges were slowly dried on a water bath, pulverized with a mortar and pestle, placed in uniform layers, and compacted by shaking or with a standard number of strokes with a blunt instrument. The bulk density was the weight of material divided by the volume of the box. Counting times for both the dry material and the empty box were 16 minutes, with counts taken at various locations.

Particle density. Particle density measurements were made on all sludges studied as well as the Ottawa sand used for drainage media. Particle density, the mass of solid per unit volume, is numerically equivalent to the specific gravity of a soil, and is

defined by Lambe (76) as the ratio of the weight in air of a given volume of soil particles to the weight in air of an equal volume of distilled water at 4°C. The specific gravities of the sludges were determined using laboratory procedures presented by Lambe (76).

Moisture profile determinations. The moisture profiles of both sludge and supporting sand layers were determined periodically during the dewatering studies. Equations 85 and 87 were used to obtain moisture or solids profiles in the sludge layers. The method for determining the moisture content of the sand was identical to that of sludge, however, the amount of water in the sand was calculated differently, because when water left the sand layer the pores were filled with air, changing the effective thickness of the sample. Equation 85 and 87 were thus not valid for drying sand since the derivation assumed the entire sample to be either solid or water. Equation 97 was used to determine the water content of sand.

DIFFUSION

Measurements of the diffusion coefficient were made in order to determine the applicability of the diffusion model to water treatmetn sludge drying. Recent studies in the soil sciences studying moisture movement in soils found the diffusion coefficient to be a function of the moisture content. Covey (77) and Wakabayashi (78,79) reported experimental values for D(U) for soils.

Where D is a function of U only, Boltzman (80) has shown that if $U=U(\eta)$, where $\eta = xt^{-1/2}$, the concentration dependent diffusion

equation

$$\frac{\partial U}{\partial t} = \frac{\partial}{\partial x}\left[D(U)\ \frac{\partial U}{\partial x}\right] \tag{104}$$

can be written as an ordinary nonlinear differential equation

$$\frac{d^2U}{d\eta^2} + \frac{\eta}{2D(U)}\ \frac{dU}{d\eta} + \frac{1}{D(U)}\ \frac{dD(U)}{dU}\ \left(\frac{dU}{d\eta}\right)^2 = 0 \tag{105}$$

The initial and boundary conditions for Equation "104"

$$U\ (x,0)=U_i \quad \text{and} \quad U(0,t) = U_s \tag{106}$$

transform to two conditions for Equation "105"

$$U(0) = U_s \quad \text{and} \quad l\ (\infty) = U_i \tag{107}$$

Equation 105may be written a.

$$\frac{d}{d\eta}\left[D(U)\ \frac{dU}{d\eta}\right] = -\frac{\eta}{2}\ \frac{dU}{d\eta} \tag{108}$$

and upon integration, rearranged as

$$D(U)_x = -\frac{1}{2t}\left(\frac{dx}{dU}\right)_{U_x} \int_{U_i}^{U_x} x\ dU \tag{109}$$

Obtaining D(U) requires measurements of U vs. X for t constant, or nearly constant. These measurements must be made experimentally by determining the moisture content along a column containing drying sludge.

After evaluating the variation of the diffusion coefficient with moisture content and using the proper boundary conditions the basic diffusion equation, Equation 12,can be solved for U at any time t by numerical techniques. This also permits calculation of the time required to dry the material to any desired moisture content.

CHAPTER V

RESULTS

Chemical Characteristics

Chemical characteristics of the sludge, decant, and filtrate samples were determined for the four water treatment sludges. Physical properties such as particle density, specific resistance, and total solids were determined for each individual study and are not included here. Samples of the clear supernatant which resulted from sedimentation, were taken as representative decant samples. Filtrate samples were collected during the dewatering studies from the column effluent. The average value of triplicate analyses was reported.

Color-turbidity-pH. Color, trubidity, and pH were determined for all samples. The average values are tabulated in Table 1.

Color was determined by a Helige Aqua Tester on unfiltered samples. This method gave values for the apparent color. The sludges exhibited a dark black color with the exception of the softening sludge. The softening sludge was reddish-brown. The dark color of the three clarifier sludges was due to the activated carbon and minute amounts of organic material. Both the filtrate and decant were relatively clear, exhibiting low color values.

Turbidity was determined by a Hellige turbidmeter. The presence in the sludge of suspended solids which could settle out rapidly, may have given false high readings. The turbidity values

Table 1 -- Average Values for Color, pH, and Turbidity for the Sludge, Filtrate, and Decant Samples

Sample	Color, color units	pH	Turbidity, JTU
Albany			
sludge	black	7.0	1200
filtrate	0.03	7.5	6.0
decant	0.10	7.7	36
Amesbury			
sludge	black	8.0	3600
filtrate	0.01	8.3	4.0
decant	0.02	7.9	3.0
Billerica			
sludge	black	4.3	2200
filtrate	0.10	7.4	65
decant	0.12	8.3	22
Murfreesboro			
sludge	reddish-brown	8.0	1700
filtrate	0.02	7.6	8.0
decant	0.02	7.6	2.0

for the sludges therefore have less significance than the values for decant and filtrate. Relatively low turbidity values were obtained for the filtrate samples with the exception of Billerica sludge. This sample apparently contained a minute amount of the activated carbon which had passed through the filter.

Values for pH were determined on a Radiometer pH meter. All pH values were near the neutral point with the exception of Billerica sludge which had an average pH of 4.3. During the time interval of transferring samples from the treatment plants to the laboratory and subsequent handling, neutralization, such as from loss of CO_2, could have taken place.

Solids. Total solids, total volatile solids, and suspended solids were determined. No established procedure for determining solids in sludge samples exists, however Standard Methods and extensive solids analysis investigations at the University of Massachusetts (53) served as guidelines. Total solids were determined by heating the samples for 8 hours at 103°C and total volatile solids were determined by heating the total solids residue at 600°C for 20 minutes. Samples for the suspended (nonfilterable) solids determinations were processed by filtering through a standard glass fiber filter. The results of the solids determinations are presented in Table 2.

The four sludges had a wide variation in total solids, the range extending from 1.45% for Albany sludge to 6.30% for Billerica sludge. The sludges were approximately 50% volatile solids with the exception of Murfreesboro (softening) sludge which was only 2.15% volatile solids.

Table 2 --Average Values for Solids for the Sludge, Filtrate, and, Decant Samples.

Sample	Total Solids,%	Volatile Solids as a % of Total Solids	Suspended Solids, mg/l
Albany			
sludge	1.45	46.0	13500
filtrate	0.029	40.0	1.5
decant	0.024	53.0	2.0
Amesbury			
sludge	3.83	43.8	37200
filtrate	0.041	12.5	0.11
decant	0.029	11.0	0.08
Billerica			
sludge	6.30	58.0	62000
filtrate	0.104	34.8	2.14
decant	0.050	40.8	2.58
Murfreesboro			
sludge	4.80	2.2	47000
filtrate	0.036	26.0	1.44
decant	0.326	19.0	0.90

A portion of the high values (50%) for volatile solids was considered to be attributed to bound water which would be retained to the solid particle at lower temperatures but driven off at higher temperatures; however, separate freeze drying studies of the sludge showed the bound water concentration was negligible. Suspended materials accounted for 98.5% of the total solids for the four sludges. The filtrate and decant samples were relatively clear.

Acidity and alkalinity. Total acidity and total alkalinity were determined by potentiometric titration. The results are tabulated in Table 3. Billerica sludge had total acidity of 2753 mg/l (as $CaCO_3$), the maximum obtained. The maximum alkalinity obtained was for the Murfreesboro (softening) sludge and was 12,950 mg/l (as $CaCO_3$).

Calcium-magnesium-total hardness. Total hardness and calcium were determined by the EDTA titrimetric method. Magnesium was determined by subtracting calcium from total hardness since hardness is usually considered to be primarily composed of calcium and magnesium. The results are presented in Table 4.

Iron and manganese. Iron and manganese were determined for the samples and the results are shown in Table 5. The Amesbury and Murfreesboro sludges contained the highest concentrations of iron, 3080 and 1990 mg/l, respectively. The Amesbury water treatment plant practices iron removal by oxidizing ferrous iron to the insoluble ferric state. A similar removal process would be produced during softening at the Murfreesboro plant. As shown by the low values for iron in the filtrate and decant samples, most of the iron was in the

Table 3 --Average Values for Total Acidity and Total Alkalinity for the Sludge, Filtrate, and Decant Samples.

Sample	Total Acidity, mg/l as $CaCO_3$	Total Alkalinity, mg/l as $CaCO_3$
Albany		
sludge	360	832
filtrate	44.2	147
decant	25.2	87.4
Amesbury		
sludge	612	1,975
filtrate	16.7	158.5
decant	-	-
Billerica		
sludge	2,753	-
filtrate	14.0	88.0
decant	253.5	2.6
Murfreesboro		
sludge	-	12,950
filtrate	6.0	74.5
decant	7.5	82.5

Table 4 --Total Hardness, Calcium, and Magnesium for the Sludge, Filtrate, and Decant Samples.

Sample	Total Hardness, mg/l as $CaCO_3$	Calcium mg/l as Ca	Magnesium mg/l as Mg
Albany			
sludge	12,900	3,060	715
filtrate	195	68	6
decant	153	58	2
Amesbury			
sludge	2,360	790	92
filtrate	182	68	3
decant	165	64	1
Billerica			
sludge	10,900	2,560	1,100
filtrate	458	172	7
decant	452	170	7
Murfreesboro			
sludge	15,100	3,990	1,240
filtrate	180	62	6
decant	182	62	7

Table 5 --Average Values for Manganese and Iron for the Sludge, Filtrate, and Decant Samples.

Sample	Manganese, mg/l as Mn	Iron, mg/l as Fe
Albany		
sludge	70.0	89.2
filtrate	12.3	0.07
decant	13.8	1.27
Amesbury		
sludge	57.6	308
filtrate	5.4	0
decant	0	
Billerica		
sludge	31.0	541
filtrate	7.4	2.38
decant	18.8	5.55
Murfreesboro		
sludge	5.6	1990
filtrate	0	0
decant	0	0

insoluble ferric state. Manganese often is present with iron in surface water supplies and is generally removed concurrently with iron. A large percentage of manganese in the Albany and Billerica sludges was in the insoluble form.

Nitrogen. Nitrogen analyses consisted of organic nitrogen, ammonia, nitrite, and nitrate. Ammonia was analyzed by the direct nesslerization method. Organic nitrogen was determined by performing total Kjeldahl and then subtracting the value obtained for ammonia. Nitrate was obtained by the phenoldisulfonic acid method which determined both nitrate and nitrite. The values for nitrate were then determined by subtracting the values previously obtained for nitrite. The results of the nitrogen analyses are presented in Table 6.

The Albany and Billerica sludges contained 479 and 612 mg/l organic nitrogen, respectively. The filtrate and decant for both sludges contained significantly less organic nitrogen, indicating the organic nitrogen was adsorbed to the sludge solids. The organic nitrogen in the Amesbury and Murfreesboro sludges was considerably less at 4.70 and 35.8 mg/l, respectively. The Albany, Amesbury, and Billerica samples contained significant amounts of free ammonia. Nitrite and nitrate values of all samples were comparatively small. The decant samples in general contained more nitrogen than the filtrate samples. The two might normally be considered equal except for the amount adsorbed to any suspended particles in the decant. Filtrate and decant samples for Albany and Billerica had a higher concentration

Table 6 --Average Nitrogen Values for the Sludge, Filtrate, and Decant Samples.

Sample	mg/l Nitrogen found as			
	Organic N	free NH_3	NO_2	NO_3
Albany				
sludge	479	58.8	0.126	2.65
filtrate	41.8	12.6	3.15	0.450
decant	25.3	24.8	11.2	2.80
Amesbury				
sludge	4.70	10.5	0.019	0.13
filtrate	1.50	10.7	0.004	0.22
decant	1.06	8.49	0.004	0.38
Billerica				
sludge	612	89.2	0.002	0.98
filtrate	10.6	41.4	0.065	0.22
decant	15.2	72.8	0.011	0.27
Murfreesboro				
sludge	35.8	2.00	0.019	0.23
filtrate	9.1	1.65	0.027	0.15
decant	15.0	3.66	0.006	0.37

of NO_2 than the sludge samples. The filtrate and decant samples were separated from any bacteria that was present in the original sludge samples. Since the amount of the different forms of nitrogen are greatly influenced by microbial activity, the rates of oxidation-reduction of the filtrate and decant samples were not equal to the oxidation-reduction rate of the sludge samples.

Phosphate. Phosphate determinations consisted of orthophosphate and polyphosphate analyses. Orthophosphate was determined by the stannous chloride method. Polyphosphates were determined by subtracting orthophosphate from the total inorganic phosphate. The phosphate results are summarized in Table 7.

Polyphosphate comprised the larger portion of phosphates in all samples except for the Murfreesboro sludge sample. The filtrate and decant samples contained much less phosphate than the sludge samples which indicated that phosphates were adsorbed to the sludge particles.

Sulfate. Sulfate analyses were performed according to Standard Methods, Method B: Gravimetric Method with Drying of Residue. Billerica sludge had the maximum value of 1240 mg/l SO_4. The results are tabulated in Table 7.

BOD-COD. Biochemical Oxygen Demand (BOD) and Chemical Oxygen Demand (COD) results are presented in Table 8. The BOD values for the filtrate and decant samples were low. The Murfreesboro sludge had the lowest BOD, 7.8 mg/l. The maximum BOD was in the Billerica sludge which also had the highest total solids content.

The COD values ranged from a minimum value of 3330 mg/l for

Table 7--Average Values of Phosphate and Sulfate for the Sludge, Filtrate, and Decant Samples.

Sample	Orthophosphate, mg/l PO_4	Polyphosphate, mg/l PO_4	Sulfate, mg/l
Albany			
sludge	2.64	54.0	209
filtrate	0.34	0.83	18.2
decant	0.08	5.4	5.35
Amesbury			
sludge	1.4	395	150
filtrate	0.15	1.6	7.20
decant	0.15	1.2	33.8
Billerica			
sludge	2.6	1803	1240
filtrate	0.15	1.6	23.8
decant	0.40	4.45	51.2
Murfreesboro			
sludge	134	61	156
filtrate	0.24	0.88	128
decant	0.25	1.25	69.0

Table 8 --Biochemical Oxygen Demand and Chemical Oxygen Demand Values for Sludge, Filtrate, and Decant Samples.

Sample	BOD, mg/l	COD, mg/l
Albany		
sludge	160	3,330
filtrate	9.6	160
decant	7.9	240
Amesbury		
sludge	180	18,500
filtrate	2.7	124
decant	1.2	98
Billerica		
sludge	190	440,000
filtrate	2.0	167
decant	2.0	289
Murfreesboro		
sludge	7.8	3,350
filtrate	0	134
decant	7.1	124

Albany sludge to a maximum of 440,000 mg/l for Billerica. The large amounts of activated carbon present and the high (6.30%) total solids content are two possible explanations for the high COD value for Billerica sludge. The COD values for the decant and filtrate samples ranged from 124 to 289 mg/l.

Preliminary Results

Preliminary studies on the evaporation rates of water and the drying rates of sludges were conducted in the environmental chamber. Results from these studies provided information for planning and refinement of later studies.

Evaporation of water. Preliminary studies on the evaporation of water were conducted in the environmental chamber to determine if there was any significant difference in the evaporation rates due to either the location in the environmental chamber or the liquid depth. Deionized water was evaporated in nine cylindrical plastic pails, 27.5 cm diameter and 35.5 cm high The pails were filled to depths of 9.6, 19.3 and 29.1 cm. The locations were on the floor near the control panel (1), on a table in the center of the room (2), and on the floor near the door (3) as shown in Figure 14. Relative humidity and temperature were controlled at 47% and 76°F, respectively. The containers were weighed to the nearest gram at intervals of approximately 1.5 days.

The average rate of water loss (gm/hr) was calculated by fitting a straight line to the weight-time data, the slope of which was obtained

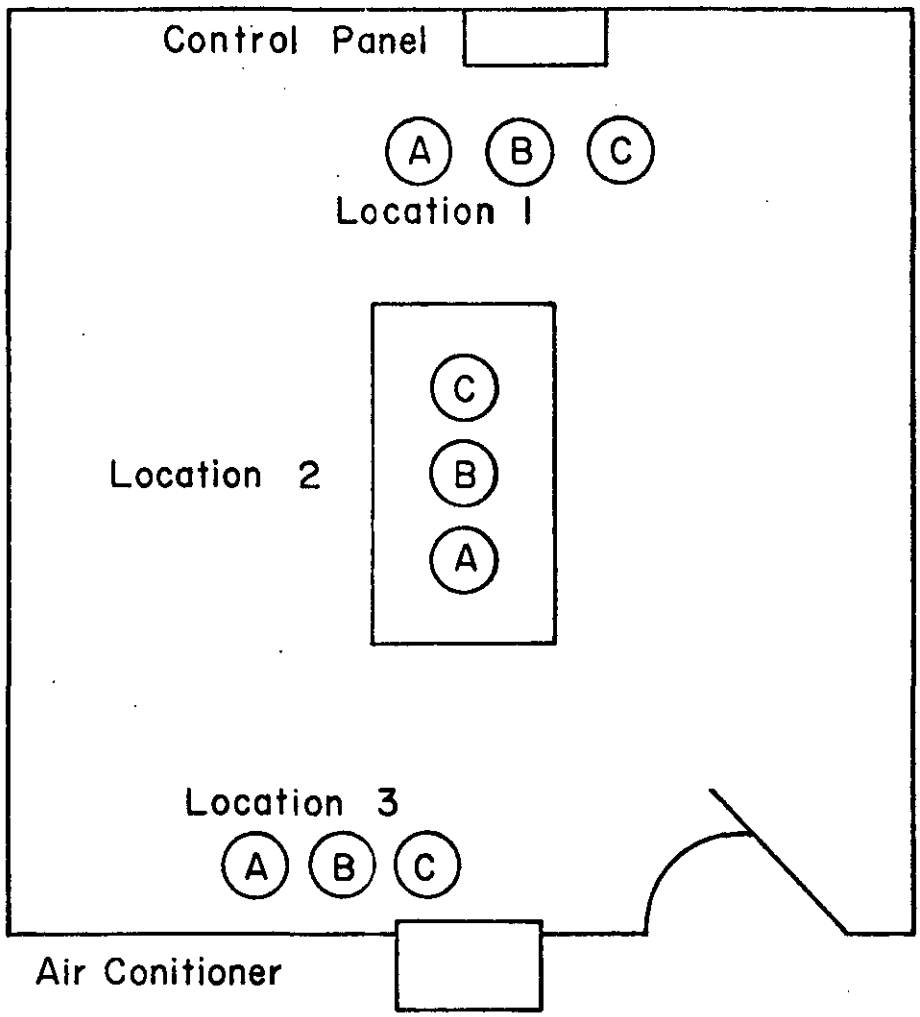

FIGURE 14 -- Location of Containers in Evaporation Study.

from linear regression analysis. The data are summarized in Table 9. A two-way analysis of variance of the drying rates showed no significant difference between depths and locations at the 5% level. A summary of the analysis of variance is shown in Table 10.

Drying studies. Two preliminary drying studies were conducted in succession using Billerica sludge. Sludges with solids contents of 2.35 and 6.12% were dried in glass pans 0.5 cm thick with inside dimensions of 35 x 22 x 4.5 cm. The initial sludge depths were 3.0 cm. Pans of distilled water were evaporated as controls. Temperature and relative humidity were controlled at 72 ± 0.5°F and 38 ± 1%, respectively. The mass of the sludges was determined on a triple-beam balance at intervals of approximately one day. When the change in mass was less than one gram per day, the sludges were assumed to be at equilibrium. Results of the two drying studies are summarized in Table 11.

Curves showing the sludge mass-time relationships are shown in Figure 15. The constant-rate drying period accounted for approximately 75% of the water loss and 75% of the total drying duration for each sample. During the early stages of drying sample D-1 appeared to have a thin film of moisture on the surface while sample D-2, the lower solids content, had clear supernatant present. The first critical moisture content was not reached, however, until after the sludges had appeared very dry and many cracks had formed. The equilibrium moisture contents were low with an average value of only 18%. At

Table 9 --Rate of Water Loss (gm/hr) of De-ionized Water at 76°F and 47% Relative Humidity.

Location	Water Depth 9.6 cm	19.3 cm	29.1 cm
1	3.77	4.05	4.39
2	2.74	3.53	4.36
3	2.77	3.18	3.67

Table 10 --Analysis of Variance for Evaporation Data

Source of Variation	Sum of Squares	Degrees of Freedom	Mean Squares	F Test
Location	2.1	2	1.05	6.20
Depth	1.6	2	0.80	4.70
Error	0.7	4	0.17	
Totals	4.4	8		

Table 11 --Results of Billerica Sludge, at Two Different Solids Contents, Dried at 72°F and 38% Relative Humidity for 3.0 cm Initial Depths.

Sample Number	D-1	D-2
Initial Solids, %	6.12	2.35
Critical Moisture Content, %	400	350
Critical Solids Content, %	20.0	22.2
Solids at equilibrium, %	90.0	79.5
Moisture at equilibrium, %	11.0	26.0
I_c, gm/cm^2-hr	0.0062	0.0070
Evaporation ratio, %	76.5	86.5

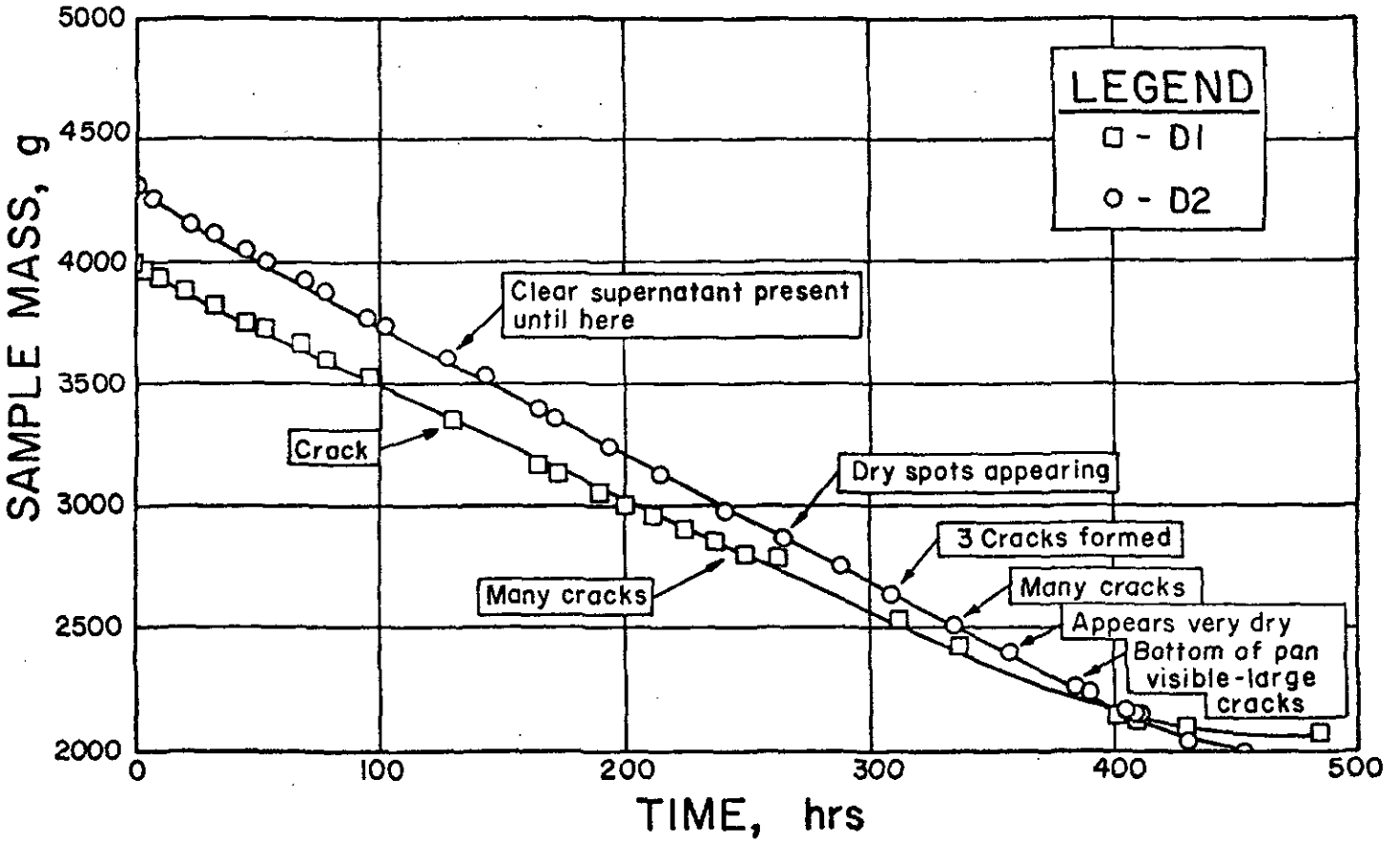

FIGURE 15 -- Sample Mass Versus Time for Billerica Sludge Drying at 72°F and 38% Relative Humidity.

equilibrium, the sludges had shrunk to only a few small, warped pieces, approximately 0.5 cm thick.

The average drying rates for the long constant-rate drying periods were determined by fitting straight lines to the sludge mass-time data. The average drying rates for samples D-1 and D-2 were 0.0062 and 0.0070 gm/cm^2-hr, respectively. When tested by comparison of regression lines the two drying rates were affected due to the different initial solids concentrations. The average evaporation rate of water for the same conditions was 0.0081 gm/hr-cm^2. The evaporation ratios (the ratio of sludge drying intensity to evaporation rate of water) for samples D-1 and D-2 were therefore 76.5 and 86.5%, respectively.

Drying-rates for the entire drying duration were calculated by Equation 62 and are shown in Figure 16. The initial decrease in the drying rate was due to the sample storage temperature having been higher than the environmental chamber temperature. The drying rate decreased while the surface temperature lowered to the ultimate value. This initial adjustment period was so short that it was ignored in subsequent analysis of the drying times.

The first critical moisture content was reached at a higher moisture content (shorter drying time) for the sample with the higher solids content, D-1. This follows with the general theory for critical moisture content in that sample D-1 had a higher solids content,

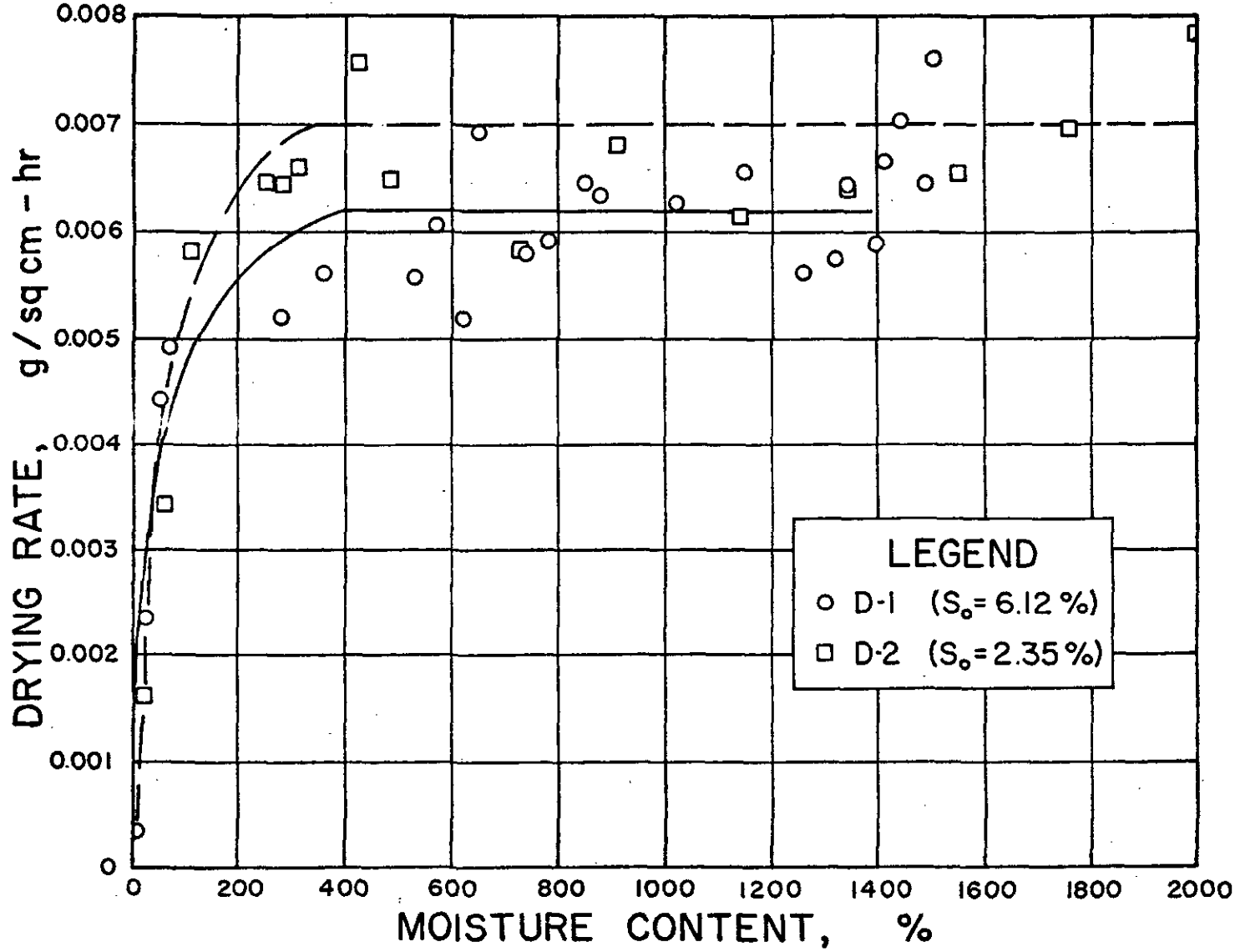

FIGURE 16 -- Drying-Rate Curves for Billerica Sludge Drying at 72°F and 38% Relative Humidity.

therefore a higher value for mass of total solids, W_{TS}. A second critical moisture content could not be clearly established for either sample.

Drying

Drying studies were conducted to determine the drying rates and evaporation ratios of thin layers of sludge under controlled drying conditions.

During the drying of water treatment sludges, shrinkage and crack formations occurred which changed the drying surface area. In order to show the relative magnitude of shrinkage, pans containing the four types of sludges were dried in the oven at 103°C for approximately two days. The sludge mass was determined periodically to provide values for the solids contents. The relative amount of shrinkage and crack formation is shown in Figure 17 . The softening sludge (Murfreesboro) settled rapidly leaving a clear supernatant to be evaporated during most of the drying period. The Billerica sludge had less shrinkage, probably due to the large amounts of activated carbon present.

Drying-rate studies. Drying-rate study D-3 was conducted to study the drying and evaporation ratios of thin layers of sludge under controlled drying conditions. Albany, Billerica, and Amesbury sludges were dried at depths of 2 and 4 cm in heavy glass pans. The pans were 0.5 cm thick walls and were 22 x 35 x 4.5 and 19 x 30 x 4.5 cm, inside dimensions. Temperature and relative humidity were controlled

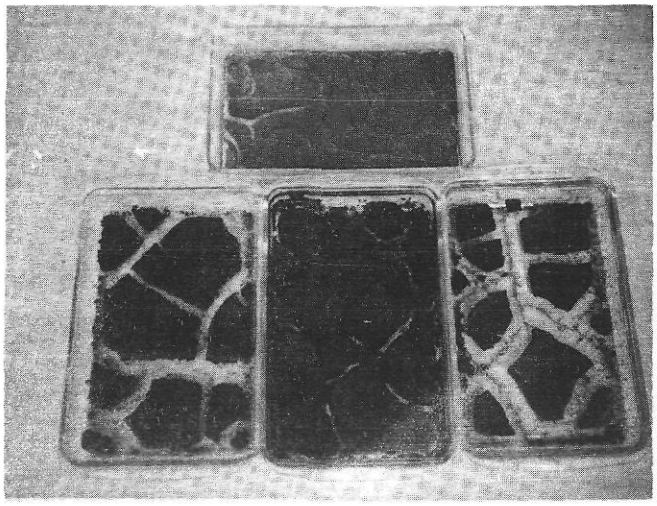

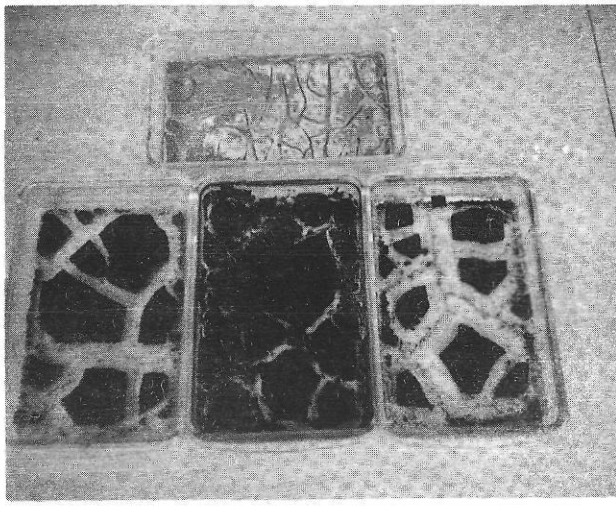

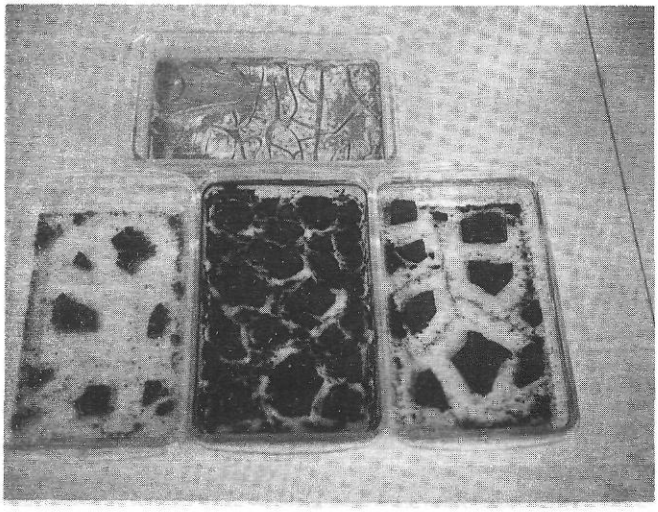

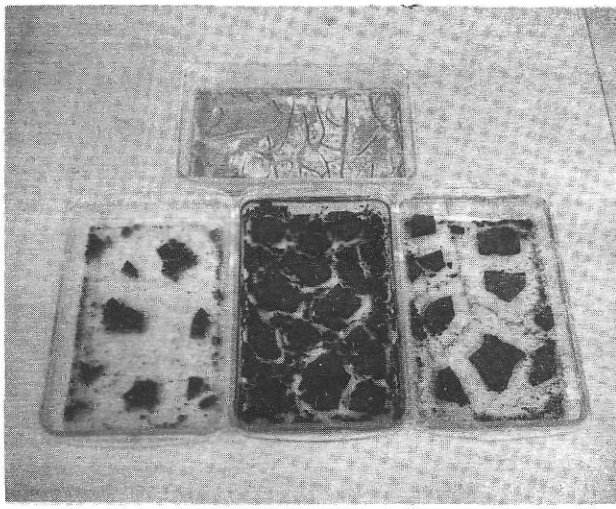

FIGURE 17 -- Photograph of Four Types of Water Treatment Sludge at Various Solids Contents.

at 75°F and 65%, respectively. All Billerica samples had initial solids contents of 6.20%. Two different solids contents were studied for Amesbury and Albany sludge. The higher solids contents were obtained by decanting some of the clear supernatant from the original sludge samples. The experimental conditions are tabulated in Table 12.

The sludge mass-time curves for the samples are shown in Figure 18 and Figure 19. Two control pans of water filled to 2 cm depth for ease of handling, served as controls. Toward the end of the drying run, water had to be added to the control pans to prevent the pans from becoming dry. This was due to the 2 cm initial depth of water evaporating in less time than some of the pans containing 4 cm of sludge. The pans of sludge were divided between two tables, located near the center of the environmental chamber. Each table contained one control pan of water. No difference in drying rates is attributed to the different locations; however, as a precautionary measure, the evaporation ratios for sludge samples on a given table were calculated using as the denominator, the values of the control pan of that table. Results are presented in Table 13.

As indicated for the sludge mass-time curves, the constant-rate drying period was the dominant one. The constant-rate period accounted for 80 to 85% of the water lost and 65 to 75% of the drying duration.

The sludges shrank vertically and appeared to have a free water surface in the early stages of drying. Cracks appeared when a solids

Table 12 --Experimental Arrangement for Drying Study D-3 Conducted at 75°F and 60% Relative Humidity.

Sample Number	Material	Initial Depth, cm	Area cm^2	S_o,%
1A	Amesbury	2	770	3.15
1B	Billerica	2	770	6.20
1C	Albany	2	770	0.92
1D	Water	2	770	-
2A	Amesbury	4	570	3.15
2B	Billerica	4	570	6.20
2C	Albany	4	770	0.92
2D	Water	4	770	-
3	Albany	2	570	1.40
4	Albany	4	570	1.40
5	Amesbury	4	570	4.47
6	Amesbury	2	570	4.47

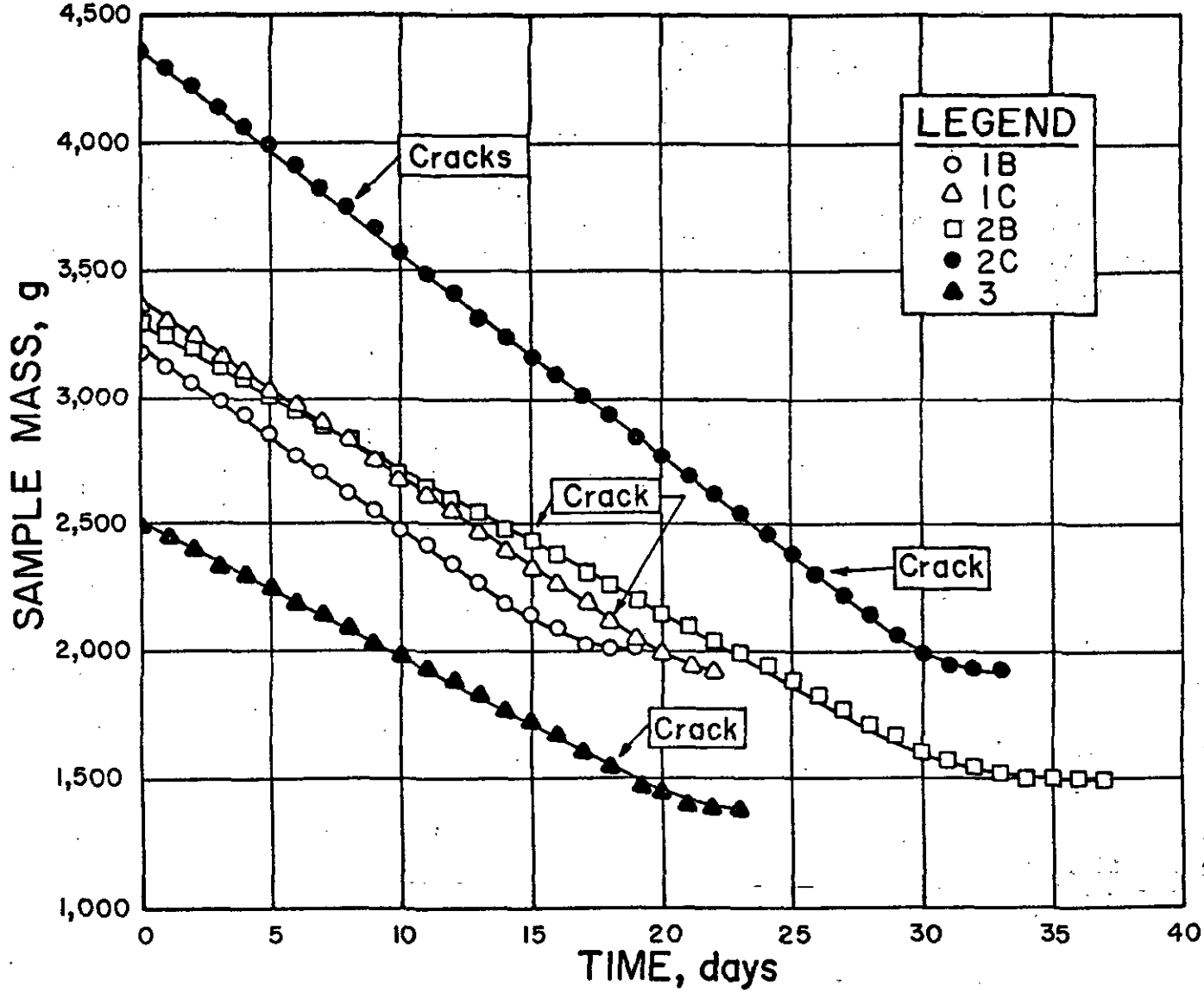

FIGURE 18 -- Sample Mass Versus Time Curves for Sludges (D-3) Drying at 75°F and 60% Relative Humidity.

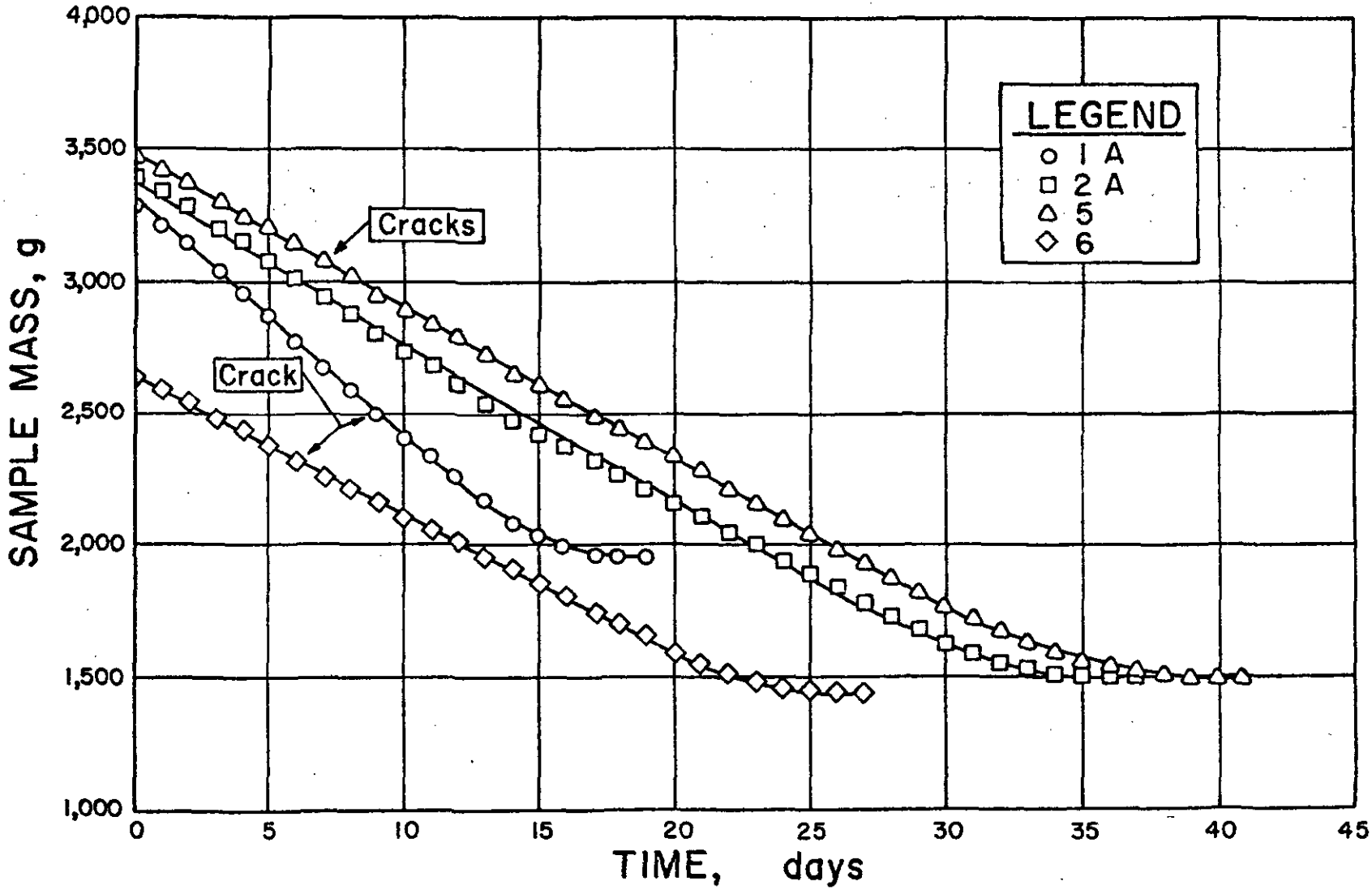

FIGURE 19 -- Sample Mass Versus Time Curves for Sludges (D-3) Drying at 75°F and 60% Relative Humidity.

Table 13 --Summary of Results for Drying Study D-3 Conducted at 75°F and 60% Relative Humidity.

Column Number	Material	Initial Depth, cm	Solids, %			U_{CR}, %	Constant-Rate Drying	
			S_o	S_{CR}	S_e		I_c, gm/hr-cm^2	E,%
1A	Amesbury	2	3.15	16.1	76.5	640	0.0045	118
1B	Billerica	2	6.20	21.8	81.1	360	0.0039	103
1C	Albany	2	0.92	6.1	75.0	840	0.0038	84
1D	Water	2	-	-	-	-	0.0038	-
2A	Amesbury	4	3.15	15.4	76.5	600	0.0044	116
2B	Billerica	4	6.20	23.6	82.5	270	0.0042	93
2C	Albany	4	0.92	13.2	80.8	780	0.0043	96
2D	Water	4	-	-	-	-	0.0045	-
3	Albany	2	1.40	14.3	75.0	460	0.0038	84
4	Albany	4	1.40	24.4	78.8	380	0.0040	105
5	Amesbury	4	4.47	15.4	75.3	480	0.0042	93
6	Amesbury	2	4.47	17.2	73.5	440	0.0038	84

content of 7 to 10% was reached which caused a larger surface area to be exposed. The increased surface area would increase the drying rate possibly offsetting any decrease in the drying rate due to the surface becoming dry. After cracks were formed in the sludge samples, horizontal shrinkage became more pronounced. At equilibrium the sludge samples had shrunk to irregular-shaped pieces with a maximum dimension of 2 cm and approximately 0.5 cm thick. The pieces appeared completely dry and were warped, exposing the bottom, therefore exposing a maximum surface area.

Evaporation ratios ranged from 84 to 118%. Pans with lower initial solids contents gneerally dried at a faster rate than samples with higher initial solids. The larger evaporation ratios can be attributed to heat advection since these samples generally contained a larger amount of solids, W_{TS}.

Curves showing the drying rate-moisture content relationships are shown in Figures 20, 21, and 22 . After the initial temperature adjustment, the sludges remained in the constant-rate drying period while 80 to 85% of the water was lost. Only 15 to 20% of the water was lost during the falling-rate drying period. It was studied for theoretical interest only since the sludges could have been removed from a drying bed before the critical moisture content was reached. No distinct second critical moisture content was established, therefore the falling-rate drying period was considered as one period. Both a straight line and a parabola were fitted to the falling rate portion by regression analysis. As a rule, the parabola gave a higher value

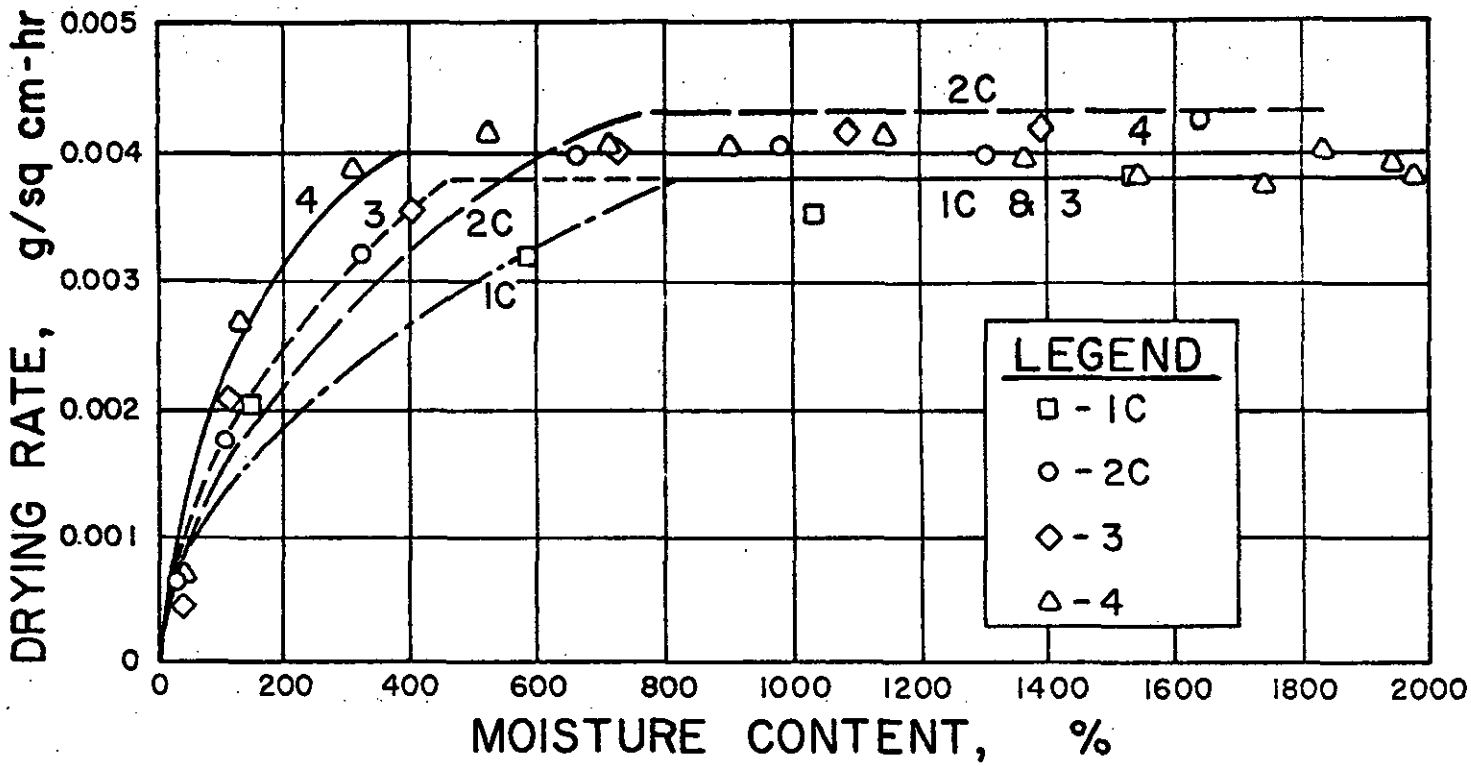

FIGURE 20 -- Drying-Rate Curves for Sludges (D-3) Drying at 75°F and 60% Relative Humidity.

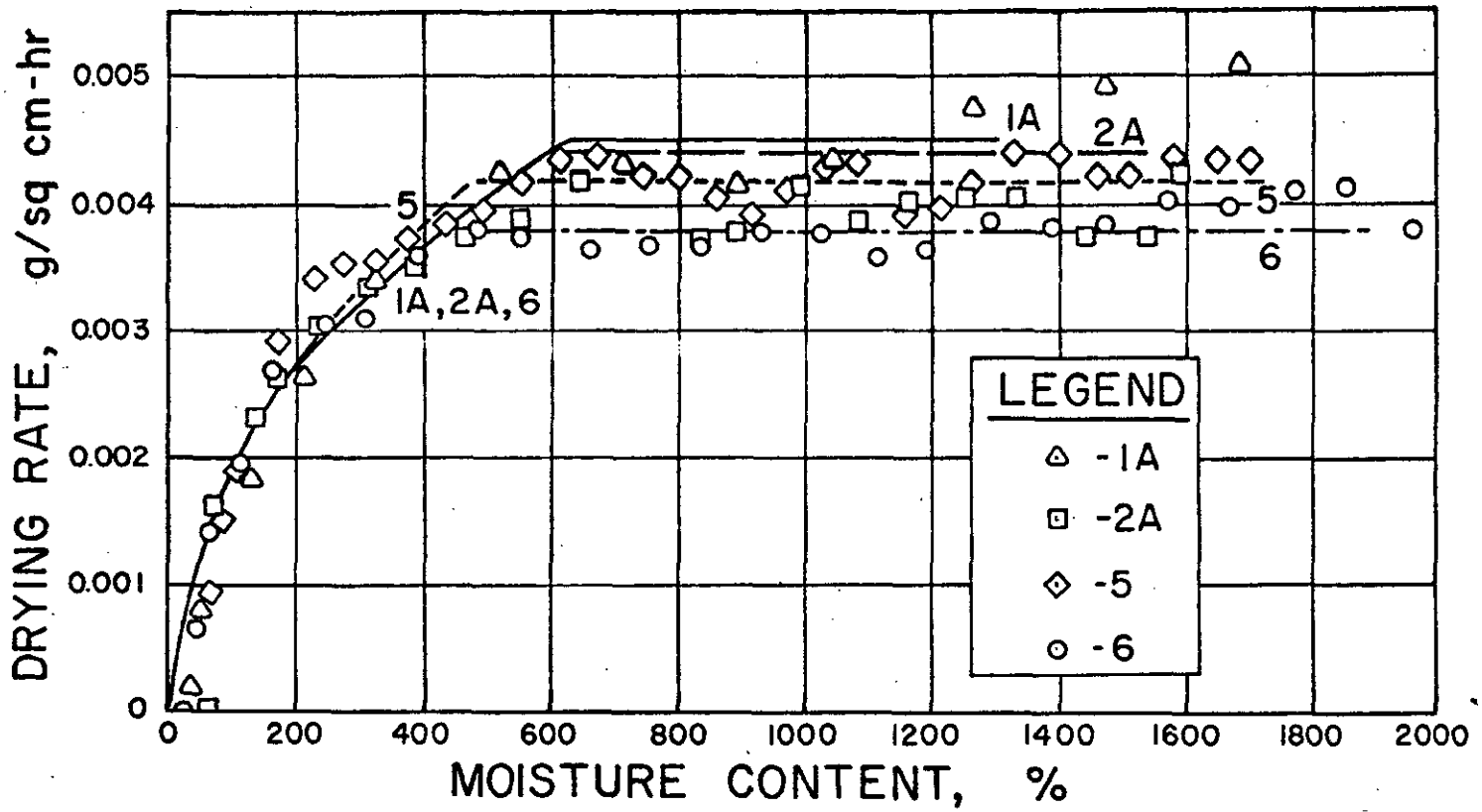

FIGURE 21 -- Drying-Rate Curves for Sludges (D-3) Drying at 75°F and 60% Relative Humidity.

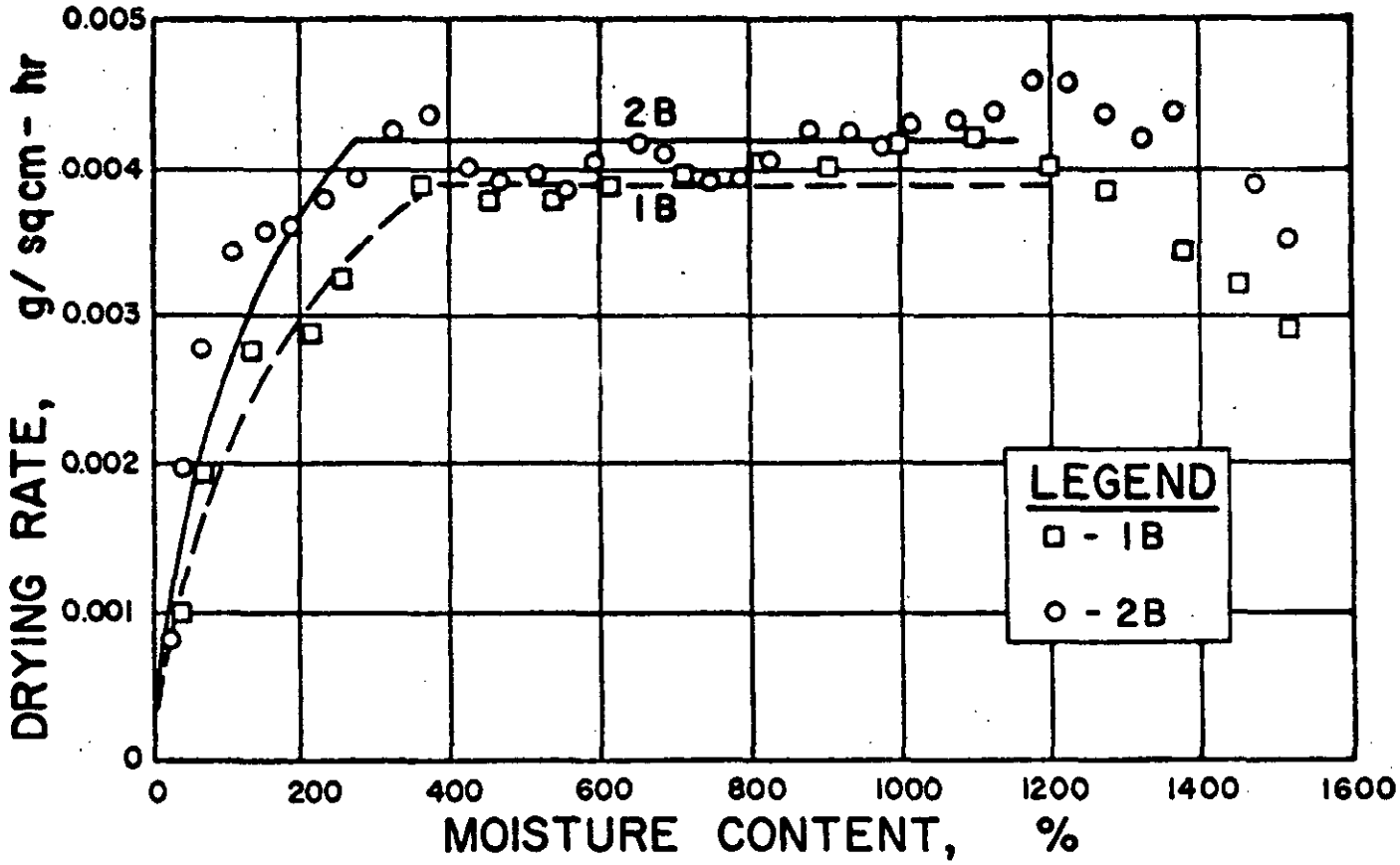

FIGURE 22 -- Drying-Rate Curves for Sludges (D-3) Drying at 75°F and 60% Relative Humidity.

for the correlation coefficient. Values for the first critical moisture content ranged from 270 to 840.

Critical moisture content. Both straight lines and parabolas were fitted by regression analysis to the drying intensity-moisture content data in order to obtain values for the first critical moisture content. As a rule, the parabola provided a better fit and gave a higher value for the correlation coefficient. The intersection of the parabola with the constant rate curve was taken as the critical moisture content.

Relationship for drying time. A relationship for calculating the drying duration in the falling-rate portion was developed assuming the relationship between drying intensity and moisture content was parabolic. The relationship can be expressed as

$$I^2 = 4pU \tag{110}$$

or

$$I = 2p^{1/2}U^{1/2} = I_c\left(\frac{U}{U_{CR}}\right)^{1/2} \tag{111}$$

where

$$2p^{1/2} = I_c / U_{CR} = \text{Constant.} \tag{112}$$

From Equation 15,

$$t = \frac{W_{TS}}{100A} \int_{U_t}^{U_o} \frac{dU}{I} \tag{15}$$

Substituting Equation 111 into Equation 15 and performing the integration gives the drying duration in the falling-rate period as

$$t_f = \frac{2W_{TS}\, U_{CR}^{1/2}}{100\, A \cdot I_c} \left(U_o^{1/2} - U_t^{1/2}\right) \tag{113}$$

$$(U_t \leq U \leq U_{CR})$$

For a sample drying in both the constant and falling-rate period, the total drying duration would be

$$t = \frac{W_{TS}}{100AI_c} \int_{U_{CR}}^{U_o} dU + \int_{U_t}^{U_{CR}} \left(\frac{U}{U_{CR}}\right)^{1/2} dU$$

$$= \frac{W_{TS}}{100A\, I_c} \left[U_o - U_{CR} + 2U_{CR}^{1/2} \left(U_{CR} - U_t^{1/2}\right)\right] \tag{114}$$

$$(U_t \leq U_{CR} \leq U_o)$$

Dewatering

Preliminary Studies. A preliminary investigation was conducted to study the comparison of water treatment sludge drying and dewatering (drying and drainage) simultaneously. Dewatering study DW-1 consisted of two columns of Albany sludge dewatering at 76°F and 46% relative

humidity. Column 1 was permitted to drain while undergoing drying but Column 2 dewatered by drying only. Column 1 contained 8.0 cm Ottawa sand supported by 2.5 cm coarse sand and 8.0 cm small stone. The experimental arrangement is given in Table 14 along with experimental results.

The sludge mass-time curves for both columns are shown in Figure 23. Both samples remained in the constant-rate drying period for practically the entire dewatering run. The average drying rate for Column 1 was 0.0057 gm/hr-cm^2 as compared to 0.0063 gm/hr-cm^2 for Column 2.

Shrinkage-time curves for both samples are shown in Figure 24. The depth-time curve for Column 2 was linear over most of the dewatering period indicating constant-rate drying. Vertical shrinkage in Column 2 diminished at a solids content of 4.6% and horizontal shrinkage began with cracks forming throughout the depth of the sludge cake.

Dewatering study DW-2. Dewatering study DW-2 consisted of three columns of water used as a control. In addition, three large pails of water in various locations within the environmental chamber were evaporated concurrently as controls. Temperature and relative humidity remained constant at 76 ± 1°F and 30 ± 2%.

The dewatering columns contained 45.7 cm of sludge on 11.5 cm of Ottawa sand supported by 3.8 cm of stone. The initial solids content of the sludge was 1.3%. The initial depth of water in the control column was 30 cm in order to eliminate any "freeboard" effects caused by the surfaces of the columns being at different elevations after

TABLE 14 --Results of Albany Sludge, DW-1, Dewatering at 76°F and 46% Relative Humidity.

Column Number	1	2
Drainage permitted	Yes	No
Initial solids, %	1.22	1.22
Initial sludge depth, cm	13.5	13.5
Final solids content, %	75.5	73.8
I_c, gm/cm^2-hr	0.0057	0.0063
Support media	sand-stone	none

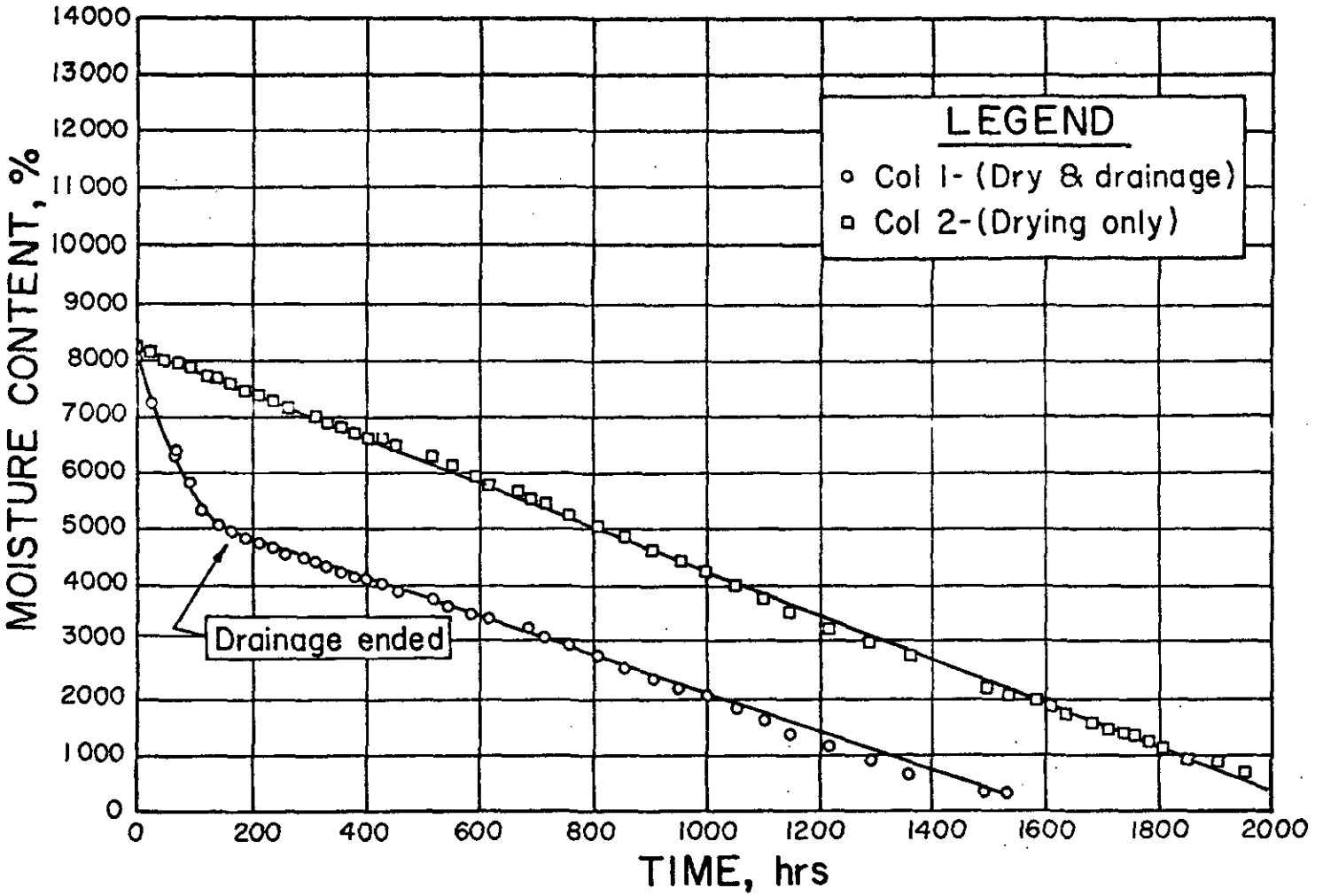

FIGURE 23 -- Sample Mass Versus Time Curves for Albany Sludge Dewatering at 76°F and 46% Relative Humidity.

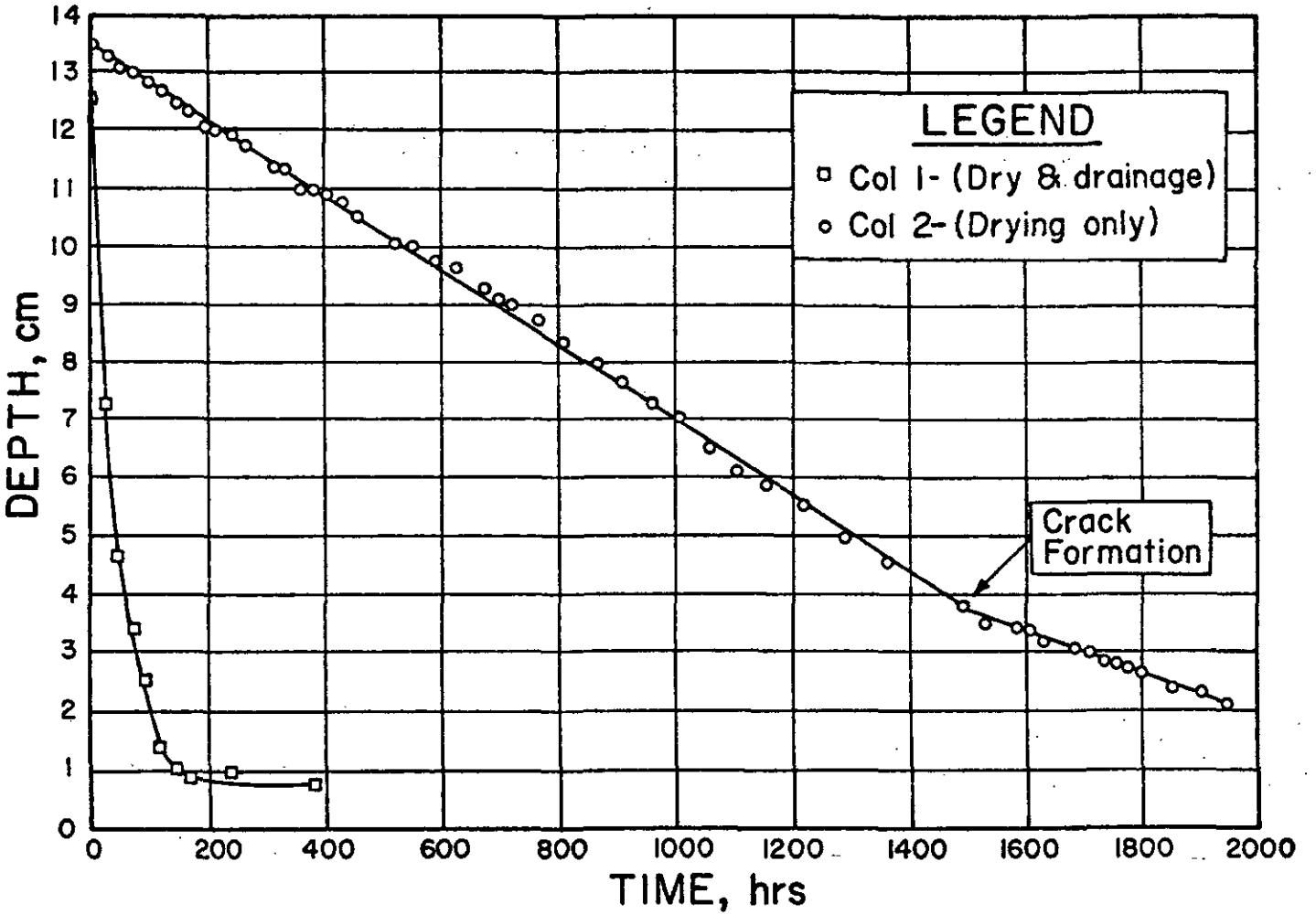

FIGURE 24 -- Change in Depth of Albany Sludge Dewatering at 76°F and 46% Relative Humidity.

drainage had occurred in the sludge columns. A picture of the dewatering columns is shown as Figure 25.

The three large pails of water showed no significant difference among the evaporation rates indicating constant drying conditions. The average evaporation rate for the three pails was 0.0064 gm/hr-cm^2.

The mass of the dewatering columns were determined periodically after drainage ended. The sludge mass-time curves for the columns are shown in Figure 26. Column 3 was omitted from the data analysis since some water was accidentally lost early in the study. The sludge columns remained in the constant rate drying period throughout the drying run. The average drying rate for the two columns of sludge was 0.00524 gm/hr-cm^2 and the average evaporation ratio was 87.5%. At the end of the drying run the columns were dismantled and the sludge cakes carefully removed. The sludge cakes appeared dry and could be readily picked up by hand. However, the average solids contents were only 10-12%, demonstrating that this particular sludge contained large amounts of bound water. Figure 27 is a photograph of one of the sludge cakes. A thin layer approximately 5 mm thick and lighter in color encased the sludge mass causing the sludge cake to appear to be drier on the outside than in the interior. This layer was removed from one cake, cut into small pieces and a gravimetric solids content analysis performed. The solids content was 10.7% in the interior and 12.3% in the outer layer.

The accumulated volume of filtrate for each of the three sludge columns is shown in Figure 28 and the variation of total head (H_o)

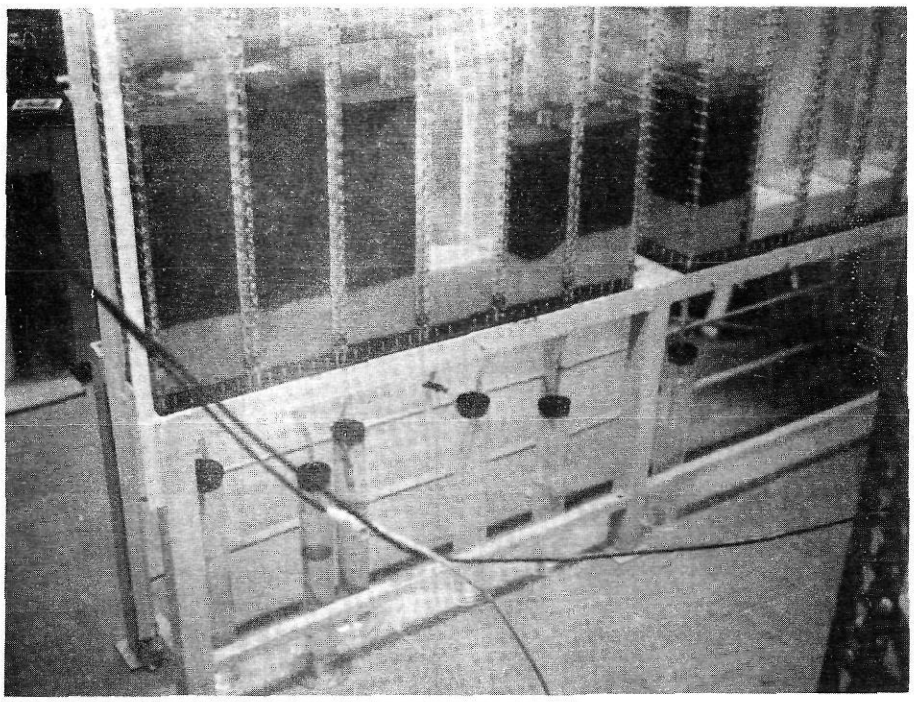

FIGURE 25 -- Photograph of Sludge Dewatering Columns in Dewatering Study DW-2.

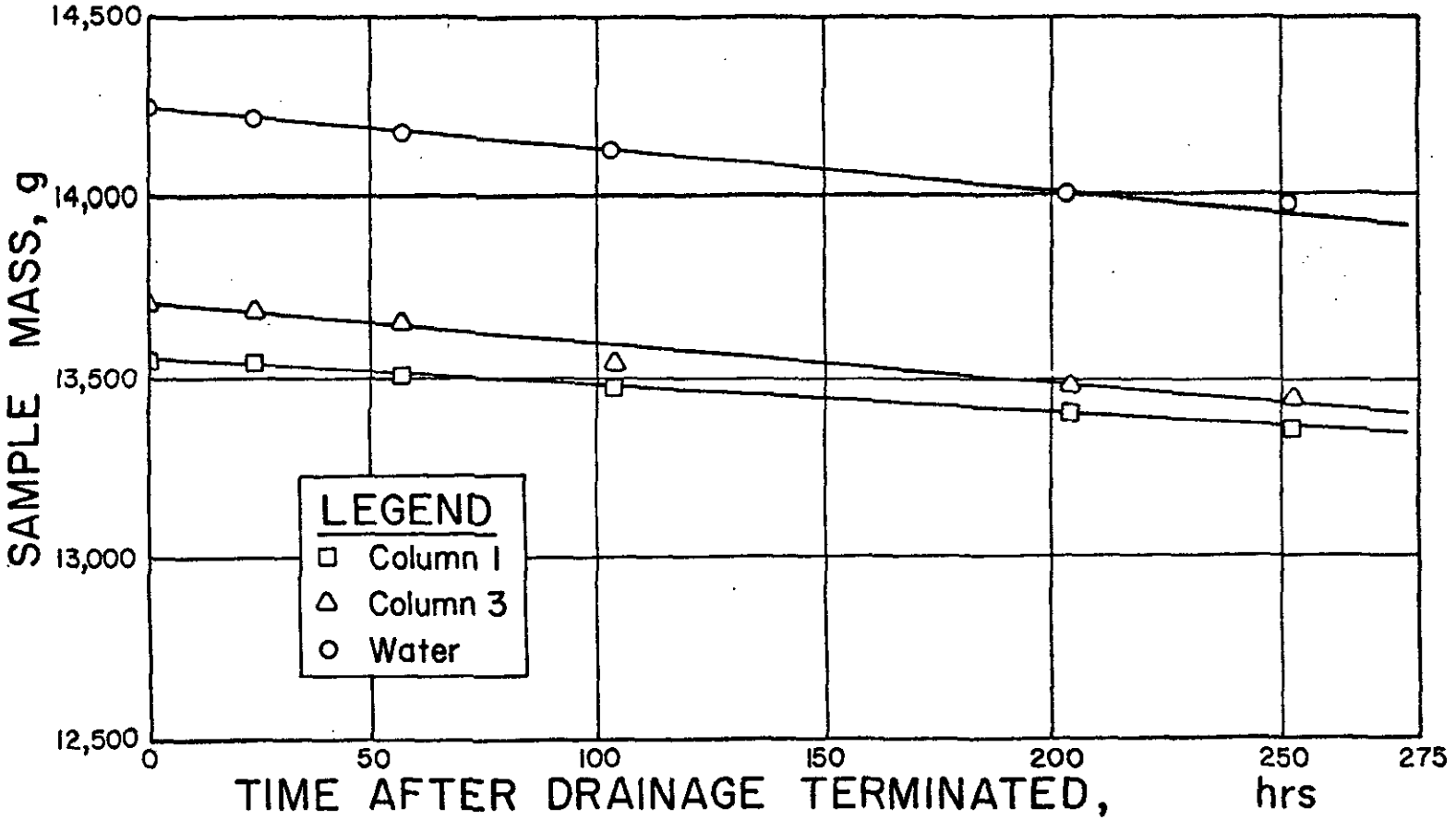

FIGURE 26 -- Sample Mass Versus Time Curves for Drying Period of Dewatering Study DW-2.

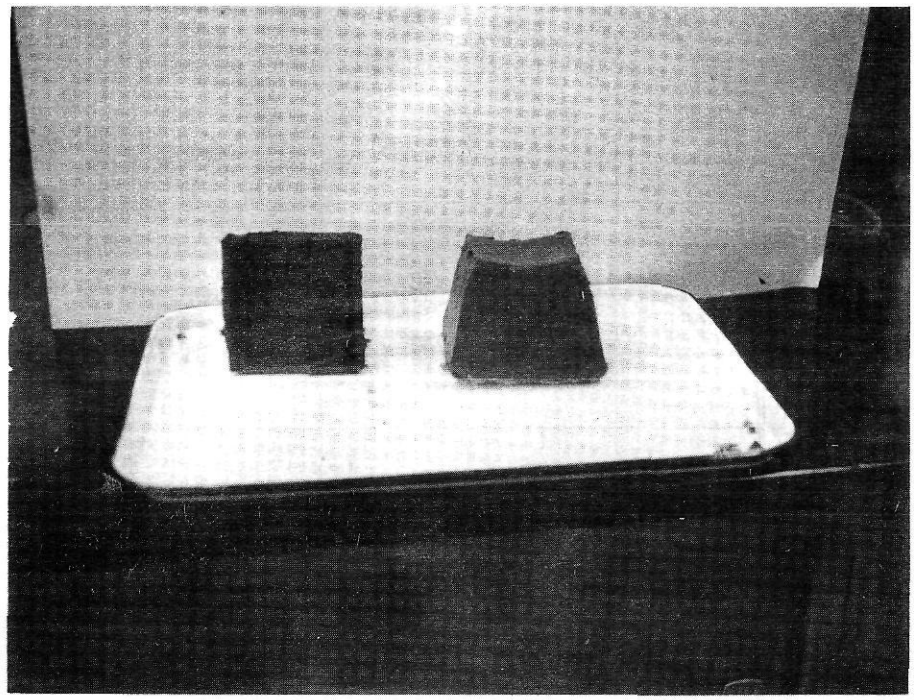

FIGURE 27 -- Photograph of Dewatered Sludge Cake.

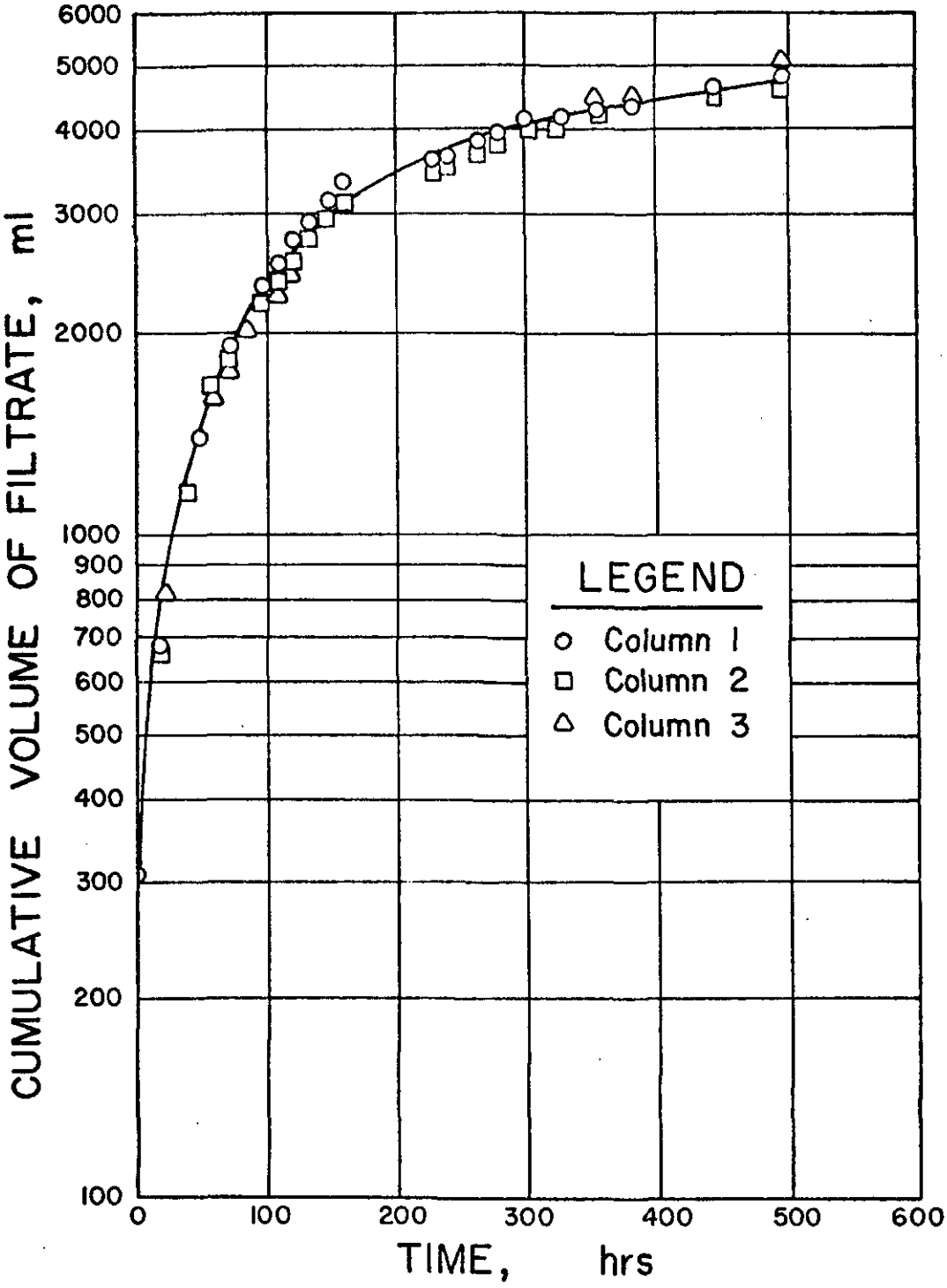

FIGURE 28 -- Cumulative Volume of Filtrate Versus Time for Albany Sludge Dewatering on Ottawa Sand (DW-2).

is shown in Figure 29. The predicted head values using empirical media factors and Equation 53 are shown as solid lines.

Dewatering study DW-3. Dewatering study DW-3 consisted of 9 columns of sludge and 2 columns of water dewatering under controlled conditions. Temperature and relative humidity were maintained at 76 ± 1°F and 35 ± 2%. Air was supplied uniformly to each column to expedite the dewatering process. Each column contained 9 cm of Ottawa sand supported by 2.5 cm of stone. The experimental conditions and results are shown in Table 15.

The two columns of water (columns 4 and 8) had an average drying rate of 0.0097 gm/hr-cm^2 as calculated from the slopes of the sludge mass-time data. There was no significant difference in the drying rates of the two columns of water, thus indicating constant drying conditions. The evaporation rate for water at 76°F and 35% relative humidity, with negligible wind and sunlight, is 0.02 in/day from Figure 2. Converted to comparable units, this would be 0.0021 gm/cm^2-hr, considerably less than the control column value of 0.0097 gm/cm^2 - hr. If the vertical air stream alone accounted for the difference in drying rates, the equivalent horizontal wind velocity from Figure 2 would be 7.5 miles per hour for the control columns.

Dewatering with and without drainage was studied with Billerica sludge in columns 5 and 6, and column 1, respectively. The drying rates for columns 5 and 6 (drying and drainage) were lower than column 1 (drying only). This could have resulted from the higher solids content in columns 5 and 6 due to drainage or the larger amount of

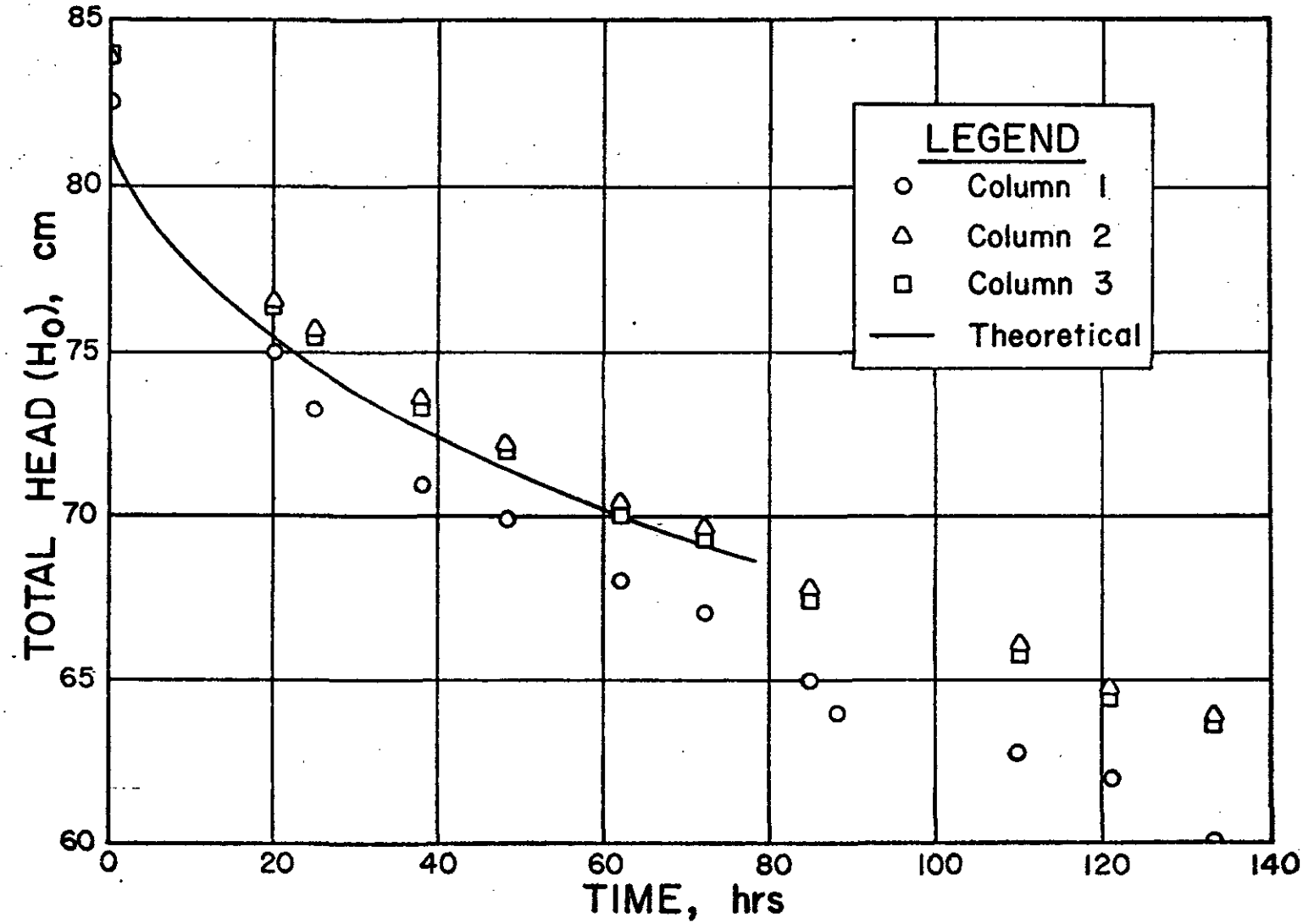

FIGURE 29 -- Drainage Curves for 45.7 cm of Albany Sludge (DW-2) Dewatering on Ottawa Sand.

Table 15 ==Results of Four Sludges DW-3 Dewatering at 76°F and 35% Relative Humidity.

Column Number	Material	Initial Depth, inches	Solids,%			I_c gm/cm^2-hr	E,%
			Initial	After Drainage	Final		
1*	Billerica	18	6.10	-	12.4	0.0128	136
2*	Albany	18	1.86	-	3.7	0.0120	128
3	Albany	12	1.86	5.8	15.2	0.0070	74
4*	Water	12	-	-	-	0.0093	-
5	Billerica	12	6.10	10.4	20.6	0.0075	79
6	Billerica	12	6.10	9.1	22.8	0.0086	91
7	Amesbury	12	3.67	7.1	20.6	0.0115	122
8*	Water	12	-	-	-	0.0096	-
9	Amesbury	12	3.67	6.2	33.4	0.0148	157
10	Murfreesboro	12	4.80	41.0	81.0	0.0055	58
11	Murfreesboro	12	4.80	29.2	92.5	0.0060	64

*Denotes Drying Only.

freeboard due to the smaller initial depth. Columns 5 and 6 differed significantly in their drying rates, column 6 having the faster rate. The amount of water lost by drainage was larger for column 5 than the drainage volume from column 6. This resulted in a higher solids content and a lower drying rate for column 5. The evaporation ratio for column 1 was 137% which was partially due to the high rate of heat transfer by radiation and conduction to the dark sludge surface. The sludge mass-time curves for columns 1, 5, and 6 are shown in Figure 30. The cumulative volume of filtrate-time curves for each sample are shown in Figures 31 and 32.

Dewatering of Albany sludge with and without drainage was studied in columns 3 and 2, respectively. The drying rates were significantly different, column 2 having the larger rate. Again, the lower drying rate occurred in the column with the higher solids content. The average evaporation ratios for column 2 and 3 were 128% and 74% respectively. Sludge mass-time curves for columns 2 and 3 are shown in Figure 33.

Columns 7 and 9 contained Amesbury sludge dewatering by simultaneous drying and drainage. These two sludges had an average evaporation rate of 140%. Immediately after drainage stopped, the sludge cakes shrank horizontally, pulling away from the container walls. The shrinkage left a large porous surface exposed, greatly increasing the drying area. The sludge was dark in color, thus, some of the increased drying rate may be attributed to heat advection. The mass-time curves for columns 7 and 9 are shown in Figure 33.

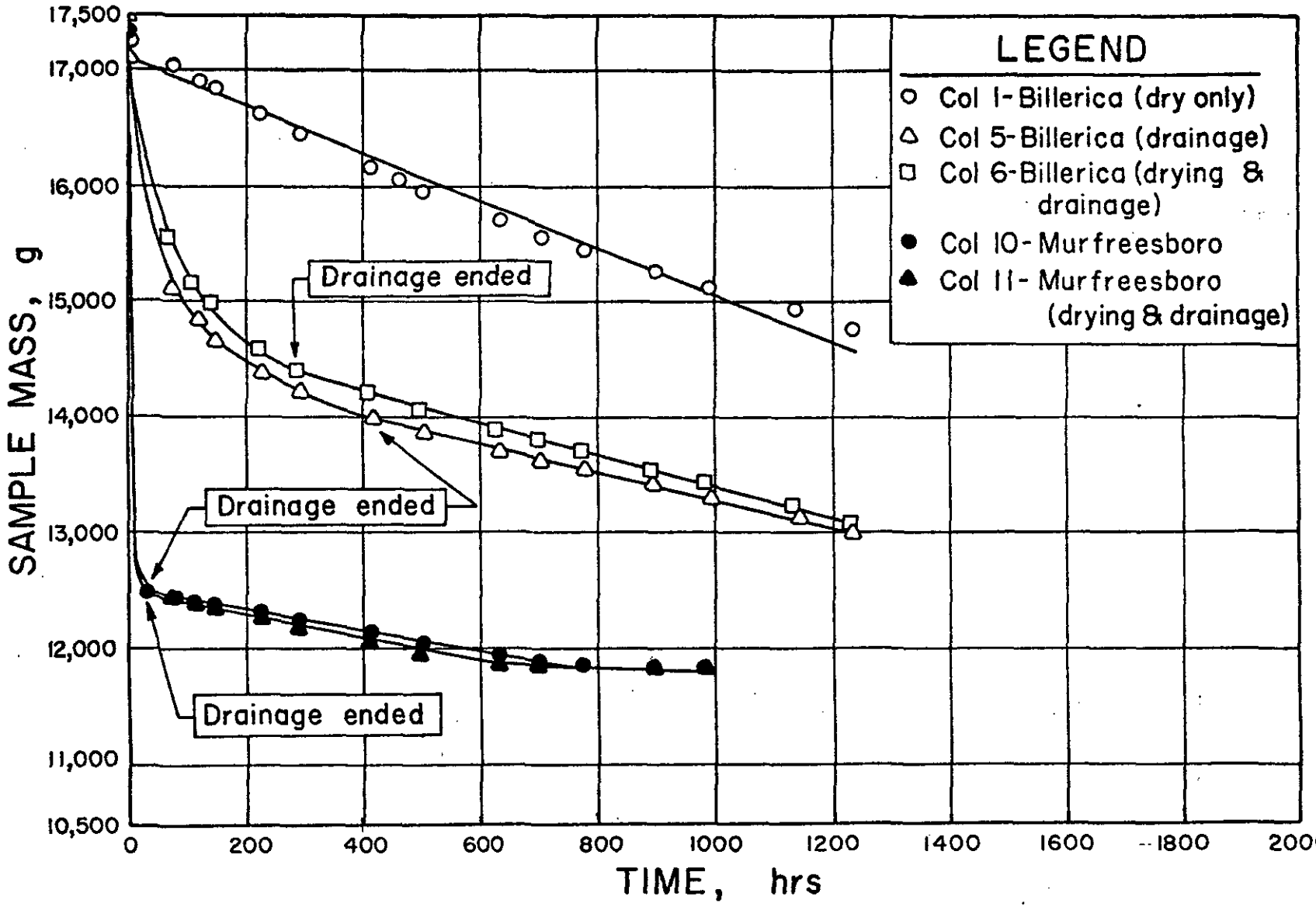

FIGURE 30 -- Sample Mass Versus Time Curves for Sludges (DW-3) Dewatering at 76°F and 35% Relative Humidity.

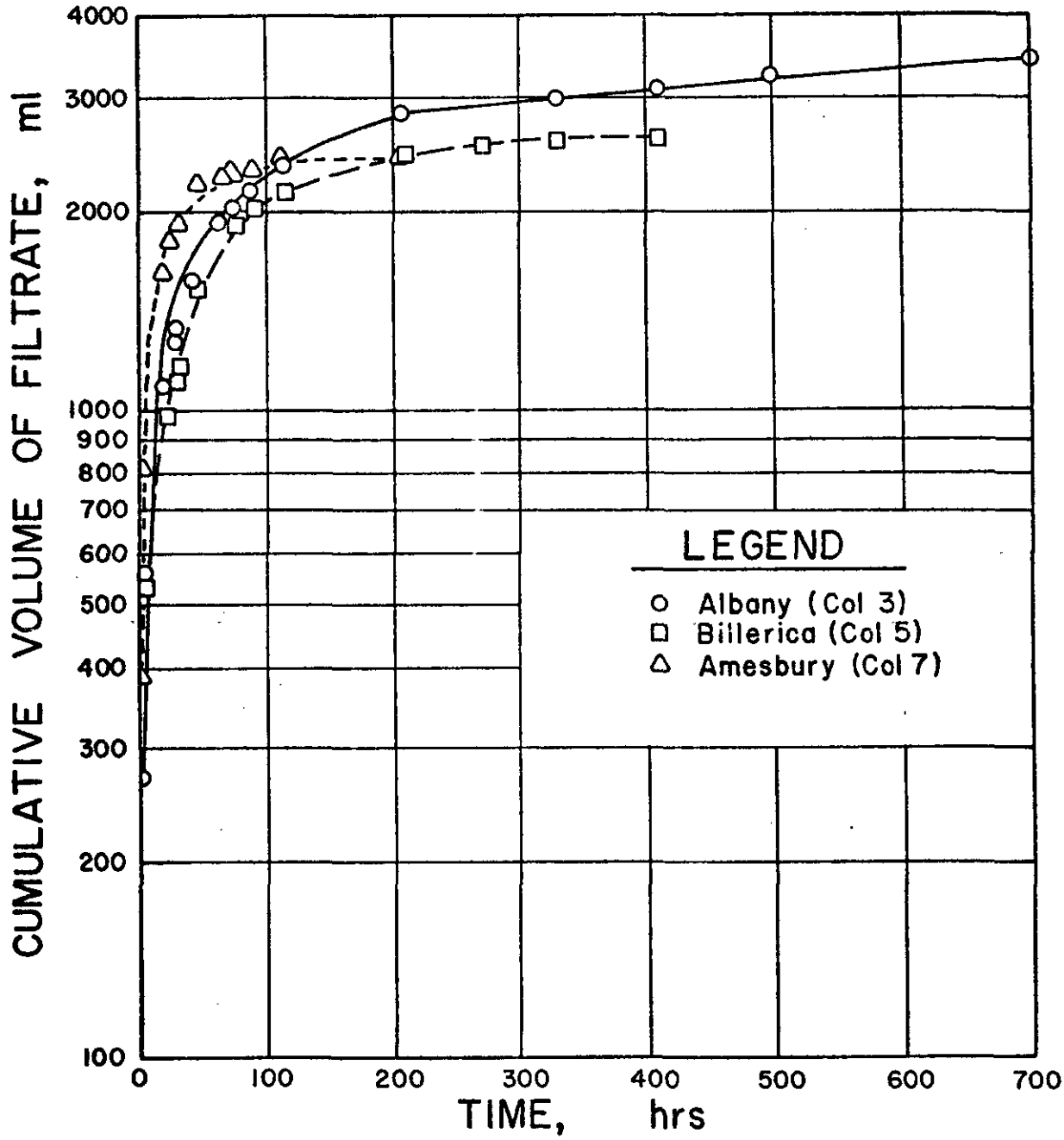

FIGURE 31 -- Cumulative Volume of Filtrate Versus Time for Sludges (DW-3) Dewatering on Ottawa Sand.

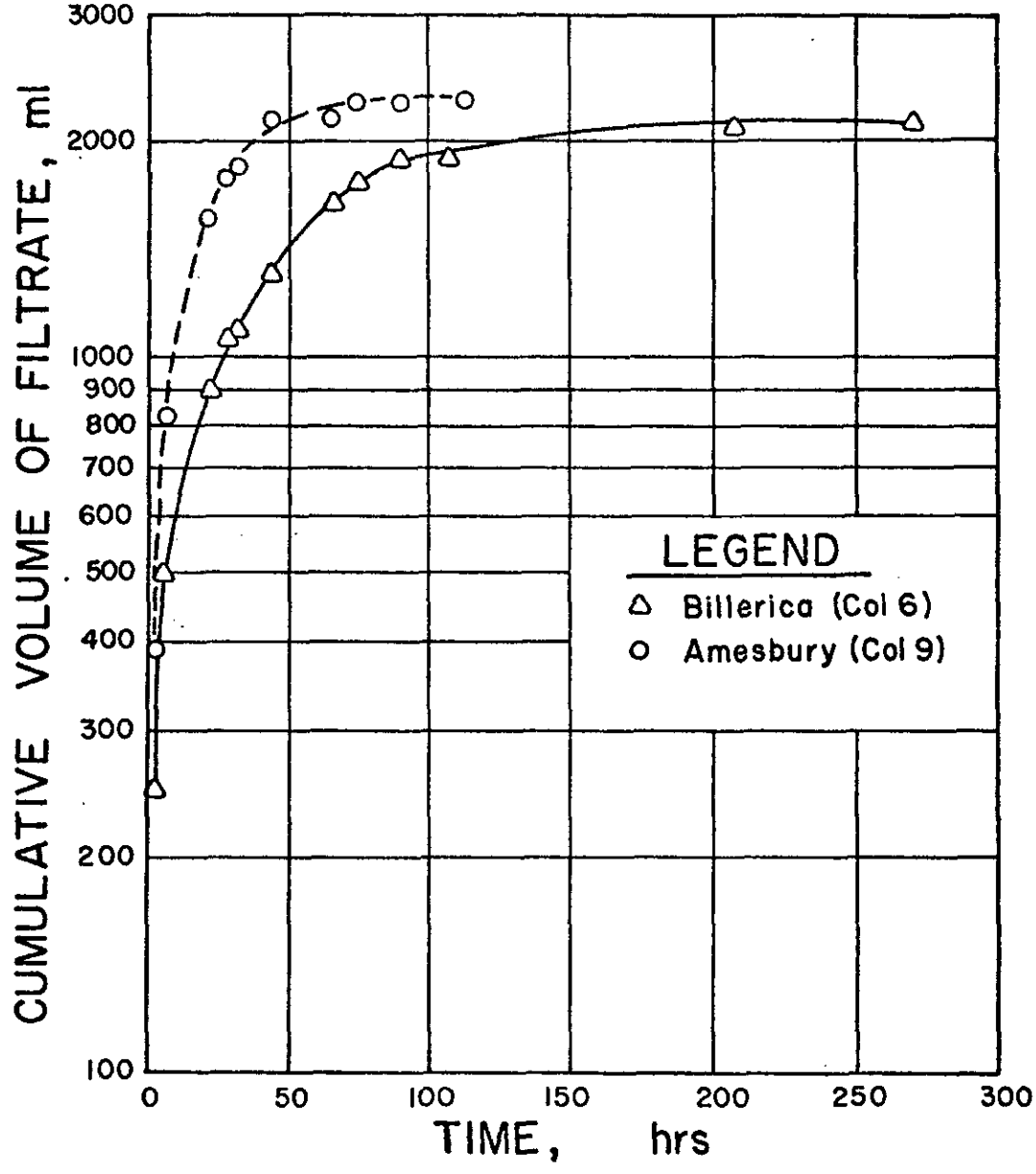

FIGURE 32 -- Cumulative Volume of Filtrate Versus Time for Sludges (DW-3) Dewatering on Ottawa Sand.

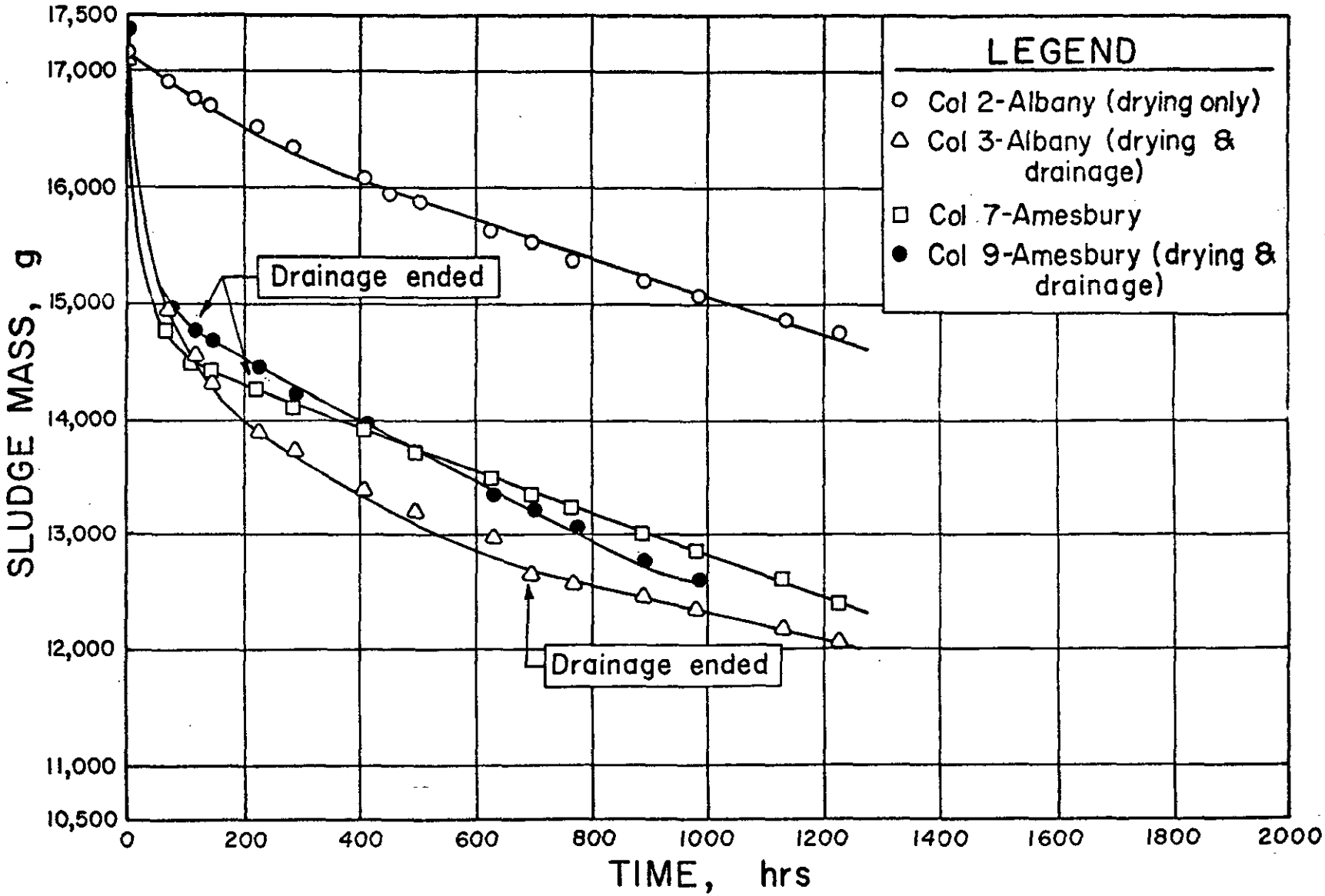

FIGURE 33 -- Sample Mass Versus Time for Sludges (DW-3) Dewatering at 76°F and 35% Relative Humidity.

Murfreesboro sludge was dewatered by drying and drainage in columns 10 and 11, respectively. The sludge dewatered very rapidly, drainage being completed in approximately 20 hours. Although the sludge initially contained 4.8% total solids, the solids settled rapidly to a dense layer approximately 3 cm thick, leaving a large amount of clear supernatant. The solids content was approximately 35% and the depth of sludge cake was 2.3 cm when drainage ended. Although some vertical cracks appeared, the sludge cake did not have a large exposed drying surface. The average evaporation ratio was 62%, the smallest of any sludges investigated. The sludge mass-time curves for columns 10 and 11 are shown in Figure 30.

The variation of total head (H_o) for the sludge samples are shown in Figure 34 along with predicted H_o values from Equation 53. The time span covered by Equation 53 is less than the total time span for total drainage. This is due to two reasons: first, approximately 25% of the filtrate was due to the distilled water used to saturate the sand columns initially; second, Equation 53 does not cover the entire drainage period but is valid only until the decreasing sludge surface adjoins the increasing sludge cake. The remaining drainage, affected by consolidation and shrinkage, is unaccounted for by the drainage model. The drainage data for dewatering study DW-3 are shown in Table 16.

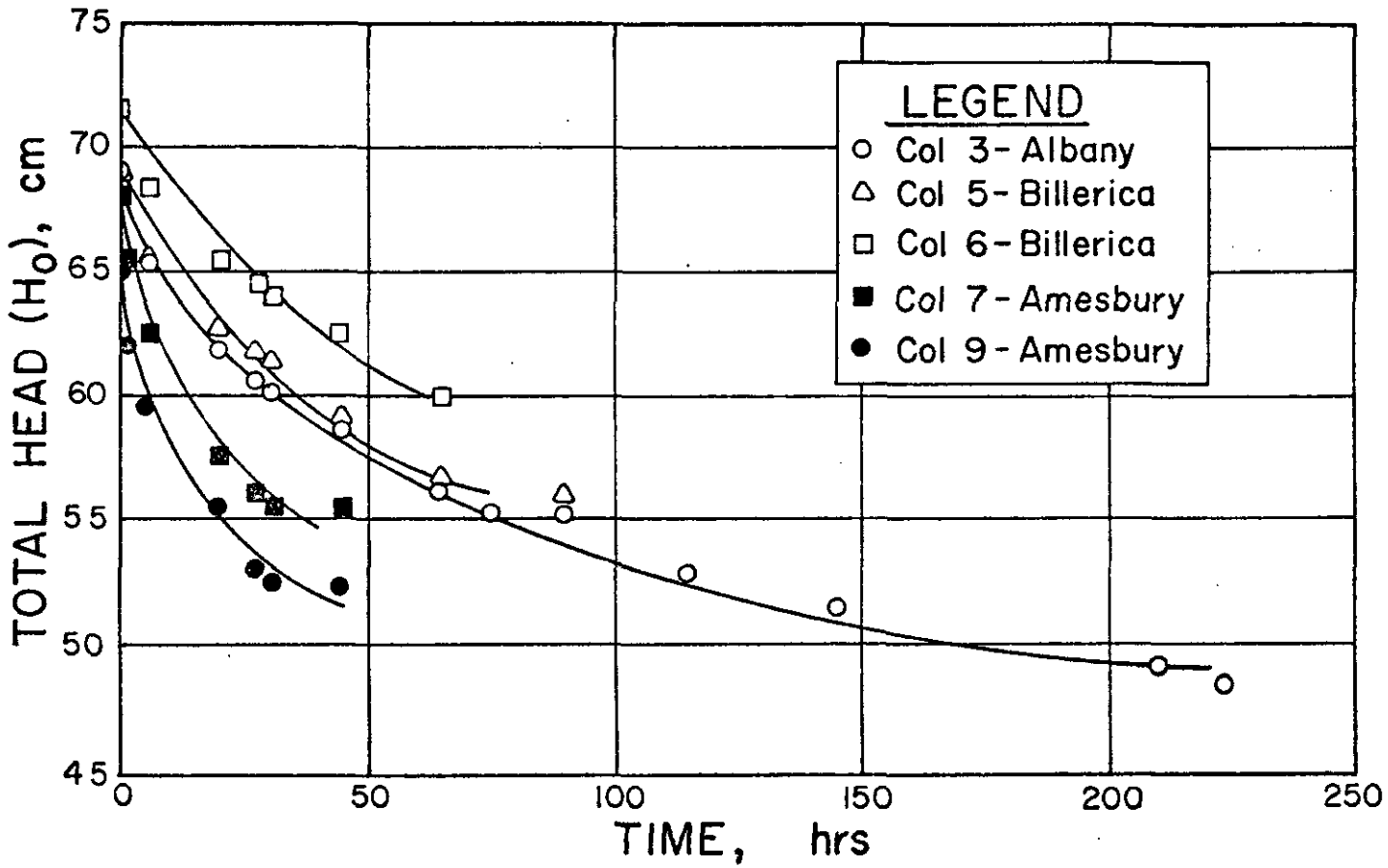

FIGURE 34 -- Drainage Curves for 30.8 cm of Sludge (DW-3) Dewatering on Ottawa Sand.

Table 16 --Drainage Data for Dewatering Study, DW-3.

Sludge	Amesbury	Albany	Billerica
Initial Solids, %	3.67	1.86	6.10
Final Solids, %	6.65	5.80	10.40
Specific Resistance, sec^2/gm	1.04×10^9	8.0×10^9	3.5×10^9
Coefficient Compressibility	0.802	0.49	0.83
Media Factor	0.12	0.17	0.06

Moisture and Solids Profiles

Preliminary measurements. The gamma-ray attenuation method of moisture and solids profiles measurements required prior determinations of attenuation coefficients and particle densities. The energy spectrum of the Cs^{137} source was determined as a check on the calibration and performance of the counting equipment. The familiar Cs^{137} spectrum as shown in Figure 35 was determined.

The attenuation coefficients were determined by measuring the attenuation of the gamma beam through water in the small plastic boxes. A plot of N/N_p for 16 minute counts through water is shown in Figure 36. The slope of the line is equal to $\mu\rho$. The values for attenuation coefficients obtained are shown in Table 17 along with values from the literature.

Particle density measurements of sand and dry sludge solids were made by the specific gravity method. The results are presented in Table 18.

Moisture movement in sand. Moisture profiles were determined for the sand layers of the dewatering columns by the attenuation method. The sand layers remained saturated until drainage from the sludge layers terminated. After drying caused cracks to appear in the sludge layer, or the sludge cake receded from the column walls, the water in the sand layer was lost. The sand layers were devoid of water at the termination of the drying period.

Table 17--Attenuation Coefficients at 0.661 Mev for the Various Materials

Material	μ, cm^2/gm	Standard Deviation	Reference
Albany sludge	0.0780	0.0048	Data
Amesbury sludge	0.0792	0.0050	Data
Billerica sludge	0.0781	0.0031	Data
Average Value for sludges	0.0784	-	Data
Ottawa sand	0.0765	0.0060	Data
Water	0.0842	0.0007	Data
Water	0.0839	-	Adrian
Water	0.0815	0.0008	Davidson et al.
Soil (average value)	0.0775	-	Reginato and Van Bavel

Table 18 --Particle Density Values, g/cm^3, for Water Treatment Sludge Solids and Ottawa Sand.

Name	ρ, gm/cm^3	Standard Deviation
Billerica	1.95	0.025
Amesbury	2.64	0.049
Albany	2.36	0.023
Murfreesboro	2.75	0.019
Ottawa sand	2.64	0.009

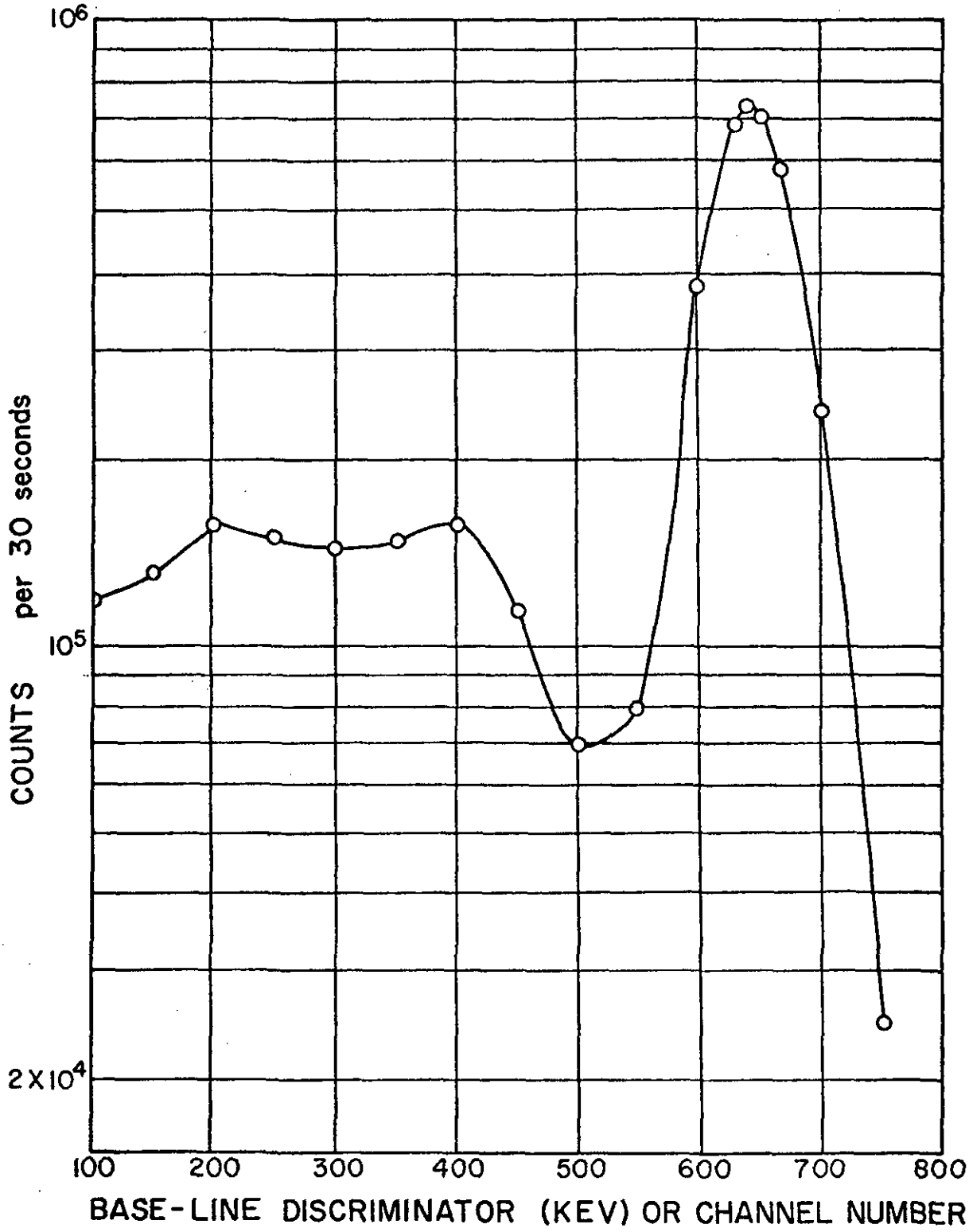

FIGURE 35 -- Energy Spectrum for 250 millicuries Cs^{137} Source.

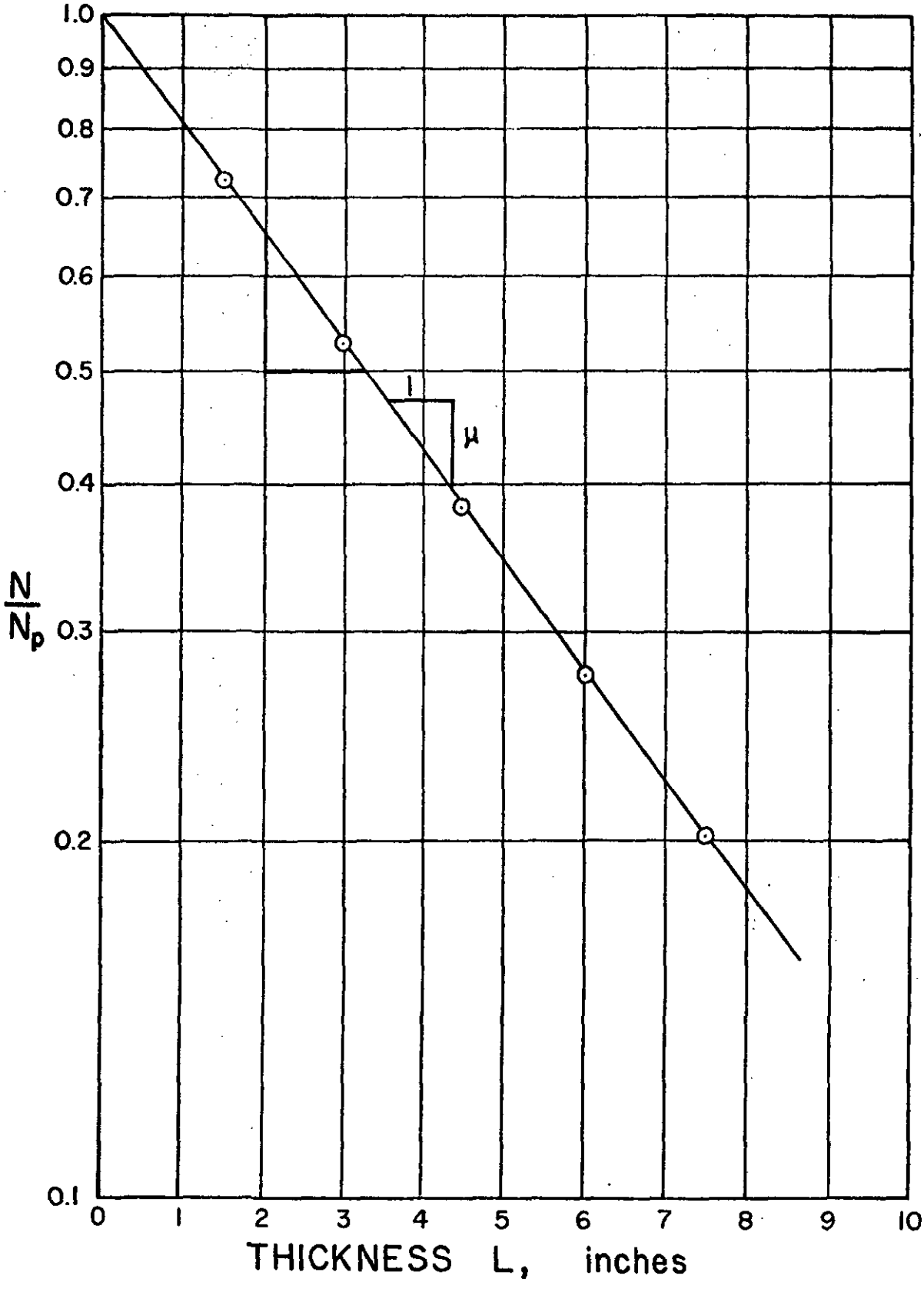

FIGURE 36 -- Variation of the Ratio N/N_p with Thickness of Water at 0.661 Mev.

The method for measuring water content in sand was tested using Ottawa sand in the small plastic boxes. Values of water content in the sand as determined from Equation 97 are shown in Table 19 along with values obtained by volumetric measurements. There was 2.6% difference between the two methods. The slight variations in water content (θ) at various depths was attributed to differences in the bulk density of the compacted sand.

Profiles of water content in the supporting sand layers were vertical during the initial dewatering stages as shown for column 3 in Figure 37 and column 5 in Figure 38. During the drying of sludge when drainage was not permitted, the water content remained constant, as shown for column 2 in Figure 38, when dewatering occurred by drying only. After enough water was lost from the sludge to cause the sludge cake to recede from the container walls, water was lost from the sand layer as shown in Figures 38 and 39. Column 2, containing a lower initial solids content (1.86 compared to 6.1% for column 1) did not dry sufficiently during this study to shrink horizontally, thus the sand layer remained saturated.

Moisture and solids profiles in sludge. The moisture and solids profiles of sludge undergoing drying and drying with drainage were measured periodically by the attenuation method. Since the mass of the samples had been determined periodically, the average values for solids content and moisture content could be calculated for comparison purposes. Measurements obtained in the early stages of dewatering agreed well with gravimetric measurements and showed no significant variations in the moisture and solids profile. As dewatering progressed,

Table 19--Summary of Water Content Measurements for Ottawa Sand by the Attenuation Method.

Ratio of distance from bottom to total length, x/L	Water content (θ), gm/cm^3
0.20	0.36
0.40	0.34
0.60	0.37
0.80	0.42
Average (Attenuation Values)	0.37
Average (Volumetric Measurement)	0.38
Difference in two methods, %	2.6

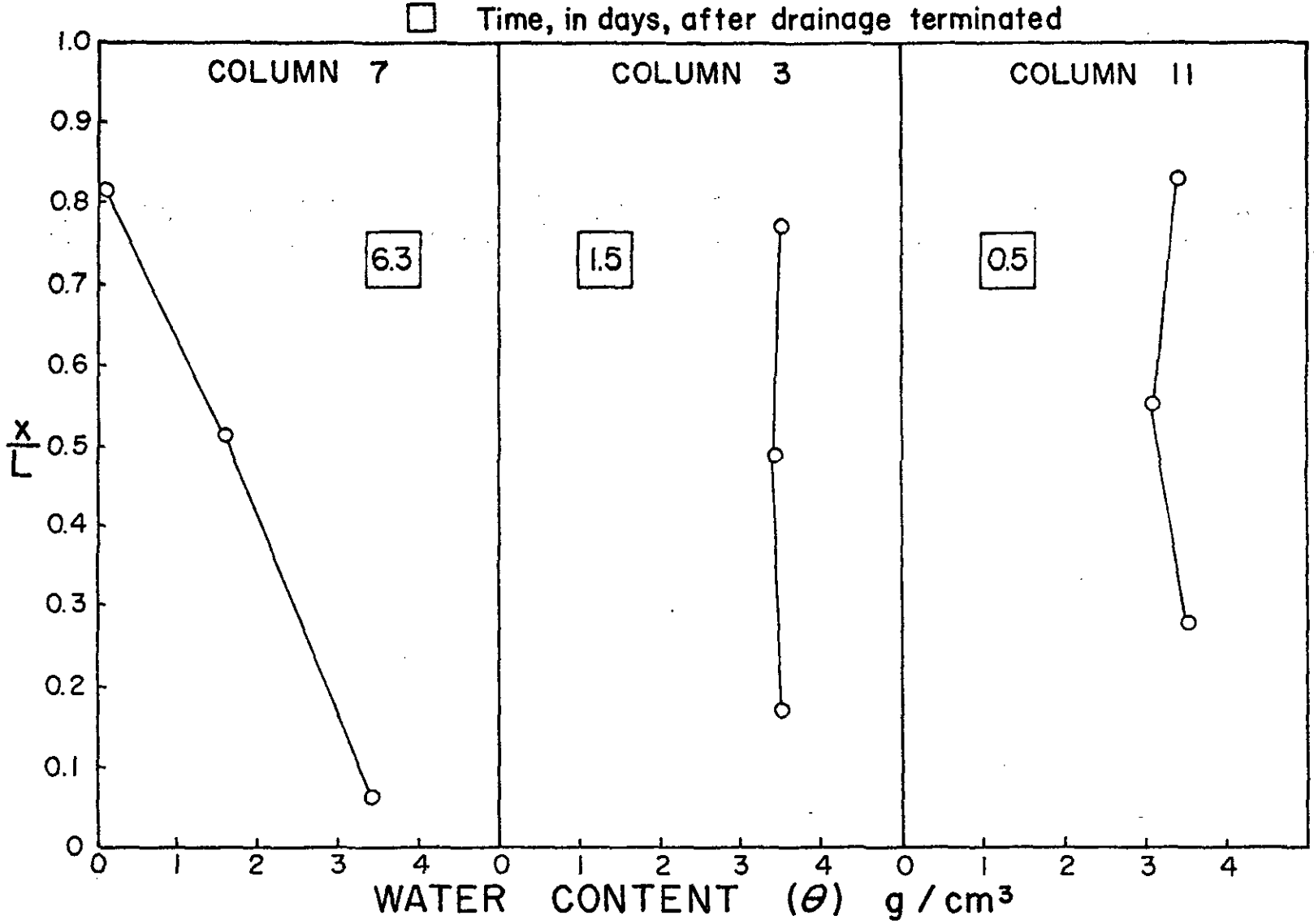

FIGURE 37 -- Profile of Water Content in Sand Layers (DW-3) After Drainage Terminated.

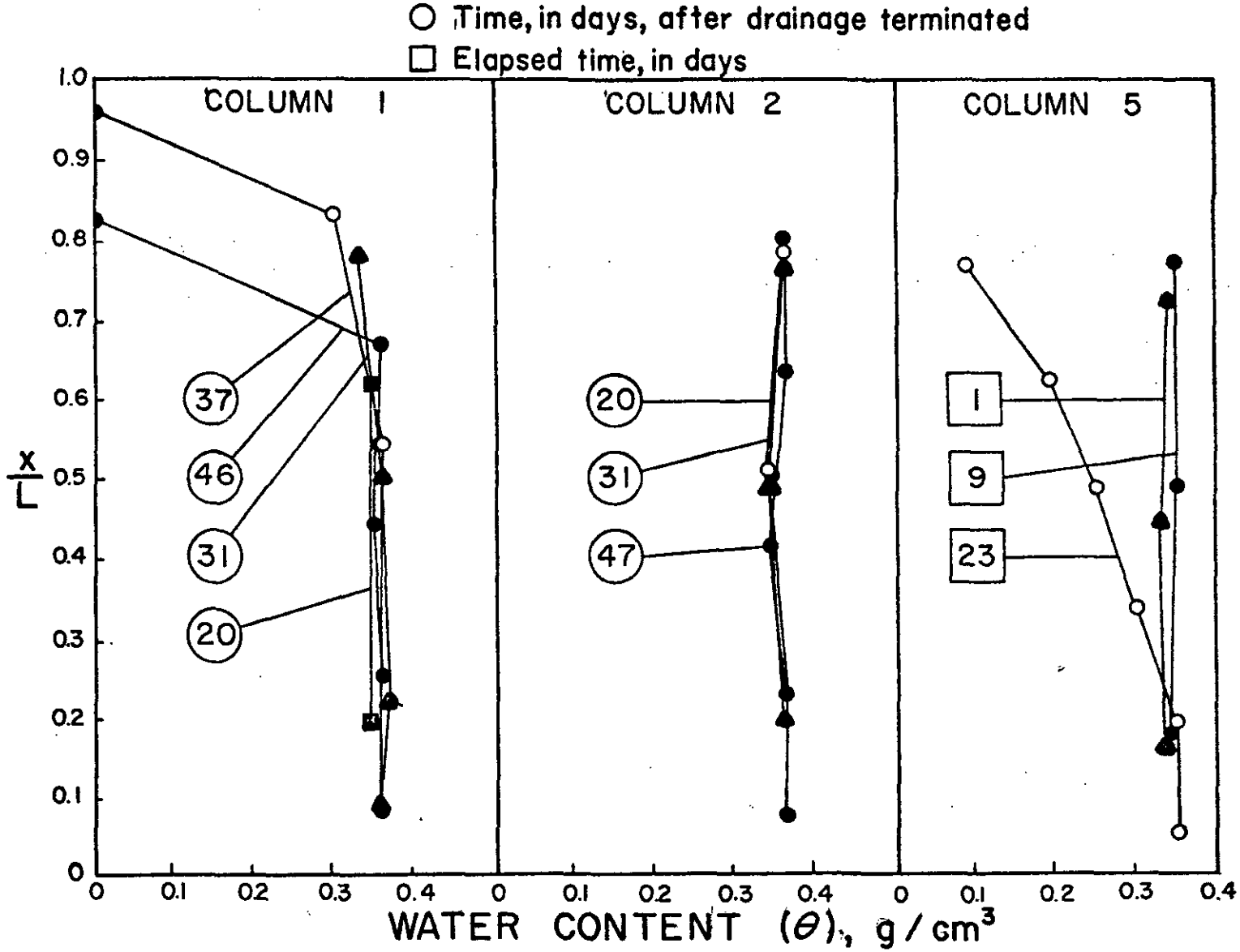

FIGURE 38 -- Profiles of Water Content in Sand Layers for Dewatering Study DW-3.

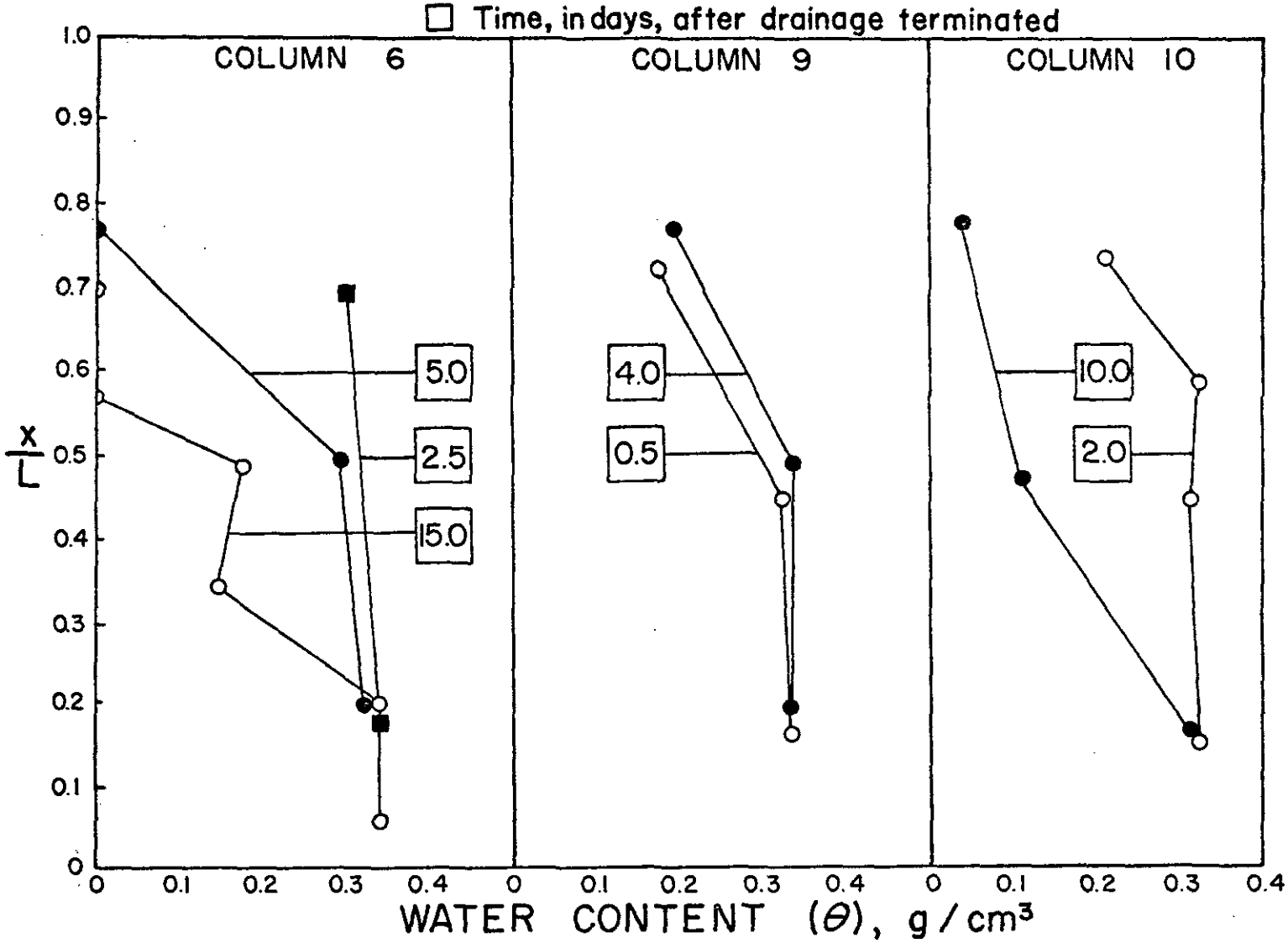

FIGURE 39 -- Profiles of Water Content in Sand Layers (DW-3) After Drainage Terminated.

the sludge cake receded from the column walls and horizontal and vertical cracks appeared. As the theoretical equations for the solids content had been derived on the basis that the column was filled with water or solids, the net result of the shrinkage, or cracks, was to change the sludge thickness making this method inapplicable during the final stages of dewatering.

The method for measuring moisture and solids content was tested using Billerica sludge in the small plastic boxes. The sludge was thoroughly mixed initially and an aliquot was taken for solids content measurement by the gravimetric metnod (oven drying). The solids profile as determined by the attenuation method is shown in Figure 40 along with the average solids content by gravimetric method. The difference between the average solids content by the gravimetric method and gamma-ray attenuation method was 6.0 %. Since the profile determination required some 1.5 hours, some sedimentation occurred causing higher solids concentrations near the bottom of the sample. An error analysis of the attenuation method was performed and is described in the Appendix. The method was found to be very accurate for high values of solids content with the accuracy diminishing as solids content decreased. The results of the error analysis for Billerica sludge are shown in Figure 41.

Solids profiles for sludge dewatering by drying only are shown in Figure 42 for Albany sludge (DW-3). The initial depth and solids content were 40.6 cm and 1.86%, respectively. Calculated average values of the solids content are shown for comparison. During the initial

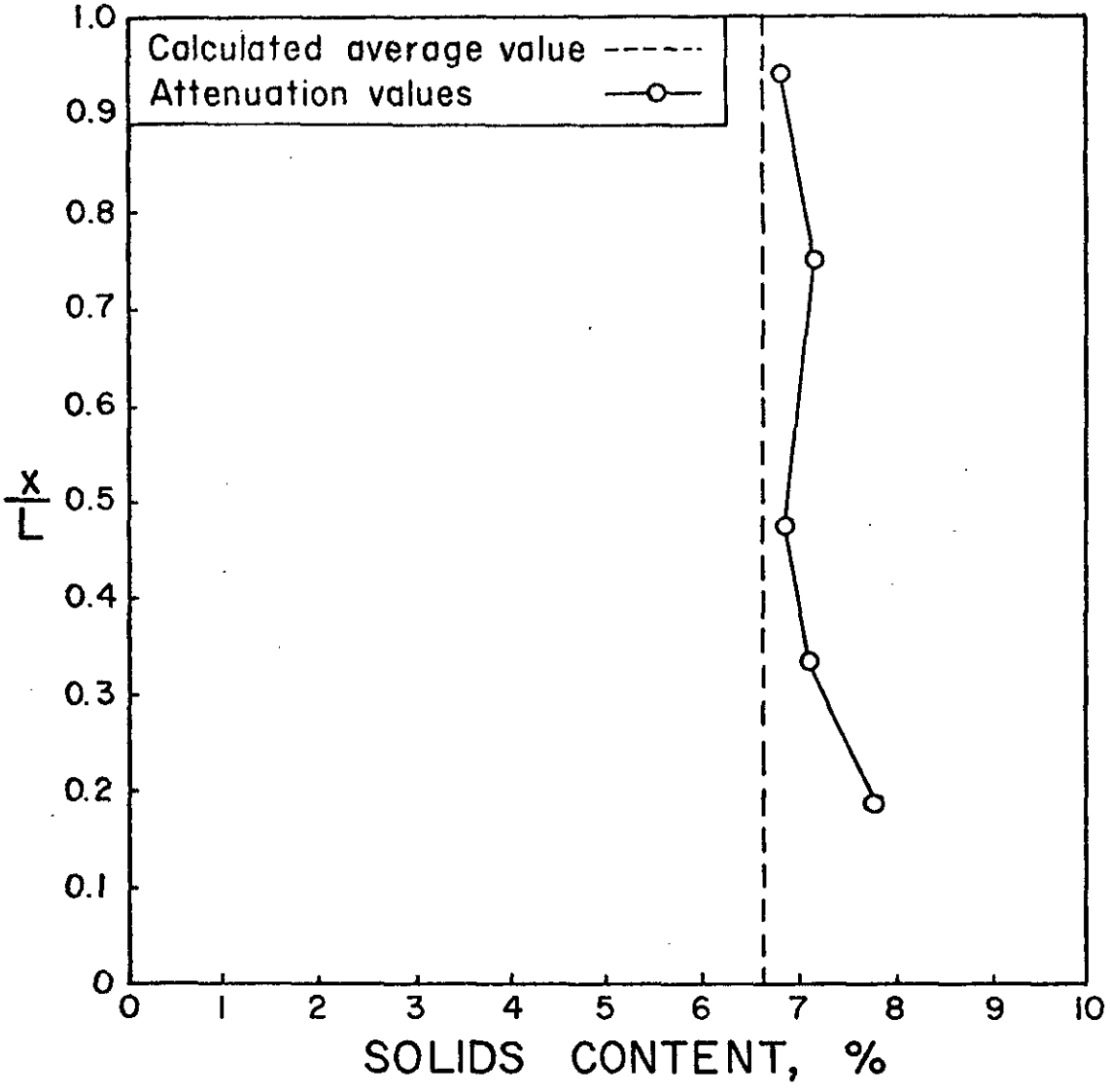

FIGURE 40 -- Variation of Solids Content with Depth for Billerica Sludge.

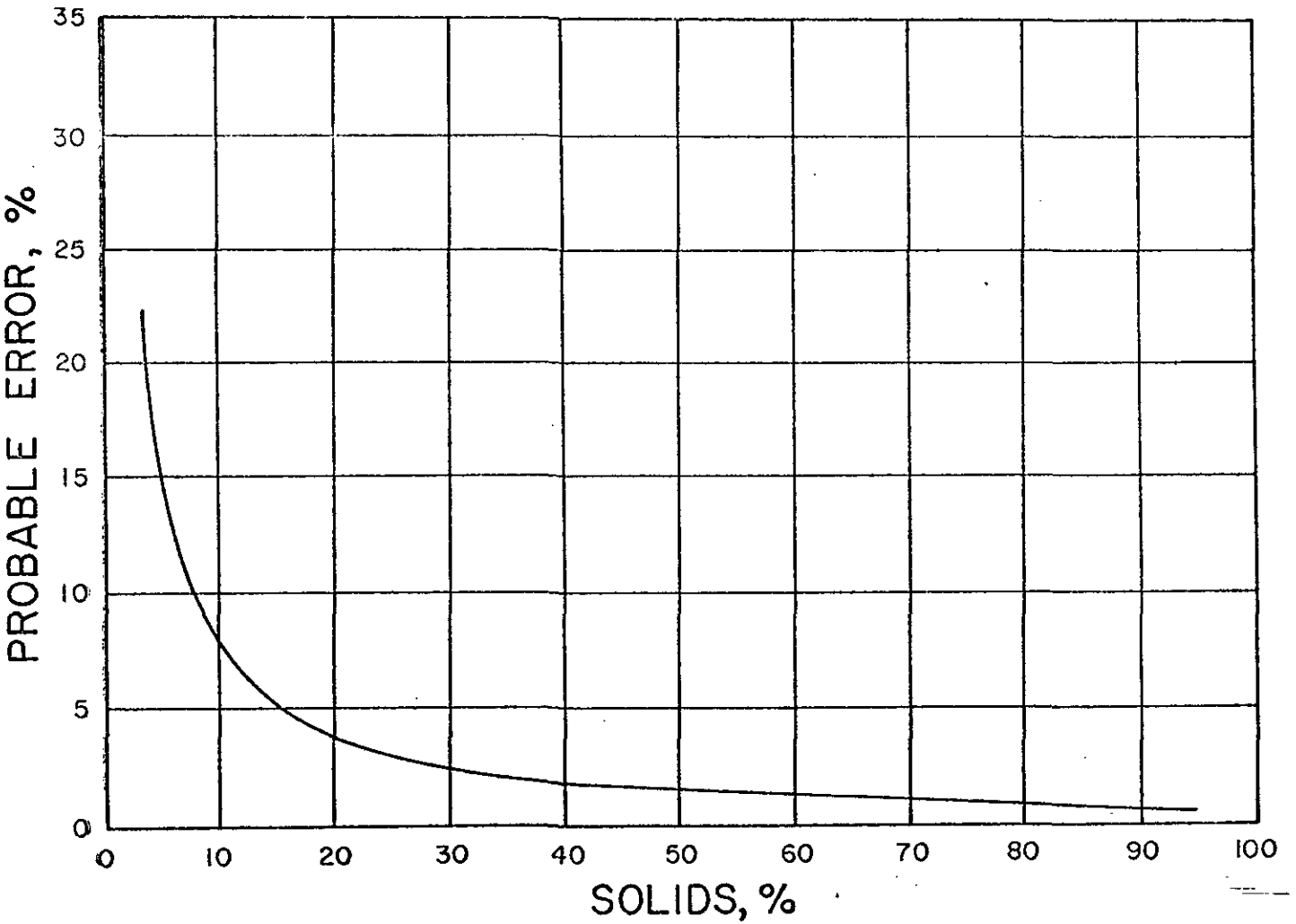

FIGURE 41 == Error Analysis.

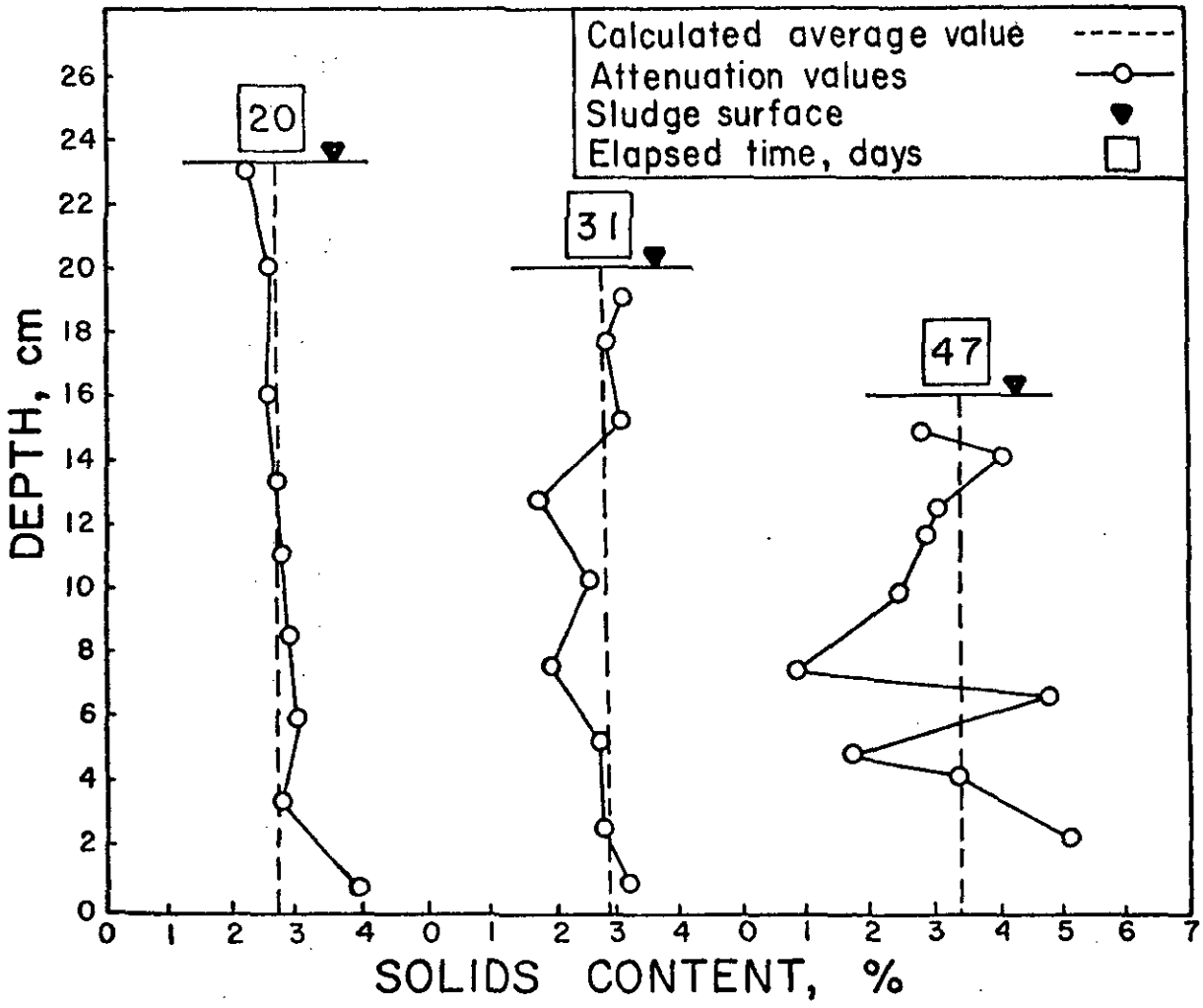

FIGURE 42 -- Variation of Solids Profiles with Time for Albany Sludge (DW-3) Drying on Ottawa Sand.

stages of drying, the solids profile was uniform with somewhat higher values near the bottom of the column due to sedimentation. As the drying time increased the solids became more varied due to shrinkage and consolidation. The final solids profile shows the solids profile after horizontal and vertical cracks had formed. Values for solids content near the top of the column could not be determined after the sludge cake had receded from the sludge surface, changing the thickness.

Solids profiles for Billerica sludge (DW-3) dewatering by drying only are shown in Figure 43 . The initial depth and solids content were 40.6 cm and 6.10%, respectively. The sludge cake shrank both horizontally and vertically during dewatering as shown in Figure 44 .

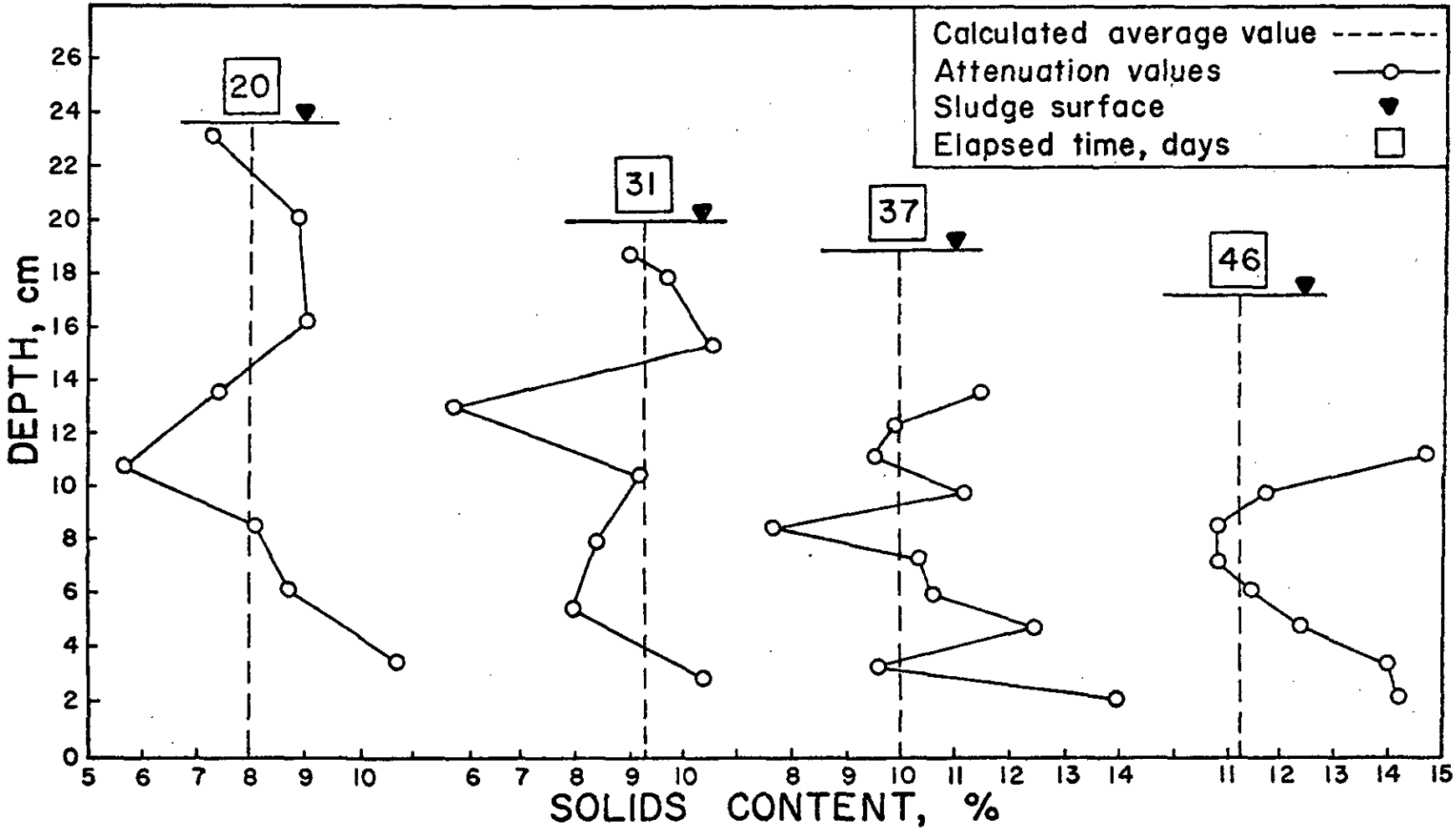

FIGURE 43 -- Variation of Solids Profile with Time for Billerica Sludge (DW-3) Drying on Ottawa Sand.

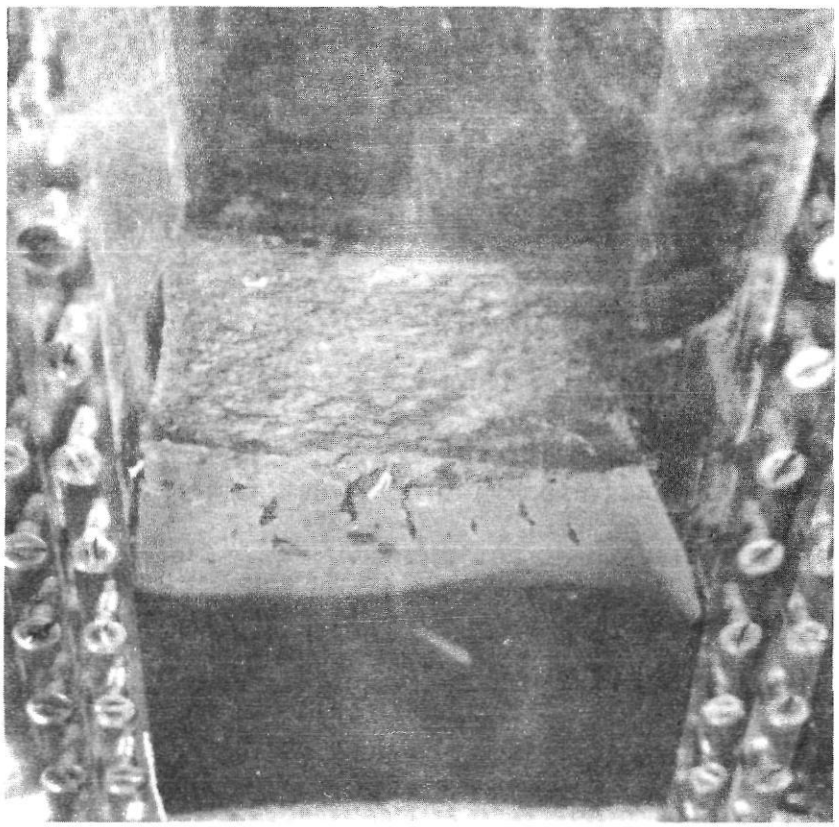

FIGURE 44 -- Photograph of Dewatered Sludge Cake.

CHAPTER VI

SUMMARY, CONCLUSIONS, AND RECOMMENDATIONS

Summary

The collection, handling and disposal of water treatment solid residues, or sludge, is one of the most vexing problems in environmental engineering. Reduction of the water content of sludge prior to ultimate land disposal reduces the volume of material handled, promotes handling and minimizes additional pollution problems. Previous studies have shown that disposal of sludge on land after drainage and drying on sand beds is economically competitive, however no rational design criteria exist.

The sludges used in this investigation were from four different types of water treatment plants. Plants represented consisted of alum coagulation, alum coagulation with iron removal, alum coagulation with activated carbon added, and lime and soda softening. A wide variety of chemical analyses were performed on the sludge, filtrate, and decant samples. The sludges had a wide variation in chemical characteristics. Many of the chemical constituents were adsorbed to the sludge solids and only small amounts appeared in the decant and filtrate samples.

Dewatering studies were conducted under controlled conditions with four types of water treatment sludge. Moisture and solids profiles were determined periodically for the sludge and supporting sand layers by use of the gamma-ray attenuation method.

All dewatering studies were conducted in a specially constructed environmental chamber. Temperature and relative humidity were carefully controlled for each study. Preliminary evaporation studies for water showed no significant difference in the evaporation rate between the location in the environmental chamber and depth of water in the container.

The evaporation ratio of water treatment sludges varied from 85 to 130% depending upon the sludge type and initial solids content. The evaporation rate of a solution is theoretically lowered due to solids being present, however, this is compensated for in some cases due to the heat conduction and convection in the small drying containers. Sludges with activated carbon present generally had an evaporation ratio in excess of 100%.

In the drying-rate studies, approximately 80 to 85% of the water loss occurred in the constant-rate drying period. The constant-rate drying period also accounted for 65 to 75% of the drying duration. Shrinkage was very pronounced in the constant-rate drying period, the change in depth approximating that of a free water surface. The sludge could have been removed from a drying bed during the constant-rate drying period, at a solids content of 12 to 20%. Constant-rate drying dictated that the sludge mass-time function be linear. Experimental results verified this postulate. The slope of the sludge mass-time curve was proportional to the constant-rate drying intensity and was easily obtained from linear regression analysis.

The falling-rate portion of the sludge mass-time curve was approximated with a parabola. The parabolic relationship between the drying

rate and moisture content differs from the linear relationship used in previous studies and gives a more accurate estimate for the drying duration.

Drainage studies were conducted in plastic columns using Ottawa sand as the filter media. Drainage increased the initial solids content of the sludge by a factor of 2 to 8, the higher value being for the softening sludge. The specific resistance determined by the Buchner funnel procedure was corrected for use in the sludge drainage equation to account for its variation with pressure. Media factors, used previously for sewage sludge drainage studies and thought to be a function of the ratio of the sludge particle size to the sand particle size, were determined empirically. Discrepancies between the actual drainage times and times predicted by the sludge dewatering equation are attributed to drainage occurring after the limitations of the drainage equation were reached. The percentage of total drainage time Equation 53 is applicable for water treatment sludges is less than the applicable time for sewage sludges.

A gamma-ray attenuation method which had been used in soil studies and more recently in sewage sludge studies was used to non-destructively measure the solids or moisture profile in the sludge. Separate procedures were developed for calculating the moisture for the two distinct conditions involved in the sand and sludge layers. Both procedures required prior determination of attenuation coefficients and specific gravity measurements of the solid material.

The gamma-ray attenuation method showed that at the end of sludge drainage, virtually no water had been drained from the supporting sand layer. Later as drying proceeded, shrinkage and crack formations exposed the sand surface to the drying atmosphere and practically all the water was lost from the sand layers. The attenuation method also showed that the moisture, or solids, profile was linear during most of the drying process.

Conclusions

Chemical properties of water treatment sludges vary widely depending upon the nature of the raw water supply, the degree and type of treatment, and the method of sludge removal from the sedimentation basin. Filtrate and decant from water treatment sludges contain considerably less pollutional strength than the sludge samples and their disposal should be determined on an individual basis.

Of the three basic mechanisms involved in water treatment sludge disposal, drying and drainage account for the majority of water removal. Both drying and drainage are now developed to a state where reasonable engineering designs can be made.

Drainage times can be predicted from Equation 53 to provide a good estimate for design purposes. Water treatment sludges with initial solids contents from 1 to 6 percent can be concentrated by drainage to 5 - 12 percent solids in 40 to 100 hours.

Drying durations can be calculated from the drying equations presented as Equation 114. Drying rates for use in Equation 114 can be determined by the model for predicting lake evaporation. The evapor-

ation ratios for the particular type of sludge and the average local weather conditions provide drying rates for any locality or climate. Under normal conditions, water treatment sludges can be removed from the drying beds while in the constant-rate drying period. The solids content for a forkable sludge ranges from 10 to 20 percent.

The moisture gradient in water treatment sludge is constant during most of the drying period, indicating that evaporation from the surface--not internal diffusion--is the major resistance to drying.

The gamma-ray attenuation method is applicable to sludge drying studies but needs some refinements to cover the dewatering period after lateral shrinkage of the sludge cake becomes pronounced. After the critical moisture content is reached the moisture profile provides useful information on the moisture content and the moisture transport mechanisms during the falling-rate period.

Recommendations

Recommendations for future studies and design of water treatment sludge dewatering beds can be made from this investigation.

Future studies. Future studies should concentrate on the quantities of sludge produced by waters of various qualities being treated in different ways and the method of removal of sludge from the sedimentation basins. Thickening of certain types of sludge, such as softening sludge, by sedimentation and decantation could remove large amounts of relatively clear water.

The effect of sludge conditioners such as polyelectrolytes on the dewatering rates should be investigated.

A study of the sludge particle sizes would lead to relationships for determining media factors for the drainage model.

Further refinements are needed in the gamma-ray attenuation method for determining moisture profiles in water treatment sludge. During the drying period of interest in sand bed dewatering, the moisture profile is constant indicating that moisture evaporation at the surface governs rather than internal diffusion moisture. However, for certain applications such as drying of thick layers of sludge and determination of the critical moisture content, the moisture profile is required. Shrinkage and crack formation of the sludge cake in the early stages of water treatment sludge dewatering change the horizontal thickness of the cake rendering Equation 85 invalid. Possible refinements in the attenuation method to overcome this limitation include the use of a different radioactive source and a combination of two sources.

King (82) discussed the advantages of using Americium 241, a gamma emitter, for attenuation measurements. The Am^{241} spectrum has a major peak at about 0.06 Mev and a lower peak of about .026 Mev. Values for the attenuation coefficient of soil were reported as 0.267 cm^2/gm and 0.077 cm^2/gm for the Am^{241} and Cs^{137} sources, respectively. Thus the beam from Am^{241} would be attenuated more by soil than would a beam from a cesuim source making the method more sensitive. Another advantage of Am^{241} over Cs^{137} is the reduction in biological shielding required. The half-thickness of lead is about 31 times greater for Cs^{137} than the half-thickness of Am^{241}. One disadvantage is the

limitation of source strength of Am^{241} due to self adsorption. For a smaller source strength, longer counting times would be required in order to obtain the desired accuracy. The relative cost of Am^{241} would also be much more than that of Cs^{137}.

The method of using both Cs^{137} and Am^{241} concurrently to overcome the limitations due to horizontal shrinkage seems promising. The ratio of transmitted beams and the ratio of the incident beams for the two sources should give information on both the moisture content and the sample thickness.

Design recommendations. Technology from various disciplines was assembled to enable the design engineer to more rationally design sand dewatering beds. Drainage times can be accurately predicted from Equation 53 requiring prior knowledge of specific resistance and coefficient of compressibility, initial and final solids content, and media factors, all of which are readily determined in the laboratory. Values for final solids content and media factors must be determined from pilot studies; however, sufficient data are present for preliminary design purposes.

Drying rates for sludge were shown to approximate those of water. Evaporation rates of water are easily determined by the Kohler model if local weather conditions are known. In the absence of local weather data, the average evaporation rate may be approximated from the U.S. Evaporation Map (Figure 3). For thin layers of sludge application, water treatment sludge has been shown to dry in the constant-rate period. This eliminates need for determining the critical moisture content and makes the calculation of drying times straightforward.

With the dewatering relationships presented, the design engineer can easily optimize the design beds by varying the various parameters involved. A method such as that used by Nebiker and Adrian (81) wherein land costs were included provides a rational design method.

BIBLIOGRAPHY

1. Hudson, H. E., Jr., "How Serious is the Problem?" Proceedings, Tenth Sanitary Engineering Conference, Urbana, Ill., 1968.

2. Russelmann, H. B., "Characteristics of Water Treatment Plant Wastes," Proceedings, Tenth Sanitary Engineering Conference, Urbana, Ill., 1968.

3. Dean, R. B., "Ultimate Disposal of Waste Water Concentrates to the Environment," Environmental Science and Technology, Vol. 2, 1968, p. 1079.

4. Aultman, W. W., "Lime and Lime-Soda Sludge Disposal," Journal of the American Water Works Association, Vol. 41, No. 9, Sept., 1949, pp. 819-829.

5. Black, A. P., "Disposal of Softening Plant Wastes," Journal of the American Water Works Association, Vol. 41, No. 9, Sept., 1949, pp. 819-829.

6. Haney, P. D., "Brine Disposal from Zeolite Softeners," Journal of the American Water Works Association, Vol. 39, No. 12, Dec., 1947, pp. 1215-1219.

7. Haney, P. D., "Brine Disposal from Cation-Exchange Softeners," Journal of the American Water Works Association, Vol. 41, No. 9, Sept., 1949, pp. 829-836.

8. Hall, H. R., "Disposal of Wash Water from Purification Plants," Journal of the American Water Works Association, Vol. 39, No. 12, Dec., 1947, pp. 1219-1223.

9. Dean, J. B., "Disposal of Wastes from Filter Plants and Coagulation Basins," Journal of the American Water Works Association, Vol. 45, No. 11, Nov., 1953, pp. 1226-1237.

10. Disposal of Wastes From Water Treatment Plants, American Water Works Association Research Foundation, New York, Aug., 1969.

11. O'Brien and Gere, "Waste Alum Sludge Characteristics and Treatment," Research Report No. 15, New York State Department of Health, Albany, N. Y., 1966.

12. Gates, S.D., and McDermott, R. F., "Characteristics and Methodology for Measuring Water Filtration Plant Wastes," Research Report No. 14, New York State Department of Health, Albany, N. Y., 1966.

13. Doe, P. W., "The Treatment and Disposal of Wash Water Sludge," Journal of the Institute of Water Engineers, Vol. 12, 1958, pp. 409-445.

14. Gauntlett, R. B., "Waterworks Sludge-I," Technical Paper 30, Water Research Association (British), Medmenham, Marlow, Bucks., Aug., 1963.

15. Gauntlett, R. B., "Waterworks Sludge-II," Technical Paper 38, Water Research Association (British), Medmenham, Marlow, Bucks., Oct., 1964.

16. Gauntlett, R. B., "Waterworks Sludge-III," Technical Paper 46, Water Research Association (British), Medmenham, Marlow, Bucks., June, 1965.

17. Wertz, C. F., "Miami in the Limelight and at a Profit," Water and Sewage Works, Vol. 100, No. 3, Mar., 1953, pp. 98-103.

18. Mace, H. H., "Disposal of Wastes from Water Treatment Plants," Public Works, Vol. 84, No. 7, 1953, pp. 73 and 88-90.

19. Burd, R. S., "A Study of Sludge Handling and Disposal," Publication WP-20-4, Federal Water Pollution Control Administration, U.S. Department of the Interior, Washington, D.C., May, 1968.

20. Tang, W., "Moisture Transport in Sludge Dewatering and Drying on Sand Beds," thesis presented to Vanderbilt University, in 1969, in partial fulfillment of the requirements for the degree of Doctor of Philosophy.

21. Sanders, T. G., "A Mathematical Model Describing the Gravity Dewatering of Wastewater Sludge on Sand Drainage Beds," thesis presented to the University of Massachusetts, Amherst, Mass., in 1968, in partial fulfillment of the requirements for the degree of Master of Science.

22. Adrian, D. D., and Nebiker, J. H., "Irrigation and Reclamation Using Sanitary Sludges," presented at the Annual Meeting of the Soil Science Society of America, New Orleans, La., Nov., 1968.

23. Nebiker, J. H., "The Drying of Wastewater Sludge in the Open Air," Journal of the Water Pollution Control Federation, Vol. 39, No. 4, April, 1967, pp. 608-626.

24. Quon, J. E., and Tamblyn, T. A., "Intensity of Radiation and Rate of Sludge Drying," Journal of the Sanitary Engineering Division, A.S.C.E., Vol. 91, No.SA-2,April, 1965, pp. 17-31.

25. Quon, J. E., and Ward, G. B., "Convective Drying of Sewage Sludge," International Journal of Air and Water Pollution, Vol. 9, 1965, p. 311.

26. Coackley, P. and Allos, R., "The Drying Characteristics of Some Sewage Sludges," Journal of the Institute of Sewage Purification, Vol. 6, 1962, p. 557.

27. Spangler, M. G., "Soil Water," Soil Engineering, 2nd ed., International Textbook Co., Scranton, Pa., 1960, pp. 84-90.

28. Treybal, R. E., "Drying," Mass-Transfer Operations, McGraw-Hill Co., New York, 1955, pp. 524-583.

29. McCabe, W. L., and Smith, J. C., Unit Operations of Chemical Engineering, 2nd ed., McGraw-Hill Co., New York, 1967, pp. 512-515.

30. Badger, W. L., and Banchero, J. T., "Drying", Introduction to Chemical Engineering, McGraw-Hill Co., New York, 1955, pp. 469-519.

31. Eagleson, P. S., "Evaporation and Transpiration," Dynamic Hydrology, McGraw-Hill Co., New York, 1970, pp. 211-241.

32. Boelter, L. M. K., Gordon, H. S., and Griffin, J. R., "Free Evaporation into Air of Water From a Free Horizontal Quiet Surface," Industrial and Engineering Chemistry, Vol. 38, No. 6, June, 1946, pp. 596-600.

33. Penman, H. L., "Natural Evaporation from Open Water, Bare Soil, and Grass," Proceedings, Royal Society (London), Ser. A, Vol. 193, 1948, pp. 120-145.

34. Kohler, M. A., Nordenson, T. J., and Fox, W. E., "Evaporation from Pans and Lakes," Research Paper No. 38, U.S. Weather Bureau, 1955.

35. Instructions for Climatological Observers, U.S. Department of Commerce, Weather Bureau,Circular B, 10th ed., rev., Washington, D.C., Oct., 1955.

36. Kohler, M. A., Nordenson, T. J., and Baker, D. R., Evaporation Maps for the United States, Technical Paper No. 37, U.S. Department of Commerce, Weather Bureau, Washington, D.C., 1959.

37. Marshall, W. R., and Friedman, S. J., "Drying", Chemical Engineers' Handbook, 3rd ed., J. H. Perry, ed., McGraw-Hill Co., New York, 1950, pp. 799-884.

38. Sherwood, T. K., "The Drying of Solids-I," Industrial and Engineering Chemistry, Vol. 21, No. 1, Jan., 1929, pp. 12-16.

39. Sherwood, T. K., "The Drying of Solids-II," Industrial and Engineering Chemistry, Vol. 21, No. 10, Oct., 1929, pp. 976-980.

40. Sherwood, T.K., "The Air Drying of Solids," Transactions, American Institute of Chemical Engineers, Vol. 32, 1936, pp. 150-168.

41. Sherwood, T.K., "Application of Theoretical Diffusion Equations to the Drying of Solids," Transactions, American Institute of Chemical Engineers, Vol. 27, 1931, pp. 190-202.

42. Newman, A. B., "The Drying of Porous Solids: Diffusion and Surface Emission Equations," Transactions, American Institute of Chemical Engineers, Vol. 27, 1931, pp. 203-217.

43. Luikov, A. V., "Heat and Mass Transfer in Some Engineering Processes," Heat and Mass Transfer in Capillary-Porous Bodies, 1st English ed., Pergamon Press, New York, 1966, pp. 341-376.

44. Carslaw, H. S., and Jaeger, J. C., Conduction of Heat in Solids, 2nd ed., Oxford University Press, Amen House, London E. C. 4, 1959.

45. Crank, J., The Mathematics of Diffusion, Oxford University Press, Amen House, London E. C. 4, 1956.

46. Ozisik, M. N., Boundary Value Problems of Heat Conduction, International Textbook Co., Scranton, Pa., 1968.

47. Gilliland, E. R., and Sherwood, T. K., "The Drying of Solids VI - Diffusion Equations for the Period of Constant Drying Rate," Industrial and Engineering Chemistry, Vol. 25, No. 10, Oct., 1933, pp. 1134-1136.

48. Hougen, D. A., McCauley, H. J., and Marshall, W. R., "Limitations of Diffusion Equations in Drying," Transactions, American Institute of Chemical Engineers, Vol. 36, 1940, pp. 183-209.

49. Ceaglske, N. H., and Hougen, D. A., "The Drying of Granular Solids," Transactions, American Institute of Chemical Engineers, Vol. 33, 1937, pp. 283-312.

50. Sherwood, T. K., and Gilliland, E. R., "The Drying of Solids VI - Diffusion Equations for the Period of Constant Drying Rate," Industrial Engineering Chemistry, Vol. 25, 1933, pp. 1134-1136.

51. Broughton, D. B., "The Drying of Solids--Prediction of Critical Moisture Content," Industrial and Engineering Chemistry, Vol. 37, No. 12, Dec., 1945, pp. 1184-1185.

52. Haseltine, T. R., "Measurement of Sludge Drying Bed Performance," Sewage and Industrial Wastes, Vol. 23, No. 9, 1951, pp. 1065-1083.

53. Jeffrey, E. A., "Laboratory Study of the Dewatering Rates for Digested Sludge in Lagoons," Proceedings, 14th Industrial Waste Conference, Purdue University, West Layfette, Ind., 1959, pp. 359-384.

54. Adrian, D. D., Lutin, P. A., and Nebiker, J. H., "Source Control of Water Treatment Waste Solids," Report No. EVE-7-68-1, Dept. of Civil Engineering, University of Massachusetts, Amherst, Mass., April, 1968.

55. Carman, P. C., "A Study of the Mechanism of Filtration - Part I," Journal of the Society of Chemical Industry, Vol. 52, Sept., 1933, pp. 280T-282T.

56. Carman, P. C., "A Study of the Mechanism of Filtration - Part II: Experimental," Journal of the Society of Chemical Industry, Vol. 53, June, 1934, pp. 159T-165%.

57. Carman, P. C., "A Study of the Mechanism of Filtration - Part III," Journal of the Society of Chemical Industry, Vol. 53, Sept., 1934, pp. 301T-309T.

58. Coackley, P. and Jones, B.R.S., "Vacuum Sludge Filtration: Interpretation of Results by the Concept of Specific Resistance," Sewage and Industrial Wastes, Vol. 28, Sept., 1956, pp. 963-968.

59. Nebiker, J. H., Sanders, T. G., and Adrian, D.D., "An Investigation of Sludge Dewatering Rates," Presented at the 23rd Annual Meeting of the Purdue Industrial Waste Conference, Purdue University, Lafayette, Ind., May, 1968.

60. Lutin, P. A., Nebiker, J. H., and Adrian, D. D., "Experimental Refinements in the Determination of Specific Resistance and Coefficient of Compressibility," Proceedings, 1st Annual New England Anti-Pollution Conference, University of Rhode Island, Kingston, R.I., 1968, pp. 120-126.

61. Gardner, W. H., "Water Content," Methods of Soil Analysis: Part 1, C. A. Black, ed., Academic Press, Madison, Wis., 1965, pp. 82-127.

62. Blizard, E. P., "Nuclear Radiation Shielding," Nuclear Engineering Handbook, H. Etherington, ed., McGraw-Hill Co., New York, 1958.

63. Standard Methods for the Examination of Water and Wastewater, 12th ed., American Public Health Assocation, Inc., New York, 1965.

64. FWPCA Methods for Chemical Analysis of Water and Wastes, Federal Water Pollution Control Administration, U.S. Department of the Interior, Washington, D.C., Nov., 1969.

65. Hald, A., Statistical Theory with Engineering Applications, John Wiley and Sons, Inc., New York, 1952, pp. 571-584.

66. Salvadori, M. G., and Baron, M. L., "Finite Differences and Their Applications," Numerical Methods in Engineering, Prentice-Hall, Inc., New York, 1952, pp. 45-75.

67. Reginato, R. J., and VanBavel, C.H.M., "Soil Measurement with Gamma Attenuation," Proceedings, Soil Science Society of America, Vol. 28, No. 6, 1964, pp. 721-724.

68. Davidson, J. M., Biggar, J. W., and Nielsen, D. R., "Gamma-Radiation Intensity for Measuring Bulk Density and Transient Water Flow in Porous Materials," Journal of Geophysical Research, Vol. 68, No. 16, 1963, pp. 4777-4783.

69. Ferguson, H., and Gardner, W. H., "Water Content Measurement in Soil Columns by Gamma Ray Adsorption," Proceedings, Soil Science Society of America, Vol. 26, No. 1, 1962, pp. 11-14.

70. Gurr, C. G., "Use of Gamma Rays in Measuring Water Content and Permeability in Unsaturated Columns of Soil," Soil Science, Vol. 94, 1962, pp. 224-229.

71. Evans, R. D., "Attenuation and Absorption of Electromagnetic Radiation," The Atomic Nucleus, McGraw-Hill Co., New York, 1955, pp. 711-745.

72. VanBavel, C.H.M., Underwood, N., and Ragar, S. R., "Transmission of Gamma Radiation by Soils and Soil Densitometry," Proceedings, Soil Science Society of America, Vol. 21, 1957, pp. 588-591.

73. Chase, G. D., and Rabinowitz, J. L., "Scintillation Techniques of Nuclear Emulsions," Principles of Radioisotope Methodology, 3rd ed., Burgess, Minneapolis, 1967, pp. 283-323.

74. Kohl, J., Zenter, R. D., and Lukens, H. R., Radioisotope Applications Engineering, Van Nostrand Co., New York, 1961.

75. Steel, R.G.D., and Torrie, J. H., Principles and Procedures of Statistics, McGraw-Hill Co., New York, 1951, pp. 15-19.

76. Lambe, T. W., "Specific Gravity Test," Soil Testing for Engineers, John Wiley and Sons, New York, 1951, pp. 15-19.

77. Covey, W., "Mathematical Study of the First Stage of Drying of a Moist Soil," Proceedings, Soil Science Society of America, Vol. 27, No. 2, 1963, pp. 130-134.

78. Wakabayashi, K., "Moisture Diffusion Coefficient of Solid During Drying Process," Kagaku Kogaku (Abridged ed.), Vol. 2, No. 2, 1964, pp. 132-136.

79. Wakabayashi, K., "Calculation of Moisture Distribution in Clay During Drying Process," Kagaku Kogaku (Abridged ed.), Vol. 2, No. 2, 1964, pp. 146-149.

80. Ames, W. F., Nonlinear Partial Differential Equations in Engineering, Academic Press, New York, 1965, p. 34.

81. Nebiker, J. H., and Adrian, D. D., "Cost Evaluation of Sand Bed Dewatering and Drying of Wastewater Sludges," Filtration and Separation (British), May-June, 1969, pp. 246-248 and p. 300.

82. King, L. G., "Gamma-Ray Attenuation for Soil-Water Content Measurements Using Am^{241}," Isotope and Radiation Techniques in Soil Physics and Irrigation Studies, International Atomic Energy Agency, Vienna, 1967, pp. 17-29.

83. Mickley, H. S., Sherwood, T. K., and Reed, C. H., "Interpretation of Engineering Data," Applied Mathematics in Chemical Engineering, McGraw-Hill Co., New York, 1957, pp. 46-104.

APPENDIX A-1 --Error Analysis of Moisture Profile Measurements.

An error analysis for the moisture profile measurements by gamma-ray attenuation was performed. The relationship for solids content as given in Equation 85, is written as

$$\frac{S}{100} = \frac{\rho_d[\mu_w\rho_w L_s - \ln (N_p/N)]}{(\rho_w-\rho_d) \ln (N_p/N) + \rho_w\rho_d L_s(\mu_w-\mu_d)} \qquad (A\text{-}1)$$

S becomes an indirectly measured quantity since it is related to the indirectly measured quantities μ_w, ρ_w, L_s, and N/N_w. The true value of S cannot be known because the true values of the indirectly measured quantities are unknown. The most probable value of S can be determined, however, by the method discussed in Mickley et al. (83). According to this method the term S in Equation A-1 can be written as a function of the indirectly measured quantities as

$$s = \frac{S}{100} = f\ (\rho_w,\rho_s,L_s,\mu_s,\mu_w,\ Y) \qquad (A\text{-}2)$$

where $Y = N_p/N$

s = fractional solids content

and the other terms are as previously described. In Equation A-2 the terms for density of water, ρ_w, and length of sludge, L_s, were considered as constants since they could be determined very accurately. The differential change in s corresponding to a differential change in

ρ_d, μ_s, μ_w, and Y is

$$ds = \frac{\partial f}{\partial \rho_d} d\rho_d + \frac{\partial f}{\partial \mu_s} d\mu_s + \frac{\partial f}{\partial \mu_w} d\mu_w + \frac{\partial f}{\partial Y} dY \qquad \text{(A-3)}$$

Replacing the differentials $d\rho_d$, $d\mu_s$, $d\mu_w$, dY by small finite increments $\Delta\rho_d$, $\Delta\mu_s$, $\Delta\mu_w$, ΔY, results in a good approximation (83) for Δs. The expression is

$$\Delta s = \frac{\partial f}{\partial \rho_d} \Delta\rho_d + \frac{\partial f}{\partial \mu_s} \Delta\mu_s + \frac{\partial f}{\partial \mu_w} \Delta\mu_w + \frac{\partial f}{\partial Y} \Delta Y \qquad \text{(A-4)}$$

The quantities $\Delta\rho_d$, $\Delta\mu_s$, $\Delta\mu_w$, ΔY may be considered as errors in the measurements of ρ_d, μ_s, μ_w, and Y. Equation A-4 overestimated the uncertainty in s since the equation comprises the assumption that the maximum error in each of the terms occurs simultaneously. If the error in each of the terms in Equation A-4 is thought of as a random variable for any set of measurements, then the standard deviation of s would be

$$\sigma(\Delta_s) = \left[\sigma^2\left(\frac{\partial f}{\partial \rho_d} \Delta\rho_d\right) + \sigma^2\left(\frac{\partial f}{\partial \mu_s} \Delta\mu_s\right) + \sigma^2\left(\frac{\partial f}{\partial \mu_w} \Delta\mu_w\right) + \sigma^2\left(\frac{\partial f}{\partial Y} \Delta Y\right)\right]^{1/2} \qquad \text{(A-5)}$$

A percentage error, ε , may be expressed as

$$\varepsilon = \left(\frac{\Delta s}{s}\right) 100 \qquad \text{(A-6)}$$

The term $\partial s/\partial \rho_d$ is obtained by differentiating Equation A-1 with respect to ρ_d, holding all the other terms constant and is found to yield

$$\frac{\partial s}{\partial \rho_s} = (\mu_w\rho_w L_s - \ln Y)\{[\ln Y(\rho_w-\rho_d)+ \rho_w\rho_d L_s(\mu_w-\mu_s)] - \rho_d[\ln Y + \rho_w L_s (\mu_w-\mu_s)][\mu_w\rho_w L_s - \ln Y]\} \quad (A\text{-}7)$$
$$[\ln Y(\rho_w - \rho_d) + \rho_w\rho_d L_s(\mu_w - \mu_s)]^2$$

The other terms are found to be:

$$\frac{\partial s}{\partial \mu_s} = \frac{\rho_w\rho_d^2 L_s (\mu_w\rho_w L_s - \ln Y)}{[\ln Y(\rho_w - \rho_d) + \rho_w\rho_d L_s(\mu_w - \mu_s)]^2} \quad (A\text{-}8)$$

$$\frac{\partial s}{\partial \mu_w} = \{[(\rho_w-\rho_d)\ln Y + \rho_w\rho_d L_s(\mu_w-\mu_s)]\rho_d\rho_w L_s - L_s\rho_w\rho_d^2[\mu_w\rho_w L_s - \ln Y]\}$$
$$[\ln Y(\rho_w-\rho_d) + \rho_w\rho_d L_s(\mu_w-\mu_s)]^2 \quad (A\text{-}9)$$

$$\frac{\partial s}{\partial Y} = \{[\ln Y(\rho_w-\rho_d) + \rho_w\rho_d L_s(\mu_w-\mu_s)][-\rho_d(\tfrac{1}{Y})] - (\rho_d\mu_w\rho_w L_s - \rho_d \ln Y)[(\rho_w-\rho_d)\tfrac{1}{Y}]\}$$
$$[\ln Y(\rho_w-\rho_d) + \rho_w\rho_d L_s(\mu_w-\mu_s)]^2 \quad (A\text{-}10)$$

The error for each of the Δ terms in Equation A-4 was taken as the standard deviation of that quantity. The standard deviation of the Y term was determined by considering the quotient. The following equations were used to determine the standard deviations:

$$\sigma(N_p) = (N_p)^{1/2} \tag{A-11}$$

$$\sigma(N) = (N)^{1/2} \tag{A-12}$$

$$\sigma(Y) = Y\left[\left(\frac{\sigma(N_o)}{N_o}\right)^2 + \left(\frac{\sigma(N)}{N}\right)^2\right]^{1/2} \tag{A-13}$$

The count rate through the plastic columns varied somewhat with the counting location. The standard deviation for a typical column was determined by taking 16 minute counts at various locations. This standard deviation was used in Equation A-13. It can be seen from Equation A-6 that the accuracy of the method diminishes with decreasing solids content.

Table A-1 --Total Mass, in grams, of Water(E-I) Evaporating at 76°F and 47% Relative Humidity in 26.7 cm Diameter Pails.

Time, hrs	Container Sample Number				
	1A	1B	1C	2A	2B
tare	1358	1376	1467	1412	1345
0	6467	12253	17619	6458	12454
48.0	6303	12060	17411	6325	12284
96.0	6144	11866	17200	6195	12126
144.3	5979	11669	16987	6063	11957
168.1	5898	11572	16873	5997	11873
193.2	5796	11467	16767	5925	11781
216.0	5710	11373	16663	5863	11695
240.2	5622	11275	16552	5794	11608
267.2	5532	11182	16449	5729	11520
288.3	5440	11085	16338	5663	11429
314.0	5341	10977	16226	5594	11336
337.8	5244	10876	16113	5525	11249
361.0	5154	10782	16016	5462	11168
384.8	5061	10685	15911	5397	11089
435.6	4853	10482	15697	5257	10917
457.0	4764	10389	15607	5196	10838
481.8	4667	10293	15503	5131	10760
504.8	4600	10234	15442	5093	10713

Table A-1 --Continued

Time, hrs	Container Sample Number 2C	3A	3B	3C
tare	1282	1303	1380	1319
0	18335	6612	12490	18169
48.0	18140	6473	12333	17992
96.0	17950	6336	12181	17814
144.3	17740	6190	12016	17621
168.1	17640	6118	11935	17538
193.2	17526	6046	11858	17443
216.0	17425	5987	11781	17361
240.2	17310	5923	11712	17276
267.2	17195	5865	11638	17193
288.3	17084	5801	11569	17110
314.0	16967	5732	11490	17020
337.8	16862	5662	11407	16920
361.0	16763	5592	11329	16832
384.8	16659	5526	11250	16740
435.6	16450	5385	11082	16547
457.0	16353	5324	11014	16469
481.8	16255	5261	10939	16383
504.8	16202	5226	10910	16343

Table A-2 --Total Mass, in grams, of Billerica Sludge(D-1)

Drying at 72°F and 38% Relative Humidity in 35 x 22 x 4.5 cm Glass Pans.

Cumulative Time, hrs	Mass, grams	Cumulative Time, hrs	Mass, grams
tare	1935	189.5	3050
0	3990	201.8	2995
5.0	3960	213.7	2950
20.8	3875	225.8	2885
27.5	3840	237.0	2840
33.0	3815	248.8	2785
46.0	3750	262.8	2725
52.8	3720	312.3	2510
68.8	3650	337.1	2410
77.0	3600	406.1	2145
94.7	3510	411.9	2125
129.5	3340	431.2	2090
166.0	3160	485.5	2075
172.0	3130	509.5	2075

Table A-3 --Total Mass, in grams, of Billerica Sludge(D-2) Drying at 72°F and 38% Relative Humidity in 35 x 22 x 4.5 cm Glass Pans.

Cumulative Time, hrs	Mass, grams	Cumulative Time, hrs	Mass, grams
tare	1935	241.3	2975
0	4310	264.1	2860
8.5	4250	288.1	2740
22.8	4165	311.3	2630
32.8	4120	336.0	2500
46.5	4050	358.7	2400
54.2	4000	386.6	2260
69.5	3920	388.3	2261
78.0	3870	394.0	2228
94.5	3780	406.0	2167
102.8	3740	409.8	2148
127.3	3610	413.0	2132
142.3	3530	432.0	2049
166.3	3395	440.1	2026
173.3	3355	456.8	2006
195.3	3235	464.3	2005
214.3	3120	477.8	2004

Table A-4--Total Mass, in grams, of Water(DW-2) Evaporating at 76°F and 30% Relative Humidity in 26.7 cm Diameter Pails.

Accumulated Time, hrs	Pan Number 1	2	3
tare	13767.5	1346.0	1380.5
0	10365.0	10215.0	10468.0
25.0	10233.0	10088.0	10342.0
49.0	10136.5	9996.0	10253.0
73.0	10042.5	9907.5	10165.5
97.2	9948.5	9815.5	10076.5
121.3	9852.0	9722.0	9985.0
165.1	9681.0	9561.5	9824.0
231.1	9427.5	9321.5	9576.5
240.5	9389.0	9283.5	9538.5
263.6	9299.5	9191.5	9452.0
302.8	9150.0	9036.5	9309.5
356.3	8943.5	8824.5	9119.0
386.3	8831.0	8710.5	9014.5
445.3	8618.5	8496.0	8815.0
495.8	8429.5	8309.5	8642.0
526.8	8320.0	8200.0	8536.0
551.7	8230.0	8110.0	8498.0
594.2	8066.0	7954.0	8300.0
666.2	7813.0	7714.0	8055.0

Table A-5 --Total Mass, in grams, of Albany Sludge(DW-2)After Drainage Had Terminated. Column 4 was Distilled Water.

Accumulated Time After Drainage Terminated, hrs	Column Number			
	1	2	3	4
0	13660.0	14214.5	13710.5	14234.0
24.9	13544.5	14175.5	13693.0	14211.0
57.4	13513.0	14103.0	13665.5	14172.5
103.4	13477.0	13974.5	13539.0	14130.5
203.4	13402.5	13909.5	13476.0	14050.0
253.4	13362.0	13875.5	13442.0	14010.0

Table A-6 --Accumulated Volume of Filtrate in milliliters, for Three Columns of Albany Sludge(DW-2.) Dewatering on 11.5 cm of Saturated Ottawa Sand. Initial Sludge Depth was 45.8 cm.

Accumulated Time, hrs	Column Number 1	2	3
0	0	0	0
1.0	310	305	330
4.0	590	560	600
20.0	670	665	650
25.0	830	835	815
38.0	1160	1165	1130
48.0	1400	1400	1345
62.5	1720	1665	1605
72.0	1900	1830	1775
88.5	2185	2085	2010
97.2	2330	2210	2125
109.5	2530	2385	2290
121.5	2720	2555	2470
133.5	2920	2745	2850
147.5	3130	2945	3040
159.5	3345	3135	3210
231.2	3605	3510	3600
240.5	3680	3585	3670
263.5	3845	3755	3845

Table A-6 --Continued

Accumulated Time, hrs	Column Number 1	2	3
280.3	3930	3870	3950
303.0	4145	4015	4100
328.5	4150	4150	4230
356.5	4240	4270	4350
386.5	4330	4380	4460
447.5	4780	4560	4635
498.0	4830	4685	5165

Table A-7 --Head (H_o) Measurements, in centimeters, for Three Columns of Albany Sludge (DW-2.) Dewatering on 11.5 cm of Saturated Ottawa Sand. Initial Sludge Depth was 45.8 cm.

Accumulated Time, hrs	Column Number 1	2	3
0	82.50	84.00	84.00
20.0	75.02	76.61	76.46
25.0	73.78	75.77	75.64
38.0	71.64	73.69	73.58
48.0	70.17	72.34	72.18
62.5	68.28	70.56	70.36
72.0	67.10	69.78	69.77
85.0	65.32	67.82	67.84
88.5	64.31	67.09	67.11
109.5	62.88	66.06	66.01
121.5	61.68	64.80	64.88
133.5	59.80	63.74	62.58
147.5	58.40	62.44	61.38
159.5	56.87	61.26	60.27
186.0	54.56	58.96	58.29
210.0	52.90	57.73	56.86
231.2	51.18	56.28	55.42
258.2	49.90	54.89	53.70
280.0	49.08	53.82	53.06

Table A-7--Continued

Accumulated Time, hrs	Column Number 1	2	3
303.0	48.38	52.67	51.93
328.5	47.94	51.86	51.06
356.5	47.34	51.14	50.37
386.5	46.95	50.44	49.70
445.5	46.22	49.45	48.69
496.0	46.19	48.84	48.36
552.0	45.95	48.60	48.15
740.0	45.46	47.72	47.70
909.0	45.08	47.53	47.36

Table A-8 --Cumulative Volume of Filtrate, in milliliters, for Water Treatment Sludges(DW-3.) Dewatering on 11.43 cm Ottawa Sand.

Initial Sludge Depth was 44.8 cm.

Cumulative Time, hrs	Column Number 3	5	6	7	9
0	0	0	0	0	0
1.5	270	270	250	390	390
6.0	560	535	500	810	820
21.0	1090	980	900	1610	1560
27.5	1260	1105	1040	1810	1780
31.2	1335	1165	1090	1890	1840
44.6	1585	1535	1310	2215	2145
65.8	1900	1825	1640	2235	2145
74.0	2025	1925	1760	2260	2250
89.7	2155	2030	1880	2300	2250
113.4	2355	2160	1895	2395	2270
208.9	2855	2470	2100	2400	
270.4		2510	2120		
330.9	2995	2590			
408.4	3105	2605			
499.6	3250				
700.4	3485				

Table A-9 --Total Mass of Sludge Columns, in grams, for Dewatering Study (DW-3.)
First two values are column tare with dry and saturated media, respectively.

Cumulative Time, hrs	Column Number 1	2	3	4	5	6
	11609	11606	11560	11480	11489	11704
	12231	12258	12207	12195	12140	12377
0	17328	17136	17131	14668	17183	17509
73.0	17092	16910	14944	14490	15136	15545
114.0	16949	16779	14551	14407	14840	15156
144.5	16891	16715	14306	14381	14678	14986
223.0	16670	16521	13873	14216	14382	14596
290.8	16493	16349	13702	14070	14220	14401
410.0	16196	16081	13365	13868	13983	14231
458.5	16081	15950	-	-	-	-
501.8	15993	15878	13166	13730	13860	14087
632.8	15723	15635	12951	13539	13696	13885
701.4	15592	15509	12633	13438	13615	13800
774.5	15485	15398	12555	13355	13537	13704
894.5	15285	15206	12420	13205	13390	13537
985.0	15138	15065	12315	13090	13282	13418
1135.2	14962	14858	12152	12931	13116	13240
1231.0	14756	14716	12035	12807	12979	13077

Table A-9--Continued

Cumulative Time, hrs.	Column Number 7	8	9	10	11
	11541	11499	11589	11608	11592
	12199	12235	12328	12341	12275
0	17171	14602	17366	17352	17928
73.0	14757	14416	14974	12454	12435
114.0	14535	14349	14772	12422	12397
144.5	14475	14316	14696	12390	12366
223.0	14309	14158	14455	12333	12261
290.7	14146	13989	14235	12271	12171
410.0	13942	13788	13960	12157	12049
501.7	13764	13645	13725	12076	11940
632.7	13508		13347	11961	11860
701.3	13382		13202	11904	11853
774.5	13255		13050	11874	11845
894.5	13026		12767	11860	11832
985.0	12860		12595	11845	11823
1135.2	12615		12343		
1231.0	12426		12140		